MODELLING OF URBAN HEAT ISLAND AND QUANTIFICATION OF AMELIORATION EFFECTS OF PLANT SPECIES ON MICROCLIMATE AND HUMAN THERMAL COMFORT IN NAIROBI CITY, KENYA

EMMANUEL OCHOLA MATSABA

MASTER OF SCIENCE

(Landscape Planning & Conservation)

JOMO KENYATTA UNIVERSITY OF

AGRICULTURE AND TECHNOLOGY

2021

Modelling of Urban Heat Island and Quantification of Amelioration Effects of Plant Species on Microclimate and Human Thermal Comfort in Nairobi City, Kenya

Emmanuel Ochola Matsaba

A Thesis Submitted in Partial Fulfilment of the Requirements for the Degree of Master of Science in Landscape Planning and Conservation of the Jomo Kenyatta University of Agriculture and Technology

2021

DECLARATION

This thesis is my original work and has not been presented for a degree award in any other university.

Signature:..... Date:.....

Emmanuel Ochola Matsaba

This thesis has been submitted for examination with our approval as university supervisors.

Signature:.....Date:……

Dr. Adimo Ochieng Aggrey, PhD

JKUAT, Kenya

Signature:.....Date:.....

Prof. Mukundi John Bosco Njoroge, PhD

JKUAT, Kenya

DEDICATION

This thesis is wholeheartedly dedicated to my beloved parents Mr. and Mrs. Matsaba, and my beloved wife Juliet Koech who have been my source of inspiration and gave me strength when I thought of giving up, who continually provide moral, spiritual, emotional, and financial support. To my brothers, sisters, relatives, mentor, friends, and classmates who shared their words of advice and encouragement to finish this study, I felt so honoured and blessed to have you. Moreover, I dedicated this thesis to the Almighty God; thank you for the guidance, strength, power of the mind, protection, and skills and for giving me a healthy life. All of these, I offer to you.

ACKNOWLEDGEMENTS

Many individuals have contributed to completing my master's studies, and in extension, the research component. To them, I owe a debt of thanks for their support, moral or otherwise, in seeing me through. First and foremost, I am deeply indebted to my supervisors, Prof. John Mwibanda Wesonga, the entire ERAfrica LOCLIM3 project team, and the Africa-ai-Japan project team for their financial support and tireless lessons that they gave me during research work.

My sincere gratitude is equally extended to my research supervisors, Dr. Aggrey Ochieng' Adimo and Prof. John Bosco Mukundi, whose timeless advice and guidance. The support received from you is immensely appreciated.

I must also thank the current staff and the postgraduate students of the Department of Landscape and Environmental Sciences at Jomo Kenyatta University of Agriculture and Technology for their organised supervision and mentorship during the entire period of my studies. Many thanks to Mr. Stephen Waringo Waweru for offering field and technical support during my research.

Special thanks to Prof. Dr. Sahar Sodoudi of the Department of Earth science at the Institute for Meteorology, Freie University Berlin, and her entire research team for their ideas and advice on urban climate change and modelling the entire period of my training and research.

Finally, sincere thanks are due to my family for their support, encouragement, and perseverance during the entire length of my studies. God bless you all.

TABLE OF CONTENTS

LIST OF TABLES

LIST OF FIGURES

LIST OF ABBREVIATIONS

BLUHI	Boundary Layer Urban Heat Island
BQA	Quality Assessment Band
CBD	Central Business District
CLUHI	Canopy Layer Urban Heat Island
DI	Discomfort Index
GE	Google Earth
GIS	Geographical Information System
1D	One Dimension
JICA	Japan International Cooperation Agency
JKUAT	Jomo Kenyatta University of Agriculture and Technology
Km	Kilometre
LAI	Leaf Area Index
LCZs	Local Climate Zones
LU	Land Use
LSTs	Land Surface Temperatures
m	metre
MUKLIMO_3	Microscale Urban Climatic Model In three dimensions
NASA	National Aeronautics and Space Administration
NDVI	Normalised Difference Vegetation Index
OLI	Operational Land Imager
PET	Physiologically Equivalent Temperature

ROI	Region of Interest
RH	Relative Humidity
SAGA	System for Automated Geoscientific Analysis
SUHI	Surface Urban Heat Island
TIRS	Thermal Inferred Sensor
UHI	Urban Heat Island
UHII	Urban Heat Island Intensity
USA	United States of America
WGBT	Wet, Globe, Bulb Temperature
WUDAPT	World Urban Database Access Portal Tool

ABSTRACT

Rapid urbanisation and global warming have led to the Urban Heat Island (UHI) phenomenon in Nairobi City. The UHI phenomenon is considered the most interpretive indication of an urban climate change in the current time of increasing urbanisation. Proper climate change adaptation planning actions in Nairobi city require recognizing the possible range of UHI intensity and spatial dispersion. However, climate research and its applications in urban planning and improvement in Nairobi city is constrained by inadequate evaluation and irregular descriptions of the local city's characteristics. Therefore, there is a need to study the correlation between urbanisation and UHI and quantify the benefits of plant species on microclimate and human thermal comfort within Nairobi city. The study models and simulates the UHI of Nairobi and further quantifies environmental amelioration effect of different tree species on microclimate and human thermal comfort in the city. The city was first classified into Local Climate Zones (LCZs), then estimated the land surface temperature (LSTs) distribution using a split-window algorithm, and simulated 2m air temperature by MUKLIMO_3 model to show UHI phenomenon for Nairobi city. After that, the attenuation effects of selected plant species on microclimate and human thermal comfort were quantified. The study generated the current LCZ classification for Nairobi city. Both built-up (LCZ 1-10) and natural (LCZ A-G) areas are present. The LCZ classification captured the forms and functions of each zone and indicated the potential UHI distribution pattern of Nairobi city. The study confirmed the presence of urban heat loads in built-up areas with a high percentage of water-resistant, non-reflective surfaces and low vegetation compared to the surrounding rural areas. Statistical analysis of LSTs showed significant differences among typical LCZs. Additionally, the amelioration effects of selected individual plant species demonstrated differences in performance. *Ficus benjamina* (vast dense canopy) presented the highest ability to attenuate environmental parameters (surface temperature, ambient temperature globe temperature, and relative humidity) and reduce thermal discomfort index, followed by *Cassia spectabilis, Warburgia ugandensis, Ficus religiosa, Callistemon citrinus* followed by *Dypsis decaryi, Bambusa vulgaris, Terminalia mantaly* and *Schinus molle* (small open canopy). In conclusion, the study presented the LCZ Nairobi as a basic spatial unit for synoptic characterization and comprehensive climate-based classification of the city sites for urban planning and management. The spatial pattern of urban heat loads in Nairobi is influenced by local climate formation as differentiated by urban form (urban morphological parameters) and functions. In addition, the attenuation effects of plant species in urban spaces vary based on their allometric properties and planting designs. Therefore, proposals for urban planning and design strategies to manage urban heat in Nairobi City can optimise the form and layout of urban LCZs to enhance ventilation and promote appropriate building materials increasing the use of green and blue urban infrastructure. The study recommended further research on spatial configurations of planting designs with more cooling and fewer energy demands and their application to the whole city.

CHAPTER ONE
INTRODUCTION

1.1 Background information

Urban climate change is a severe problem for cities worldwide (Hashim & Hashim, 2016), particularly in developing countries like Kenya, where urbanisation is happening rapidly (Alavipanah *et al*., 2015). Urbanisation prompts changes in the landscape (Oyugi *et al*., 2017), as infrastructure replace vegetation and open land, making the surfaces that were once porous and sodden to end up impermeable and dry (Ali *et al*., 2017; Hashim & Hashim, 2016; Middel *et al*., 2014; Ren *et al*., 2016; See, *et al*., 2015; Singh *et al*., 2017).

Tropical cities such as Akure in Nigeria, Cairo in Egypt, and Nairobi in Kenya are experiencing heat waves; they are expected to face further the challenge of increased intensity, duration, and spatial distribution of heat waves (Connor *et al*., 2015). The rapid urbanisation and increased global warming (Oyugi *et al*., 2017) has led to a sequential of environmental problems, especially the formation of urban heat islands (UHI) (Bechtel & Daneke, 2012; Stewart & Oke, 2012) in Nairobi city, a situation whereby urban built-up zones experience hotter temperatures than their rural surroundings areas *(*Santamouris *et al*., 2017; Stone *et al*., 2010; Stone & Rodgers, 2001) and which is considered to be the most interpretive indication of urban climate change in the current time of increasing urbanisation.

The changing temperatures brought about by the UHI impacts lead to different air qualities, which relate to outdoor microclimate, cooling demands in buildings as well as human thermal comfort levels and health (Bechtel & Daneke, 2012; Ren *et al*., 2016; Stone *et al*., 2010; Vargo *et al*., 2016). The fundamental drivers of UHI are believed to identify with the three attributes of urban areas: increased roughness due to building

structural geometries, drier and progressively impenetrable surfaces, and anthropogenic warmth and moisture discharges (Bechtel *et al*., 2015; Bechtel & Daneke, 2012; Geletič *et al*., 2018; Stevan *et al*., 2013).

According to Angel *et al*. (2005), it is expected that by 2050 about 70% of the worldwide populace will live in urban territories, resulting in even greater urban sprawl. More than 100,000 cities in developing countries are expected to triple their built-up areas by 2030. Even in developed nations, urban areas will expand by 2.5 times, notwithstanding their little populace measure and a lower rate of populace development . As a result, forecasts indicate that average temperatures will continue to rise in the coming decades in most cities, mostly because of anthropogenic forcings (Oppenheimer & Children, 2016).

The concept of Local Climate Zones (LCZs) was introduced by Stewart & Oke, 2012 to provide the link between urbanisation and its corresponding thermal impacts on the landscape and to standardise the documentation and global exchange of urban temperature observations (Stewart & Oke, 2012). Most recent studies investigating urban temperature fields utilize the LCZ classification and primarily support the correspondence of LCZs with air temperature fields in cities and their surroundings (Bechtel *et al*., 2015; Geletič and Lehnert, 2016; Lehnert & Geletiˇ, 2016; Lehnert *et al*., 2015; Stewart & Oke, 2012; Stewart *et al*., 2014). However, some authors working with LCZs have pointed out that the influence of thermal properties of local climate may significantly vary concerning the geographical location of the zone, the size of the city, the position within the city, and relief (Bechtel *et al*., 2015; Bokwa *et al*., 2015).

Also, studies on vegetations indicate that plants have a significant beneficial ability to modify urban microclimate (Santamouris *et al*., 2017; Zhao *et al*., 2017) by countering the urban heat island effects (Alavipanah *et al*., 2015; Mcpherson *et al*., 2016), resulting

in improved thermal comfort (Santamouris *et al*., 2017; Abreu-Harbich *et al*., 2012, 2015; Zhao *et al*., 2017) and in the social cohesion and well-being of urban life (Alavipanah *et al*., 2015). However, the diversity of plant species could have a differentiated influence on urban microclimate and thermal comfort (Shashua-Bar *et al*., 2011).

This study incorporated the concept of LCZ classification to compute and compare the UHI phenomenon across Nairobi city. Further, it quantified the environmental amelioration effects of different plant species on microclimate and thermal comfort. The LCZ classification scheme is useful for integrating local climate knowledge into urban planning and design practices. It captures the internal structure and texture of cities to answer some crucial questions about the rapidly urbanising world.

1.2 Statement of the Problem

Advanced climate models are needed to consolidate the combined effect of urban climate change and urbanisation and assess the urban population's spatial vulnerability like Nairobi City (Oyugi *et al*., 2017; Stone & Rodgers, 2001). Despite this reality, there is also a challenge that the different interpretation of the term “urban” and “rural” by different scholars has led to vagueness in the use of urban-rural classification in climatological studies, which makes it challenging to determine which factors control the urban climate and therefore more critical in urban landscape planning and climate change management studies (Ng, 2015). Furthermore, urban climate research and its applications in urban planning and development in Nairobi city has for a long time been limited by inadequate quantification and irregular description of the city characteristics (urban form and function).

On the other hand, the diversity of plant species could have a different influence on urban microclimate and thermal comfort (Shashua-Bar *et al*., 2011). However, the

magnitude of varying plant species ameliorating urban microclimate by cooling the urban microclimate and improving thermal comfort based on their allometric properties at any particular time of the day is unknown for urban environments in tropical cities like tropical cities Nairobi. Therefore, findings from previous research on the UHI effect in Nairobi have restricted capacities to inform policymakers to mitigate the UHI effect since they did not show the correlation between urbanisation and urban climate change.

1.3 Justification

Climate monitoring of cities Nairobi is gradually becoming an essential element of urban planning and development. The forecast indicates that UHI intensity will continue to rise in the coming decades, leading to different air qualities related to human health. Therefore, this study was borne out of the need to inform policymakers to mitigate the UHI effect by showing the spatial correlation between urbanisation and urban climate change trends in the city.

The concept of LCZs was introduced by Stewart & Oke, 2012 to provide the link between urbanisation and its corresponding thermal impacts on the landscape and standardise the documentation and global exchange of urban temperature observations (Stewart and Oke, 2012). Most recent studies investigating urban temperature fields utilize the LCZ classification and primarily support the correspondence of LCZs with air temperature fields in cities and their surroundings (Bechtel *et al*., 2015; Geletič and Lehnert, 2016; Lehnert and Geletiˇ, 2016; Lehnert *et al*., 2015; Stewart & Oke, 2012; Stewart *et al*., 2014). However, some authors working with LCZs have pointed out that the influence of thermal properties of local climate may significantly vary concerning the geographical location of the zone, the size of the city, the position within the city, and relief (Bechtel *et al*., 2015; Bokwa *et al*., 2015).

Therefore, there is an urgent need for a comprehensive database on Nairobi city that goes beyond an urban footprint analysis to capture the landscape's internal structure and texture to answer some critical questions about the rapidly urbanising city. These include questions on the efficacy of urban-based adaption and mitigation policies in response to climate change and whether actions in one city are transferable. Additionally, there is a need to quantify the environmental amelioration effects of plant species diversity on microclimate and human thermal comfort levels in Nairobi city green space.

1.4 Objectives

The general objective of the study was to simulate Urban Heat Island and quantify the environmental amelioration effects of plant species as an adaptation strategy for Nairobi city. The specific objectives include:

1. To generate current Local Climate Zones for Nairobi city.
2. To estimate land surface temperature differentiation of local climate zones.
3. To simulate the Canopy layer Urban Heat Island using the MUKLIMO_3 Model.
4. To quantify the environmental amelioration effect of selected plant species on microclimate and human thermal comfort within Nairobi City.

1.5 Research Questions

1. What is the relationship between local climate zones and the spatial distribution of urban heat islands for Nairobi?
2. What are the effects of different plant species and diversity on urban microclimate and human thermal comfort?

1.6 Scope

This research incorporated the concept of LCZ classification to compute and compare urban temperature for the management of urban heat spots in Nairobi City. The study measured and simulated the UHI phenomenon's spatial configuration and further quantified the environmental amelioration effect of different plant species on microclimate and human thermal comfort in Nairobi city. The city was classified into LCZs, and then the spatial patterns of LSTs were estimated using the Split window algorithm in ArcGIS. At the same time, 2m air temperature fields were simulated using the MUKLIMO_3 microscale model at an urban scale. The distribution of urban heat load was differentiated using LCZ as a standardised scheme for documentation and global exchange of urban temperature observation. The study further explored the relationship between plant species' allometric properties and environmental parameters (ambient and relative humidity, globe temperature, infrared, and wind speed). It confirmed the importance of plant species canopy and height characteristics on the local microclimate within Nairobi city. The measurements of microclimatic parameters were carried out on isolated plant species within Uhuru Park and Central Park.

1.7 Limitations

The research study looked at the UHI and adaptation strategy for Nairobi city. The results were very positive; however, these findings may not be transferable to other Kenyan cities like Mombasa and Kisumu for urban planning and climate change management without adjustments. In addition, the study does not consider the spatial configurations of planting designs with more cooling and fewer energy demands and their application to the whole city.

CHAPTER TWO
LITERATURE REVIEW

2.1 Introduction

Relevant theories on the concept of LCZs, UHI distribution, and the effects of urban vegetations on microclimate have been reviewed to provide better insight and background on urban climate change adaptation using a diversity of plant species in Nairobi city from a broader perspective. This chapter includes the theoretical review in section 2.2, conceptual framework in section 2.3, a critical review of the existing literature significant to the study presented in section 2.4 summary in section 2.5. The research gaps are outlined in section 2.6.

2.2 The Theoretical review

The UHI manifestation accuracy is important for large urban conurbations to mitigate climate change and achieve sustainable development. This chapter presents literature on LCZs, UHI, and urban vegetations.

2.2.1 Local Climate Zones

The concept of LCZs (Bechtel *et al*., 2015) is applied to provide the link between urbanisation and its corresponding thermal impacts on the landscape, which is critical for understanding the consolidated impact of urban climate change and the vulnerability of the urban population. Spatial urbanisation extends and the potential heat spots exits because LCZs are locales of uniform land cover, structure, material, and human action at a horizontal scale of 50m-250m. (Stewart & Oke, 2012) as illustrated by parameters in *Figure 2.1*.

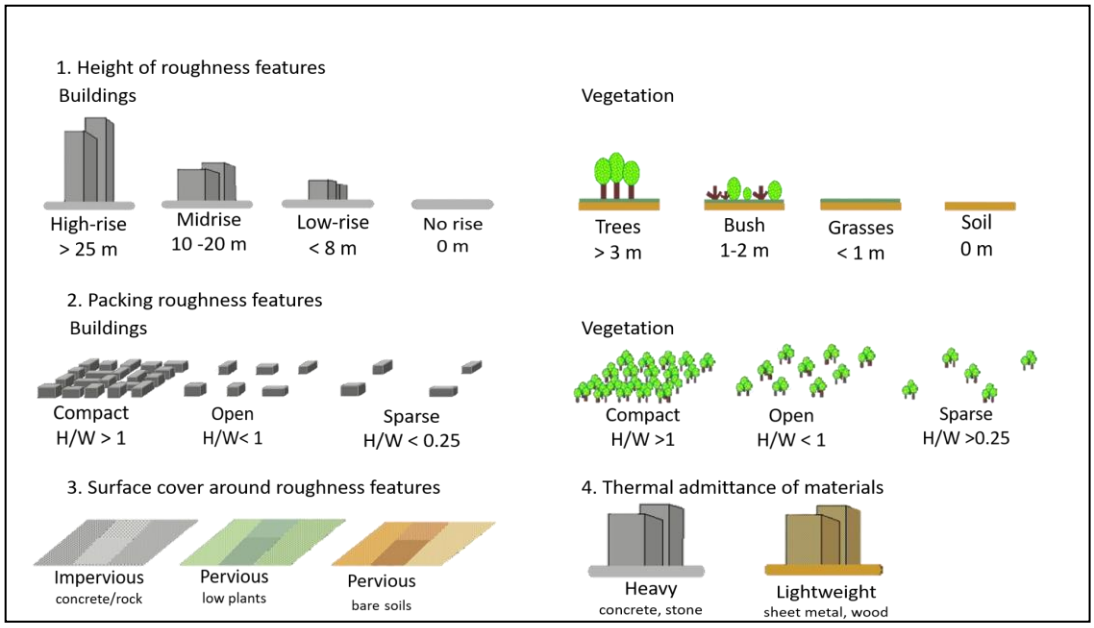

Figure 2.1: Urban parameters used for the construction of local climate zones.

The concept of LCZs is well documented and effectively definable based on the ten quantifiable based on urban canopy parameters relating to their structure (aspect ratio, roughness element height, and sky view factor), surface cover (plan fraction occupied by vegetation, buildings, and impervious ground) surface fabric (surface albedo and thermal admittance) and human activity (anthropogenic heat output) which are similar to those in urban models (Bechtel *et al*., 2015, 2017; Bechtel & Daneke, 2012; Geletič & Lehnert, 2016) as shown in *Figure 2.2*.

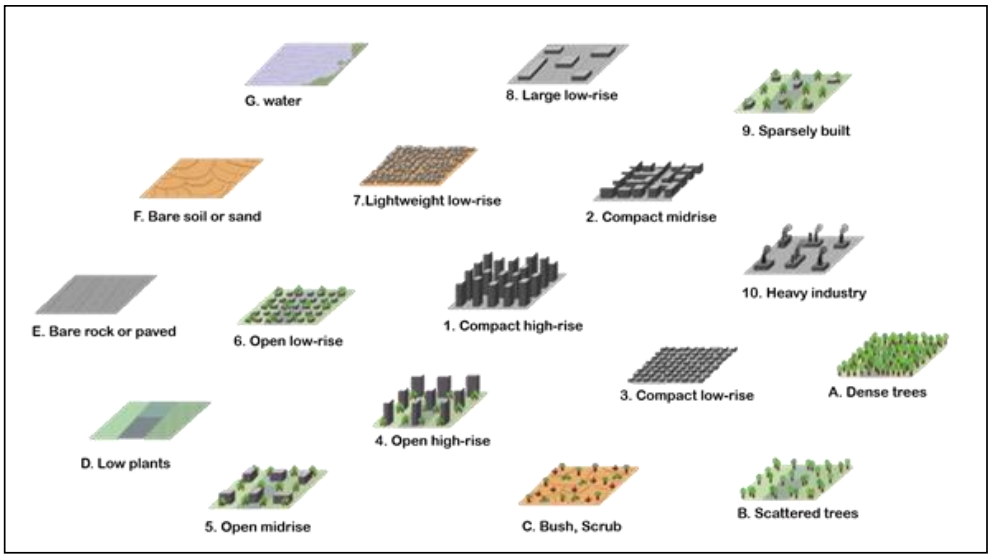

Figure 2.2: The LCZ concept with urban LCZ types (LCZ 1–10) and natural LCZ types (LCZ A–G).LCZ types and their characteristics (adapted from (Bechtel et al., 2017) and colour code used in the WUDAPT framework. Tall: >10 stories, Mid-rise: 3–9 stories, Low: 1–3 stories (Bechtel et al., 2015).)

Every zone was distinguished as a specific class if the encompassing circle of impact was uniform in geometry surface cover and human activities (Bechtel *et al*., 2015; I. D. Stewart & Oke, 2012). Unique combinations of these properties provided a distinctive thermal regime for each LCZ at screen height, best observed in clear weather conditions and areas of simple relief (Bechtel *et al*., 2015; Danylo *et al*., 2016; Stewart & Oke, 2012), as illustrated in *Table 2.1*.

Table 2.1 shows the quantifiable properties relating to surface structure, surface cover, and human activities for all the urban LCZ types according to Oke and Stewart 2012 *Table 3*. The data include:1: The ratio of the amount of sky hemisphere visible from ground level to that of an unobstructed hemisphere (%); 2: Mean height-to-width ratio of street canyons (LCZs 1–7), building spacing (LCZs 8–10), and tree spacing (LCZs A–G);3: The ratio of building plan area to total plan area (%); 4: The ratio of impervious

plan area (paved, rock) to total plan area (%); 5: The ratio of pervious plan area (bare soil, vegetation, water) to total plan area (%); 6: The geometric average of building heights (LCZs 1–10) and tree/plant heights (LCZs A–F) (m); 7: Davenport et al.'s (2000) classification of effective terrain roughness (z0) for city and country landscapes.; 8: The ability of a surface to accept or release heat (J m^{-2} $s^{-1/2}$ K^{-1}); 9: The ratio of the amount of solar radiation reflected by a surface to the amount received by it. It varies with surface colour, wetness, and roughness; 10: Mean annual heat flux density (W m^{-2}) from fuel combustion and human activity.

Table 2.1: Physical properties (characteristics and surface cover description) of the Local Climate Zones, modified from Stewart & Oke, 2012, table 3 and 4. Source: (Bechtel et al., 2015b; Stewart & Oke, 2012).

LCZ	1 (Ψsky)	2 (λs)	3 (λb)	4 (λ_I)	5 (λp)	6 (m)	7 (m)	8 (J.m-2.S-$1^{/2.K-1.}$)	9 Albedo	10 (W.m-2)
LCZ 1	0.2-0.4	>2.00	40-60	40-60	<10	>25	8	1500-1800	0.10-0.20	50-300
LCZ 2	0.2-0.6	0.75-2.00	40-70	30-50	<20	10-25	6-7	1500-2200	0.10-0.20	<75
LCZ 3	0.2-0.6	0.75-1.50	40-70	20-50	<30	03-10	6	1200-1800	0.10-0.20	<75
LCZ 4	0.5-0.7	0.75-1.25	20-40	30-40	30-40	>25	7-8	1400-1800	0.12-0.25	<50
LCZ 5	0.5-0.8	0.30-0.75	20-40	30-50	20-40	10-25	5-6	1400-2000	0.12-0.25	<25
LCZ 6	0.6-0.9	0.30-0.75	20-40	20-50	30-60	03-10	5-6	1200-1800	0.12-0.25	<25
LCZ 7	0.2-0.5	1.00-2.00	60-90	<20	<30	02-04	4-5	800-1500	0.15-0.35	<35
LCZ 8	>0.70	0.10-0.30	30-50	40-50	<20	03-10	5	1200-1800	0.15-0.25	<50
LCZ 9	>0.80	0.10-0.25	10-20	<20	60-80	03-10	5-6	1000-1800	0.12-0.25	<10
LCZ 10	0.6-0.9	0.20-0.50	20-30	20-40	40-50	05-15	5-6	1000-2500	0.12-0.20	>300
LCZ A	<0.40	>1.00	<10	<10	>90	03-30	8	unknown	0.10-0.20	0
LCZ B	0.5-0.8	0.25-0.75	<10	<10	>90	03-15	5-6	1000-1800	0.15-0.25	0
LCZ C	0.7-0.9	0.25-1.00	<10	<10	>90	<20	4-5	700-1500	0.15-0.30	0
LCZ D	>0.90	<0.10	<10	<10	>90	<10	3-4	1200-1600	0.15-0.25	0
LCZ E	>0.90	<0.10	<10	<10	<10	<0.25	1-2	1200-2500	0.15-0.30	0
LCZ F	>0.90	<0.10	<10	<10	>90	<0.25	1-2	600-1400	0.20-0.35	0
LCZ G	>0.90	<0.10	<10	<10	>90	_	1	1500	0.02-0.10	0

The level 0 methodology proposed by the World Urban Database and Access Portal Tools (WUDAPT) (Bechtel *et al*., 2015) is used to map LCZs. WUDAPT level 0 method has already been developed and tested in Hamburg, Germany; Houston, USA and; Dublin, Ireland (Bechtel *et al*., 2015), medium-sized Central European cities (Geletic & Lehnert, 2016), and Wuhan and Hangzhou cities in China (Ren *et al*., 2016). It is based on the measurable physical properties of the environment and a clearly-defined decision-making algorithm. The algorithm derives from the basic physical parameters defined by Stewart and Oke in 2012 (building surface fraction, pervious surface fraction, impervious surface fraction, and height of roughness elements (Bechtel & Daneke, 2012).

The classification divides the urban landscape into 17 standard classes, ten urban (LCZ 1-10) and seven (LCZ A-F) natural zones (Bechtel & Daneke, 2012; See *et al*., 2015; Stewart & Oke, 2012). Oke and Stewart (Bechtel *et al*., 2015; Cai *et al*., 2016; Ren *et al*., 2016; Stewart & Oke, 2012) developed LCZ as an exhaustive climate-based characterisation of urban and rural sites that facilitated objective comparison of urban climates between cities using standard, routinely collected meteorological data. It emphasised the importance of intra-urban temperature comparison among different urban classes to analyse various urban morphology on local climate formation (Bechtel *et al*., 2015).

2.2.2 Urban Heat Island

Air temperatures in built-up urban areas are higher than those of their rural surroundings. This phenomenon, which is generally known as the UHI, is viewed as the most illustrative and recorded sign of climate modification in the current time of increasing urbanisation (Santamouris *et al*., 2007; Santamouris *et al*., 2017) as it is

expected that by 2050 about 70% of the worldwide populace will live in urban territories with a resulting even greater urban sprawl.

According to the World Bank, as documented in the Dynamics of Global Urban Expansion', more than 100,000 urban communities in developing nations are expected to triple their built-up zones by 2030. Even in developed nations, urban areas will expand by 2.5 times, notwithstanding their littler populace and a lower rate of populace development (Angel *et al*., 2005). As a result, future estimates indicate that average temperatures will continue to rise in most urban communities, mostly because of anthropogenic forcing (Weaner & Christopher, 2016).

UHI is a thermal inconsistency with horizontal, temporal, and vertical dimensions and may be observed in almost all types of built-up areas, and its characteristics appear to be related both to external influences (e.g.prevailing weather circumstances, climatic conditions, and seasons) as well as to the intrinsic nature of cities, e.g., land-use and land cover distribution, building size and density) (Bechtel *et al*., 2015; Bechtel *et al*., 2012; Connor *et al*., 2015; See *et al*., 2015; Stewart & Oke, 2012; Stewart *et al*., 2014a). While it is mostly a nocturnal phenomenon, it additionally occurs amid the daytime with a spatial and temporal pattern effectively controlled by the unique attributes of each urban zone (Bokva *et al*., 2014; Gulyás *et al*., 2006; Ragheb *et al*., 2016; Unger *et al*., 2014). It is typically developed during clear, calm nights and is ordinarily an after effect of the city's deferred cooling compared to surrounding rural areas (Ching *et al*., 2016; Stewart *et al*., 2014a; Stone & Rodgers, 2001).

The primary causes of the UHI are structural differences in thermal properties between the urban and rural environments, such as the thermal properties of the urban fabric and geometry, urban activities, and urban pollution (Bechtel *et al*., 2015; Gartland, 2012; Gartland, 2008; Ng, 2015; Warren, 2012). In particular, climatic parameters such as

cloud cover and wind speed have been reported to be essential factors in the development and intensity of the UHI, which appears to be more robust under a cloudless sky and light wind (Tzavali *et al*., 2015). Warmer urban temperatures could lead to human thermal discomfort, particularly at night during the heatwave period, increased energy consumptions, increased health risks, and increased mortality rate.

The UHI phenomenon may be quantified by the UHI Intensity (UHII), which is measured by the distinction between the highest sustained urban (built-up) air temperature and the background rural (natural cover) air temperature (Dobrovolný & Krahula, 2015; Parlow *et al*., 2014; Polydoros *et al*., 2018; Smoliak *et al*., 2015). The UHII variation relies on the geometry, size, density, population, and industrial advancement of the city; the surface materials (i.e., concrete, asphalt)and topography; the meteorological conditions, and; the general climate of the region (Bechtel *et al*., 2015; Bechtel & Daneke, 2012; Connor *et al*., 2015), and the industrial activities of urban areas that cause cities to maintain warmer temperatures than their rural surrounding. Three types of UHI are distinguished as follows:

The surface urban heat island (SUHI) refers to the measured infrared radiations (land surface temperatures) emitted and reflected by surfaces to identify possible hotspot locations in a city. On average, the difference in daytime surface temperatures between built-up and rural areas is 10°C to 15°C; the difference in nighttime surface temperatures is typically smaller, at 5°C to 10°C (Polydoros *et al*., 2018). The spatial extent and intensity of SUHI vary with seasons because of changes in the sun's intensity, ground cover, and weather. As a result of such variation, SUHI is typically the largest in the warm seasons (Zhou *et al*., 2014a; Zhou *et al*., 2014b).

Canopy layer heat island (CLUHI) is the canopy layer of air between the ground and treetops or roofs of buildings, where the most human activity occurs. CLUHI exists in

the air layer where people live, from the ground to below the tops of trees and roofs (Smoliak *et al*., 2015). Observations of the CLUHI are derived from air temperature measurements made within the layer of the atmosphere below the urban canopy layer. Such observations may be made using networks of either fixed stations or mobile traverses.

The boundary layer heat island (BLUHI) is located above the CLUHI. Both CLUHI and BLUHI are called ambient air temperature and start from the rooftop and treetop level and extend up to the point where urban landscapes no longer influence the atmosphere (Alexander Buyantuyev & Wu, 2010). This region typically extends beyond 1.5 km above the surface (Crawford & Christen, 2014). CLUHI and BLUHI are the two types of atmospheric UHI. CLUHI is the most commonly observed of the two types and is often referred to in discussions of UHI (Parlow *et al*., 2014). Atmospheric UHIs are often weak during the late morning and throughout the day and become more articulated after sunset due to the slow heat release from urban surfaces.

2.2.3 Urban vegetation and Human thermal comfort

One of the essential drivers of temperature increment in tropical urban communities is the absence of appropriate landscape treatment in urban green spaces (Warren, 2012), which leads to undesirable consequences such as increased thermal discomfort and potential for the urban populace (Briscoe, 2017). The warm solace of city occupants is directly (Abreu-harbich *et al*., 2012; Prasad *et al*., 2002; Abreu-Harbich *et al*., 2015) and indirectly (Stafoggia *et al*., 2008) influenced by UHI (Alavipanah *et al*., 2015). UHI's impacts aggravate social and environmental quality in cities, collectively contributing to global climate change challenges (Alavipanah *et al*., 2015).

While numerous factors contribute to UHI formation, this study focused on the vegetative cover because urban communities could straightforwardly address these

factors with available landscape design skills and technologies. In rural areas, open land and vegetation typically dominate the landscape. Plants adapt patterns to climate change, improve the microclimatic performance of the built environment and reduce energy consumptions through a blend of evapotranspiration and shading (Coutts *et al*., 2016; Fahmy *et al*., 2010; Oke, 2006) which thus may cause the diurnal patterns of cooler daytime temperatures and hotter evening time temperatures as a result of trapped heat and humidity within urban canopy layer whenever contrasted to the rapid nocturnal cooling of open natural areas (Coutts *et al*., 2016).

Conversely, urban regions are characterised by buildings and paved surfaces (impervious and dry surfaces, such as conventional roofs, sidewalks, roads, and parking lots) (Ali *et al*., 2017; Hashim & Hashim, 2016; Middel *et al*., 2014; Ren *et al*., 2016; See *et al*., 2015; Singh *et al*., 2017). The change in land cover brings about less shade and moisture to keep urban zones cool. Built-up areas evaporate less water, contributing to the raised surface and air temperatures (Golden, 2004). Hence, as a component of urban climate knowledge and optimisation of urban forms, vegetation is the essential element of the site and has to lie at the centre of any applied urban design methodology.

Human thermal comfort is subjective and is based on contextual parameters such as physiological and psychological acclimatisation to heat, air temperature, items of clothing worn, activity level, the temperature of the surrounding surfaces, airflow and relative humidity of the air as well as solar radiation (Shooshtarian & Ridley, 2017). Therefore, thermal comfort is unique to individuals, and it is impossible to define a type of thermal environment that meets everyone's requirements. Ambient temperatures must be neither too low nor too high to reduce individual vulnerability and maintain a comfortable thermal environment. However, it is possible to specify an acceptable temperature range for a high percentage of people, and this range is between 20°C and 27°C, with an optimal humidity rate of 35% to 60% (Shooshtarian & Ridley, 2017).

Body temperature, which is approximately 37°C, is kept by consuming calories from food and heat exchanges with the immediate surroundings according to the heat transmission mechanisms (Fabbri, 2015).

The thermal comfort in urban spaces is closely related to urban forestry. Vegetation has a significant ability to modify urban microclimate (Santamouris *et al*., 2017; Vieira De Abreu-Harbich *et al*., 2012, 2015; Zhao *et al*., 2017) by countering the urban heat island effects (Alavipanah *et al*., 2015; Masson *et al*., 2014; Mcpherson *et al*., 2016), resulting in improved thermal comfort (Abreu-harbich *et al*., 2012; Santamouris *et al*., 2017; Abreu-Harbich *et al*., 2015; Zhao *et al*., 2017) and the social cohesion and well-being of urban life (Alavipanah *et al*., 2015).

2.3 Conceptual framework

The theoretical framework that explains the adaptation of UHI using the concept of LCZs and environmental amelioration effects of diversity of plant species in Nairobi city was conceptualised, as illustrated in *Figure 2.3*. The conceptual framework in *Figure 2.4* illustrates the interrelationships in the study, the critical variables involved, and how they are interrelated. Urbanisation factors on urban microclimate lead to a higher temperature, lower wind speed, and relative humidity.

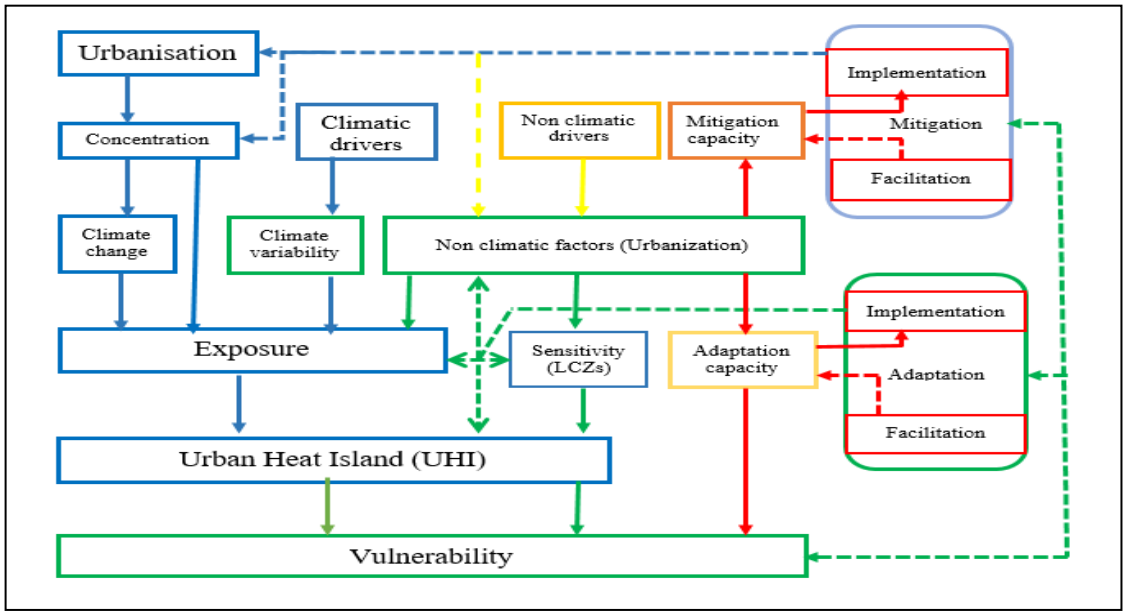

Figure 2.3: Conception framework. Source: own conceptualisation. (source:Author)

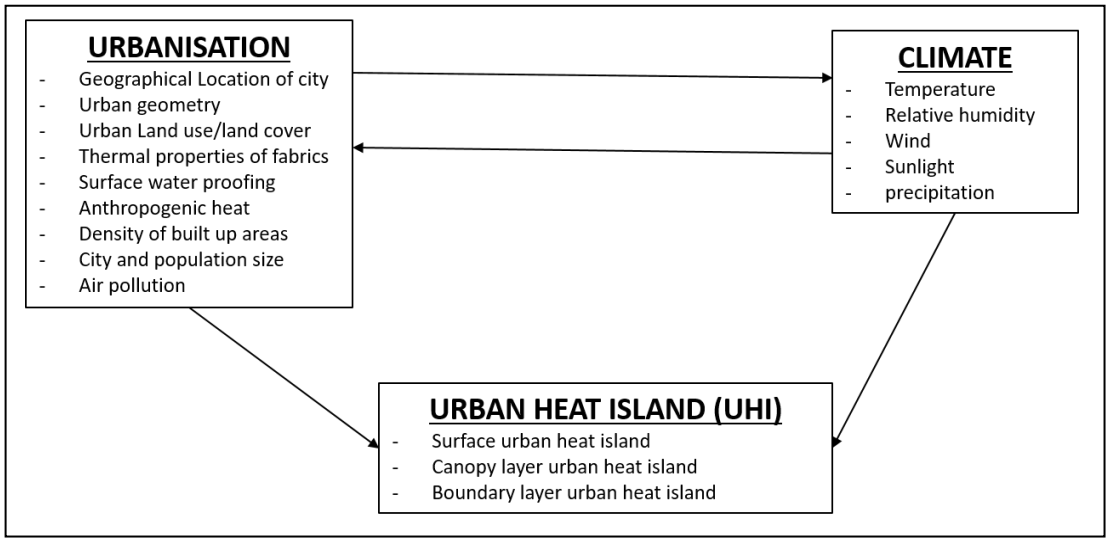

Figure 2.4: Interaction between urbanisation and climate factors. Source: own conceptualisation. (source:Author)

2.4 Critiques on the existing literature

This section includes a global critical review of the concept of LCZ classification in section 2.4.1, measurement and simulation of UHI phenomenon in section 2.4.2, case studies of UHI measurements in section 2.4.3, and measurements and simulations of the urban vegetation effects in section 2.4.4. The primary goal was to report and make sense of LCZs, UHI, and the role of urban vegetation as an adaptation strategy to UHI worldwide.

2.4.1 Local Climate Zone classifications

Steward and Oke (2012) developed LCZ to redefine and quantify the UHI effect. Each LCZ aims to have homogenous air temperature and is defined by qualitative and quantitative properties (Bechtel *et al*., 2015; Steward and Oke, 2012). Most recent studies investigating urban temperature fields utilise the LCZ classification and broadly support the correspondence of LCZs with air temperature fields in cities and their surroundings (Bechtel *et al*., 2015; Geletič & Lehnert, 2016; Lehnert & Geletiˇ, 2016; Lehnert *et al*., 2015; I. D. Stewart & Oke, 2012; Stewart, Oke, & Krayenhoff, 2014b). However, several authors working with LCZs had pointed out that the influence of thermal properties of local climate significantly varied concerning the geographical location of the zone, the size of the city, the position within the city, and relief (Bechtel *et al*., 2015; Bokwa *et al*., 2015).

One of the significant advantages of LCZ is the new perspective of UHI, looking into the temperature differentiation among LCZ classes rather than the traditional “urban” and “rural” classes. It emphasised the importance of intra-urban temperature comparison among different urban classes to analyse the influence of heterogeneous urban morphology on local climate formation (Bechtel *et al*., 2015). Existing knowledge of urban form (location, size, materials, and geometry), functions, and general

microclimates is not transferable among cities globally (Bechtel *et al*., 2015; Bechtel & Daneke, 2012; Connor *et al*., 2015). Therefore the concept of LCZs is designed to be universal, simple, and objective, which targets to be part of a global protocol to derive information about the form and function of cities with the help of free satellite images and free software of Google Earth (GE) and SAGA-GIS. LCZ has 17 standard types, including two subsets: 10 built types and 7 land cover types (Bechtel *et al*., 2015; Connor *et al*., 2015).

The LCZ classification scheme is, therefore, a valuable concept for integrating local climate knowledge into urban planning and design practices since it captures the internal structure and texture of cities to answer some crucial questions about the rapidly urbanising world (Bechtel *et al*., 2015; Connor *et al*., 2015). These include questions on the efficacy of urban-based adaptation and mitigation policies in response to climate change and whether actions in one jurisdiction are transferable. The data generated from the LCZ classification process could be applied to other studies involving weather and climate models (Brown, 2004; Geleti *et al*., 2016; Lehnert & Geletiˇ, 2016; Lelovics *et al*., 2014; Zhan *et al*., 2013); such as MUKLIMO_3 (Geleti *et al*., 2016), which require a detailed description of the urban landscape to simulate the urban effect on climate, urban planning, assessing the urban inequalities for better future climatic-spatial planning.

2.4.2 Measurement and Simulation of Urban Heat Island

The spatial and temporal variation of the UHI of local cities around the world has been studied frequently (Arnds *et al*., 2017; Arnfield, 2003) as a result of the new development of climate data sources and methodological approaches in recent years, which shifted urban climatology research from identifying UHIs and prediction of UHI

intensity to simulating for the exact patterns of the spatiotemporal variability of UHIs and temperature fields in urban environments.

Although many UHI studies are available, the results for tropical cities like Nairobi are still missing. Also, most UHI investigations have focused on atmospheric UHI, where the air temperature pattern in urban and rural areas are evaluated based on field measurements. These limited and isolated stationary networks cannot capture various thermal characteristics caused by land use and land cover (LULC) changes (Hu *et al*., 2016). As a result of these, earlier urban climate studies and their potential application(s) to inform policymakers in urban planning and management of land surface temperatures (LSTs) in a city like Nairobi is limited by the lack of systematic criteria for evaluation design and communication of UHI observations, inadequate quantification and irregular description of the city characteristics as they do not show the correlation between urbanisation and urban climate change in the city spatially.

During the current progress in exploring the complexity of the process driving the climate system, numerical models designed for application on the city scale have gradually been developed to provide more detailed and more accurate information about the spatiotemporal variability of canopy layer UHI (Bechtel *et al*., 2017; Ching *et al*., 2018, 2011; See *et al*., 2015). The present state of the art of numerical modelling makes it possible to solve the thermodynamics of the atmosphere and complex relations between variables, such as the buildings and vegetation types, on the scale of the urban environment (Bechtel *et al*., 2015; Bechtel & Daneke, 2012; Sun, 2013).

The thermodynamic version of the microscale urban climate MUKLIMO_3 model (*in German, Mikroskalige Urbane Klima Modell*) developed by Deutscher Wetterdienst (2014) is designed for urban climate studies, especially on issues of urban land use planning and the climatic effects of local land-use changes as well as for analysing the

climate of entire cities. MUKLIMO_3 model simulates and identifies Spatio-temporal variability of 2 m air temperature for a typical summer (warmest) day conditions a city and its surroundings. MUKLIMO_3 modelling applies the concept of topography and local climate zones (LCZs) to obtain representative spatial units for analyses of 2 m air temperature differences between various types of urban neighbourhoods (Alexander & Mills, 2014; Bokwa *et al*., 2015; Geletič *et al*., 2016). As a result of increased urban climate monitoring and adaptation, there is a need to expand knowledge of MUKLIMO_3 results to document the canopy UHI phenomenon for tropical cities like Nairobi, where such information is lacking. As a result, MUKLIMO_3 results can be used to assess human thermal stress utilizing the perceived temperature to inform city planners and policymakers to manage the heat load in the city.

MUKLIMO_3 considers the friction effects of building surfaces and turbulence generation due to airflow separation. A first-order closure scheme calculates turbulent fluxes of heat, moisture, and momentum (Hollosi & Zuvela-Aloise, 2017; Žuvela-Aloise, 2017; Žuvela-Aloise *et al*., 2016). Früh et al., 2011 described the numerical method for calculating short-wave irradiances at ground level, the walls, and the roofs of buildings in an environment with unresolved build-up (Geleti et al., 2016). The storage of heat within the urban fabric is simulated by calculation of the molecular heat fluxes from the outer wall surfaces into the urban fabric (or vice versa), which depend on the temperature gradient across the walls of the buildings and the predefined values of the heat transfer coefficient and the heat capacity of the walls (Früh et al., 2011).

The model also considers the effects of cloud cover on radiation. However, it does not include cloud processes, precipitation, horizontal runoff, or anthropogenic heat sources.

The vegetation in the canopy model has three vertical layers: tree crown, tree trunk, and low vegetation (Hollosi & Zuvela-aloise, 2017; Žuvela-Aloise et al., 2016).

MUKLIMO_3 was used to generate air temperature field development in the study area during the selected day. The model simulations were represented with 23 temperature maps with a resolution of 200 m; the time step between two successive modelled fields was 60 minutes.

2.4.3 Case studies of urban Heat Island Measurement

This section includes critical review sections on the UHI phenomenon in the USA, Asia, Europe, and Africa. Findings are discussed and synthesised into directions for research. Many studies on the UHI in the USA confirmed different trends in urban-rural temperatures (Hansen *et al*., 2001). From 1880-1999 the UHII in the USA was 0.65°C per century, while the mean decadal difference varied from 0.015 to 0.31°C (Liu *et al*., 2017). From 1951 to 2000, the mean decadal UHII decelerated slightly, varying from 0.05 to 0.19°C (Aguilar *et al*., 2005; Hansen *et al*., 2001; Peterson & Peterson, 2003). From 1901 to 1984, the UHI was connected strongly with the population and varied from 0.11-0.91°C (Stone, 2007).

In Arizona, the UHII was 0.072°C per year from 1920-1984 (Comrie & Comrie, 2000). While in Texas, the UHI trended by 0.3°C per decade for the period 1946-1990 (Brazel *et al*., 2000; Golden, 2004; King & Davis, 2007). In Minnesota, the mean UHII was 2.1°C from 1950 to1990 and varied from 0.5 to 1°C between 1967-1976. In Chicago, the UHII ranged from 2.34-2.68°C in 2010. It was shown that UHI is mainly a nighttime phenomenon (Coseo & Larsen, 2014).

Many studies have also been carried out for Asia, supporting the notion that the UHII was also linked to urbanisation. In China, the average UHI was 0.23°C (1954-1983) and seasonal with an intensity of 0.28-0.33°C in the spring and 0.06-0.10°C in the summer and autumn (Ching *et al*., 2016; Wang *et al*., 2001; Wang *et al*., 2018). The most prominent features of the UHI in China for 2003-2011 were geographic location, diurnal

difference, seasonality, and climate (Cai et al., 2011; Muhaisen, 2006; Zhang & Yao, 2009; Zhang *et al*., 2004). For 2001 the UHII was 4-6°C between Beijing and suburban areas and 8-10°C between the northwestern part of the city and its outer suburbs from evening to late night during the summer (Cai *et al*., 2011). Shanghai also had the characteristics of a heat island, especially in the summer of 1961- 1997 (Li *et al*., 2012; Zhou *et al*., 2014; Zhou *et al*., 2014).The UHI phenomenon was maximum during the summer and the spring and weaker during the winter for 1997-2008 with an intensity of over 0.8°C for 1997- 199 and stronger at night (Deng *et al*., 2003).

In Hangzhou (East China), the average temperature increased by 0.74°C for 2009 in the city centre because of high urbanisation with a maximum value of 1.6°C around sunset. In Suzhou, the maximum UHII varied from 0.1 to 2.2°C in the summer of 2007, with a mean value of 1.2°C (Zhang *et al*., 2011). In Hong Kong (China), the UHII was 1.5°C for 2002, with a maximum during summer (Giridharan *et al*., 2004; Ng & Cheng, 2012).

In Muscat (Oman), the maximum UHII was 2.4°C for 2008-2009, stronger at night than in the day and in the summer than in winter. During the summer, the UHII was 4.3°C during the night and 2.3°C during the day (Charabi & Bakhit, 2011).

Extensive UHI studies have been carried out in Europe. The UHI in London is a nighttime phenomenon, and the UHII varied from -4°C to 8°C from 1999 to 2000 (Koç *et al*., 2015; Kolokotroni *et al*., 2006; Kolokotroni & Giridharan, 2008; Tzavali *et al*., 2015). In Paris (France), the UHII was 8°C in 2003, mainly due to urbanisation at night, while an increase in street air temperatures of 0.5-2°C was attributed to air conditioning (Tzavali *et al*., 2015). In Palermo (Italy), the average UHII was 3°C during the night and 2°C during the day (2008) (Cellura *et al*., 2011). In Hamburg (Germany), the UHI was 0.6°C while the temperature increased by about 0.07°C per decade with the minimum temperature being 3°C higher in the summer from 1891 to 2007 (Schlünzen *et al*.,

2009). In Leipzig (Germany), the UHII varied by 2.9-3.1°C.The annual average warming difference in Istanbul (Turkey) increased by 0.17-0.39°C for 1957-1980 and 0.81-0.82°C for 1981- 2004, while Ankara had no warming trend (Ezber *et al*., 2007). The magnitude of UHI was increased over time and may be associated with increased energy consumption due to economic development (Chen *et al*., 2014; Chen *et al*., 2017). Finally, the UHI effect is virtually non-existent in the Netherlands. A large part of their territory is below sea level (Schwarz *et al*., 2012).

Turning to Kenya, in Nairobi, the cooling rates were -1.9°C from 1 hour before until 3 hours after the sunset, and the warming rates were 2.6°C 5-9 hours before sunset (2007). The most substantial cooling and warming rates were experienced during the dry-hot period of February-March (i.e., 2.6°C). In contrast, the lowest cooling and warming rates were experienced during July-August's cool-dry period (i.e., 1.7°C) (Makokha & Shisanya, 2010).

In general, several significant factors are influencing the UHI effect. The increased urbanisation (i.e., USA, Tucson, Phoenix, Delhi, Istanbul, Athens), industrialisation (i.e., Beijing, Singapore, Athens), buildings density (i.e., Beijing, Shanghai, Singapore, Bari), geometry, and construction materials (such as concrete and asphalt) caused an urban environmental deterioration, especially in summer when cities suffer from raised temperatures with direct effects on cooling energy consumption. The city location (i.e., Minneapolis, Muscat, Johannesburg, Melbourne, London, Vienna, Netherlands, and Moscow) plays a key role as cities with mountains prevent air circulation. So, topography conditions severely impact air temperature as warm air is provided over the city centre while the rough urban surface reduces horizontal airflow in the city. The anthropogenic heat release (transport, water heating, and cooling) determines how heat is absorbed, stored, released, and dispersed in the urban environment, expressed as a

temperature increase in the urban area. Therefore, the existing knowledge on urban climate change is not transferable is city-specific.

2.4.4 Urban vegetation effects on microclimate

A critical attribute of tropical cities is urban greenery in parks, gardens, along avenues, and residential areas and could be significant in developing adaptation possibilities against urban climate change effects (Abreu-Harbich *et al*., 2013). Various studies confirmed that trees could influence urban microclimate, improve human thermal comfort, and decrease the potential for health impairment of urban populations mainly because of distinct features of each species and planting strategies, especially in the tropics (Abreu-Harbich *et al*., 2013; Matzarakis, 2013).

Estimations carried out in the suburbs of Sacramento, in areas with mature trees, demonstrated that the air temperature under the tree foliage was 1.7 − 3.3◦C lower contrasted to zones where there were no trees (Bowler *et al*., 2010; Koç *et al*., 2015). In Miami, Florida, the average air temperature decrease amid summer was 3.6◦C in the shade of large trees (Gartland, 2008). Comparative research done in Sacramento and Phoenix demonstrated that a 25% increase in the number of trees could lower the temperature amid the mid-year by 3.3– 5.6◦C (Jaganmohan, Knapp, Buchmann, and Schwarz, 2016).

Jamei et al. (2006) examined three distinct species in various conditions (parks, gardens, and streets) and reported a decrease in temperature and an increase in relative humidity under the trees' foliage. The three distinct species analysed did not present statistically significant differences in the decrease of temperature and increase of relative humidity. Consequently, no association was found between the decrease of temperature and the allometric qualities of trees (tallness, the width of foliage, the thickness of the trunk, among others) (Jamei *et al*., 2016).

Acer saccharum and Juglans regia presented lower temperatures than Pinus radiata. Comparative outcomes when contrasting temperature and relative humidity of trees found in avenues and parks. They reported a higher relative humidity range from 27% to 33 %) under the trees and did not depend on tree species (Mcpherson *et al*., 2016). A study set up to look at how the road is influenced by the nearness of trees that give shade in Israel demonstrated that the solar radiation rates in the trees' shade were 10% lower than those in the open air. Measurements carried out in Tokyo's urban zones, around buildings at midday, demonstrated that the maximum variation in the average air temperature brought about by green zones was 0.47◦C (Szkordilisz & Kiss, 2015).

The shade cast by trees, and the amount of radiation filtered, is influenced by the form and density of the canopy, the density of the twigs, branches, leaf cover the individuality of trunks and leaves, which contributes to the overall characteristics of tree shape and density (Abreu-Harbich *et al*., 2012). Additionally, green coverage, leaf area index (LAI) (Abreu-Harbich *et al*., 2015), and other specific features of species (like size, shape, and colour of leaves, structure, and density of the treetop, tree age, and growth) (Abreu- Harbich *et al*., 2012; Bueno-Bartholomei & Labaki, 2003; Gulyás *et al*., 2006) which are critical arboreal characteristics could influence the ability of urban trees to reduce local air temperature, increase air humidity, reduce wind speed, and modify air pollutants (Streiling & Matzarakis, 2003). Tree canopies can modify microclimatic environments because of the reflection, transmission, and absorption of solar radiation and control wind speed (Abreu-Harbich *et al*., 2015). In tropical climates, the possibility of changing wind conditions and shade will modify the microclimate and improve human thermal comfort (Lin *et al*., 2010). Therefore, planting trees is a good solution for improving thermal comfort in tropical cities.

2.5 Summary

According to these studies, UHI is developed in areas with a high percentage of water-resistant, non-reflective surfaces and low vegetation. Materials such as stone, concrete, and asphalt trap heat at the surface, while the lack of vegetation reduces heat loss due to evapotranspiration. Also, anthropogenic heat and atmospheric pollutants contribute to increasing UHI intensity. The LCZs scheme, an international measurement protocol, was established to make comparative studies among UHI intensity measurements. The concept of LCZ classification uses remote sensing data with thermal infrared wavelengths to show both full spatial coverage and vertical variability of UHI. The LST is susceptible to changes in surface conditions and indicates much higher spatial and temporal variability than the air temperature. Although surface and air temperature heat islands are related, they are not the same, and care should be distinguished. Although the spatial structure of UHI is evident by satellite data, the value of ground-based measurements in the longitudinal study of UHI should not be underestimated. The dependence of UHI on geographical location, climate, and urban form and characteristics underscore the need for additional case study research that examines specific areas to (1) estimate the UHII with current data, (2) understand its dependence on some determining factors, and (3) target efficient adaptation measures such as those that conserve heating energy and reduce the cooling load. Such a study for the Nairobi metropolitan area will be described in the forthcoming chapters.

On the other hand, studies confirmed that trees could influence urban microclimate, improve human thermal comfort, and decrease the potential for health impairment of urban populations mainly because of distinct features of each species and planting strategies, especially in tropical cities. Urban trees can modify air temperature, increase air humidity, reduce wind speed, and modify air pollutants. Specific features of tree species, like structure and density of the treetop, size, shape, and colour of leaves, tree

age, and growth, can influence the performance of solar radiation attenuated by a canopy, air temperature, and air humidity. Therefore, planting trees is a good solution for improving thermal comfort in tropical cities.

2.6 Research Gaps

Contemporary measurements focusing on ambient temperature variability may not provide critical information about the spatial distribution of both LSTs and 2 m air temperature. Also, due to limited and isolated weather stationary networks, the studies cannot capture various thermal characteristics caused by land use and land cover (LULC) changes (Hu & Brunsell, 2015; Shen *et al*., 2016). The spatial and temporal variation of the UHI of local cities around the world has been studied frequently. However, the existing knowledge of urban climate change adaptation is not transferable because cities have unique sizes forms, functions, topographies, general climate, and meteorological conditions (Bechtel *et al*., 2015; Bechtel & Daneke, 2012; Connor *et al*., 2015) that results into differentiated UHI phenomenon. Also, different plant species' ability to create a microclimate that promotes human thermal comfort in tropical cities like Nairobi is not well understood. As a result of these, earlier urban climate studies and their potential application(s) to inform policymakers in urban planning and management of UHI in a city like Nairobi are limited by the lack of systematic criteria for evaluation design and communication of UHI observations, inadequate quantification and irregular description of the city characteristics as they do not show the correlation between urbanisation and urban climate change in the city spatially.

CHAPTER THREE
METHODOLOGY

3.1 Introduction

This chapter consists of the methodology for classifying LCZs and Simulation of UHI in Nairobi City in section and measurements and simulations of microclimate in Different Plant Species as an adaptation strategy to UHI in Nairobi city in section 3.2.

3.2 The Description of Study Area

The study focused on a tropical equatorial city, Nairobi ("city in the sun"), which is the largest (696 km^2) and the capital city in Kenya at a mean altitude of 1,684 meters above sea level (*Figure 3.1*).

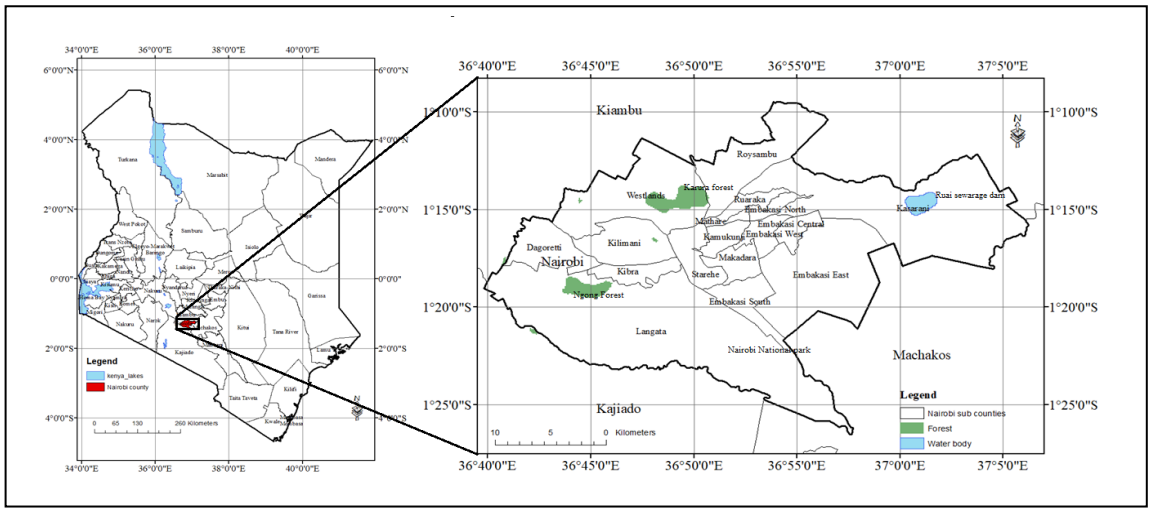

Figure *1*.1: The Location of Nairobi City.

The populace is the second-largest city in the African Great Lakes region after Dar es Salaam in Tanzania (Oyugi *et al*., 2017), with about 4,397,073 in the 2019 census. With functionalism as the main principle, Nairobi city has grown in concentric zones, reflecting the historical stages of its development with clearly-defined historical centres, residential buildings old and new, industrial areas, housing estates, modern shopping centres, malls, and allotments, resulting in a neighbourhood with irregular as well as regular (grid and radial grid), and various street plans for the city. However, the plans developed ever since 1927 up to the current Nairobi Integrated Urban Development Master Plan have never been fully realised. There is a highly polluted river (the Nairobi River) and a higher proportion of open vegetated (low plant) spaces. The landscapes beyond the city's boundaries are predominantly agricultural, with agricultural areas on the Western and sand and bare soils on the Eastern part. Patches of trees (LCZ B) and mixed forests (LCZ A) complete the landscape mosaics of the city.

3.3 Datasets

For this study, Google earth imagery was used to identify appropriate training sites. Bulk ordering of selected Landsat 8 images (Landsat paths 168 and row 61) from the USGS LandLook data store. The Landsat 8 image quality was 9, and the scene centre was latitude -1.4483^0E and longitude 37.0703^0S. Images were submitted to additional processing, such as atmospheric correction on the USGS science for changing world website. In total, six images of processed Landsat 8 data with a spatial resolution of 30m, with less than 10% cloud and haze cover (with clear sky and differentiated land use and land cover classes), were downloaded from the USGS Earth Explorer interface. Landsat-8 carries two instruments: an Operational Land Imager (OLI) sensor and a Thermal Infrared Sensor (TIRS). The OLI sensor has nine bands (Bands 1–7 and 9 at the 30-m resolution, panchromatic Band 8 at 15-m resolution), while TIRS has two bands (Bands 10 and 11, collected at the 100-m resolution and re-sampled to 30 m). To

interpret further analyses in this study, it is important to emphasise that all thermal images were recorded in the morning daylight hours (*Table 3.1*).

Table 3.1: Landsat 8 Scenes and climatic data (Atmospheric pressure, Air temperature, and relative humidity input values) used for LCZ and LST evaluation in Nairobi city. (Source: USGS science for changing world website)

Scene ID	Acquisition Date	Scene Time (UTC)	Earth-sun Distance	Solar Elevation Angle	Solar Azimuth Angle	Solar Zenith Angle	Atmospheric Pressure (Pa)	Air Temperature (C)	Relative Humidity (%)
LC81680612013159LGN01	8/6/2013	7:43:01	1.015	54.62	45.01	35.38	84.40	16.75	68.79
LC81680612014034LGN01	3/2/2014	7:44:01	0.986	56.58	118.55	33.42	84.50	21.50	56.40
LC81680612015005LGN01	5/1/2015	7:43:01	0.983	55.23	129.67	34.77	84.50	20.82	43.20
LC81680612016216LGN01	3/8/2016	7:43:01	1.015	56.09	55.07	33.91	84.63	20.53	51.32
LC81680612017362LGN00	28/12/2017	7:43:02	0.983	55.57	131.45	34.43	84.50	21.50	54.87
LC81680612018029LGN00	29/01/2018	7:43:00	0.985	55.93	120.79	34.07	85.54	22.11	39.63

3.4 Local climate zone (LCZ) Classification

The mapping procedure was carried out with the level 0 methodology proposed by the World Urban Database and Access Portal Tools (WUDAPT) *(*Bechtel *et al., 2015)* to generate the LCZ map at the city scale as follows. In part 1, Google Earth (GE) pro was used to establish the urban domain under study (Known as Region of interest, ROI) and to define areas within the domain that typified LCZ types (Stewart and Oke, 2012). In total, 319 training samples were collected saved in a kmz format. In part 2, Satellite data (Landsat 8) was acquired and processed with System for Automated Geoscientific Analysis (SAGA–GIS). The entire ROI was classified into LCZ types using the training areas provided in part one (Bechtel and Daneke, 2012), as illustrated in *Figure 3.2*.

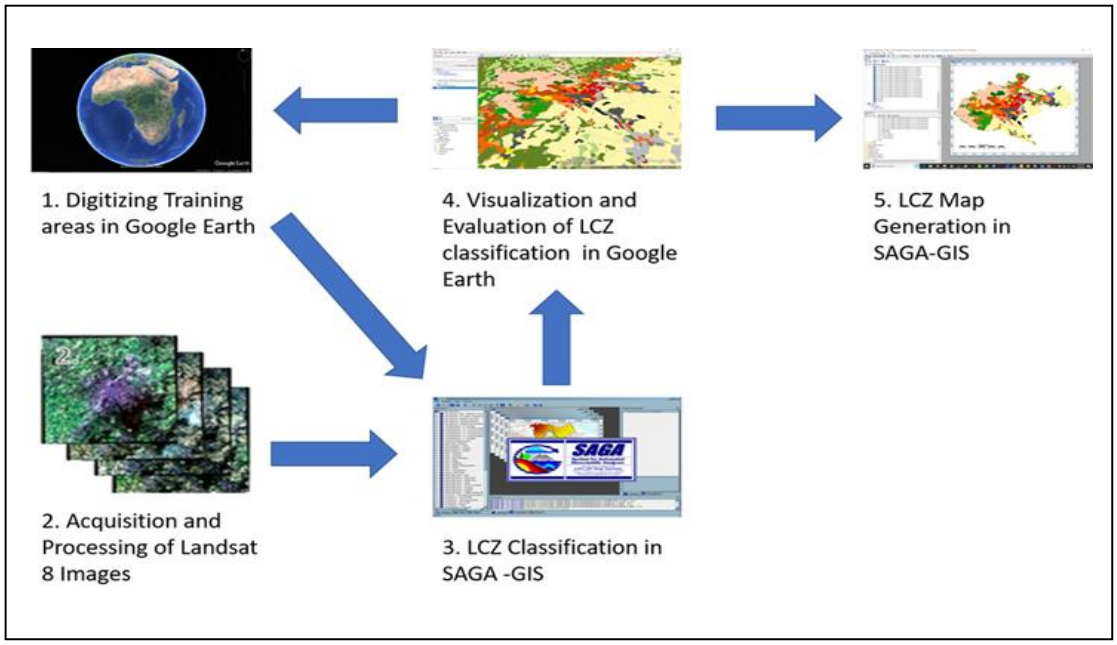

Figure 3.2. The workflow of WUDAPT level 0 methodology

The classification was conducted with the built-in random forest tree count of 128 trees and a majority post-filtering with a radius of 5 cells, which was based on the six Landsat 8 images and the training area polygons. The classifier calculated the most likely LCZ type and the probabilities for all LCZ classes for each 100 ×100 m pixel (Bechtel *et al*., 2015). The classification was conducted with the built-in random forest tree count of 128 trees and a majority post-filtering with a radius of 5 cells based on the Landsat images and the training area polygons. The classifier calculated the most likely LCZ type and the probabilities for all LCZ classes for each 100 ×100 m pixel (Bechtel *et al*., 2015) as shown in *Figure 3.3*.

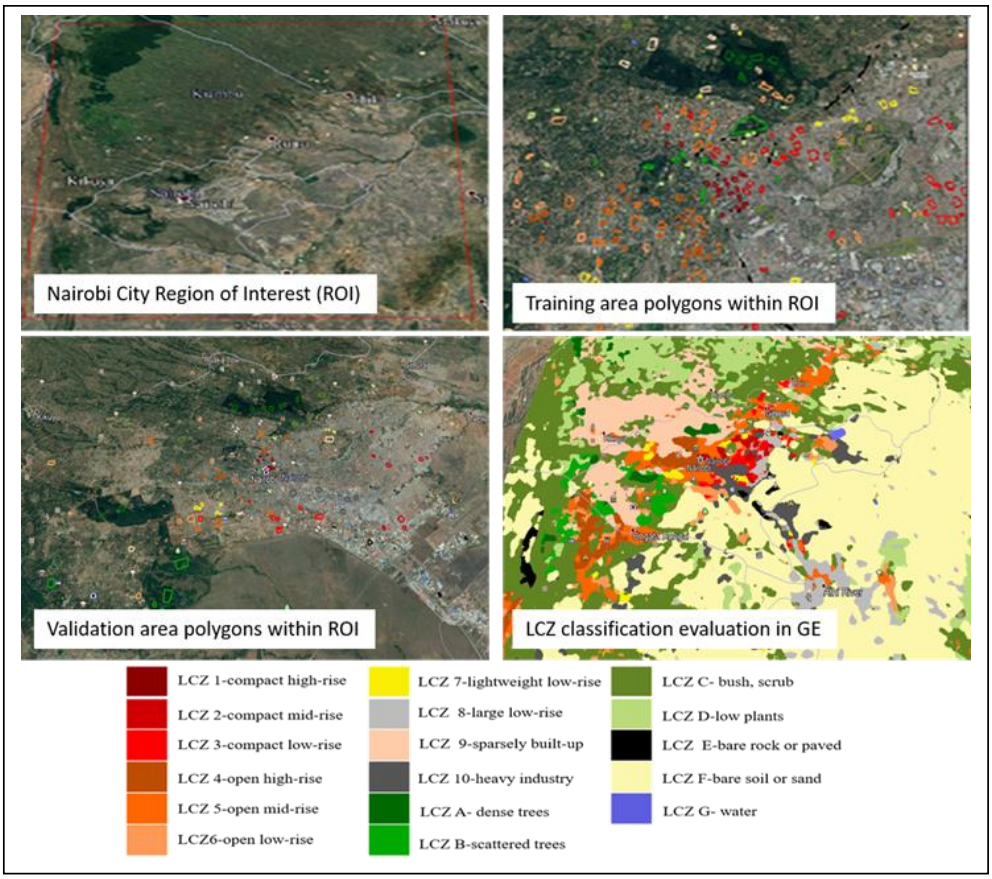

Figure 3.3: Location and visualisation of Region of interest, training samples, validation samples, and LCZ classification in Google Earth.

3.4.1 LCZ Classification Accuracy Assessment

An accuracy assessment was conducted to check the performance of the random forest classifier and the accuracy of the LCZ classification and to estimate the classification error. Since it was not feasible to check pixel by pixel whether or not the LCZ classification was correct, a new set of training samples for all LCZs has been randomly collected as reference data to estimate the classification error. The numbers of new samples of each LCZ class have been set at 0.5% of the number of each developed LCZ class (Ren *et al.*, 2016). An assessment that compared the developed LCZ classes with

reference data was used to estimate the classification error. The degree of confusion between the classification result and the ground truth was summarised in a confusion matrix (Ren *et al*., 2016).

3.4.2 Urban Morphological Properties for each LCZ Classes

To better understand these classes' accuracy in the WUDAPT Level 0 product, GIS files with the actual building height data for Nairobi were incorporated to show the spatial pattern of buildings based on height values of the LCZs. Urban surface land cover fractions were extracted for "urban LCZ types," since for the "non-urban LCZ types," it was possible to estimate the surface cover fractions using the table of the Local Climate Zones, modified from Stewart & Oke, 2012, table 3 and 4 (Bechtel *et al*., 2015; Bechtel *et al*., 2012; Bechtel *et al*., 2017; Bechtel & Daneke, 2012). Urban surface fractions were derived by launching an LCZ map in google earth pro and selecting an area of $1km^2$ for each LCZ, and then running a simple supervised classification in SAGA-GIS, according to surface cover categories (building, paved, trees, grass, soil/sand, water) *(Figure 3.4).*

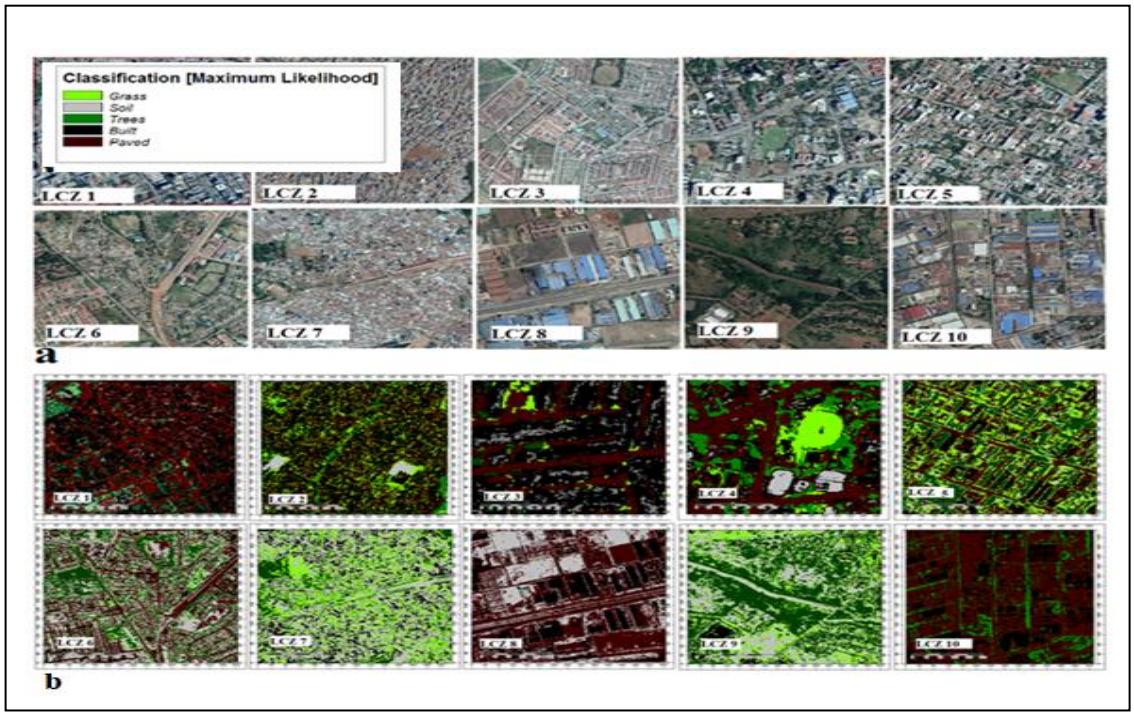

Figure 3.4: LCZ 1-10 for Nairobi city (approximately an area of 1km2 each). (b) Supervised classification for individual LCZs used for deriving surface fractions. Key: 1-compact high-rise, 2-compact mid-rise, 3-compact low-rise, 4-open high-rise, 5-open mid-rise, 6-open low-rise, 7-lightweight low-rise, 8-large low-rise 8-large low-rise, 9-sparsely built-up, 10-heavy industry.

All the ten urban LCZ types (Compact high-rise, compact mid-rise, compact low-rise, open high-rise, open mid-rise, open low-rise, lightweight low-rise, large low-rise, sparsely built, and Heavy industry) were present, so the process was done for each of them separately. The fractional coverage was computed by n/N, where n is the number of samples for each class, and N is the total number of samples. The albedo calculation inputs were Landsat bands that had been converted from digital numbers to surface reflectance. The modified Landsat formula developed by Liang (2000) and later normalised by Smith (2010) was used to calculate shortwave surface albedo, defined as the average reflectance of the sun's spectrum. These unitless quantity values ranged from 0 to 1.0 and varied based on the land cover type.

The formula was implemented in ARC-GIS using a raster calculator as:

((0.356*B2) + (0.130*B4) + (0.373*B5) + (0.085*B6) + (0.072*B7) -0.018) / 1.016) *(Equation 1).*

Where: B2 (blue band); B4 ((red band); B5 (near-infrared band); B6 (shortwave infrared 1 band); B7 (shortwave infrared 2 bands); 0.356 = Band 2 specific multiplicative rescaling factor from the metadata;0.130 = Band 4 specific multiplicative rescaling factor from the metadata; 0.373 = Band 5 specific multiplicative rescaling factor from the metadata; 0.085 = Band 6 specific multiplicative rescaling factor from the metadata: 0.072 = Band 7 specific multiplicative rescaling factor from the metadata and 1.016 = Sum of Band2, Band 4, Band5, Band 6 and Band 7 specific multiplicative rescaling factor from the metadata according to Landsat 8 bands (Smith, 2010). Output data for all the urban LCZ types were compared to Oke and Stewart, 2012 *Table 3*, which shows the quantifiable properties relating to surface structure, surface cover, and human activities *(Table 3.2).*

3.5 Land Surface Temperature Differences within Local Climate Zones

3.5.1 Land Surface Temperature

The LST_Landsat_8_split_window toolbox uses the split-window technique to estimate surface temperature from daytime Landsat -8 images (Danodia *et al*., 2017) for LST retrieval. The brightness temperature map of thermal bands (band 10, band 11), surface reflectance map of the red band (band 4), the normalized difference vegetation index (NDVI) map generated by surface reflectance data, water and cloud mask map, environmental parameters (air temperature, relative humidity, and atmospheric pressure)

and polygon map of Nairobi city were considered to explicitly to produce LST maps for Nairobi city, as conceptualised in *Figure 3.5* below.

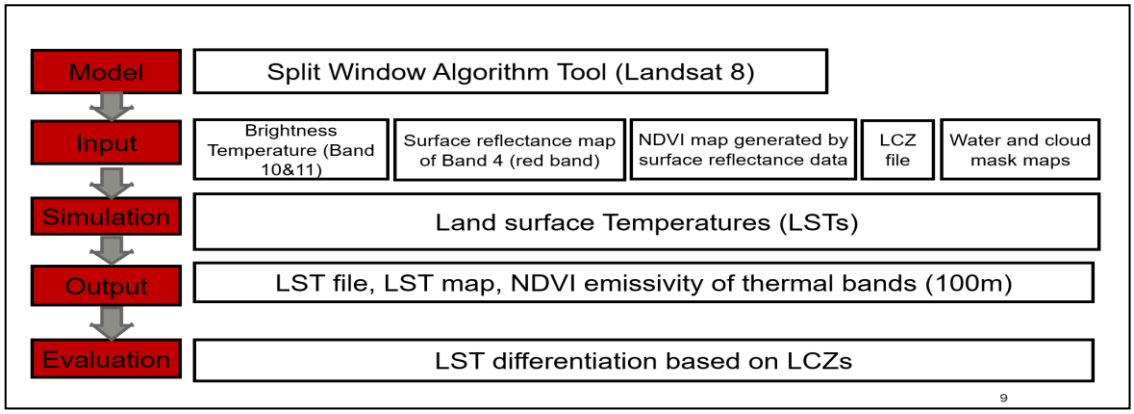

Figure 3.5: Conception framework of Land surface Temperatures (LSTs) estimation using Split Window Algorithm Tool. Source own conceptualization

The split window algorithm in the LST_Landsat_8_split_window toolbox removes the atmospheric effects and obtains the LST from the linear or nonlinear combination of brightness temperatures of two adjacent channels. In total, six Landsat images in six different years, as shown in *Table 1*, were used to retrieve and show spatial variations of the current LCZs and LSTs of the city on particular days that excluded extreme weather conditions.

3.5.2 Comparison of Land-Surface Temperatures in Local Climate Zones

To explore the application of LCZ mapping for surface urban heat island (SUHI) characterisation, the thermal analysis was based on the assumption that individual LCZs exhibited characteristic features typical of a given LST regime. LST fields were overlaid with LCZs, and typical LSTs were calculated for each zone. Boxplots were used to summarise the statistical distribution of LST within LCZs for all the Landsat 8 scenes examined. The t-test analysis was performed to examine the mean significant differences

between individual LCZs regarding LST in all the Landsat 8 scenes. For testing true difference (t-test), a null hypothesis for the one-way t-test ($p<0.05$) was that the actual difference in the means was equal to 0.

3.6 Simulation of Spatio-Temporal Variability of 2m Air Temperature

MUKLIMO_3 model was employed on the urban scale to simulate the 2 m air temperature field, relative humidity field, and wind field for Nairobi city and its surroundings on a three-dimensional (3D) model grid. The MUKLIMO_3 model provided the best radiation-driven climatic conditions characterised by an almost clear sky (Bokva *et al*., 2014; Hollosi & Zuvela-aloise, 2017) conceptualized in *Figure 3.6* below.

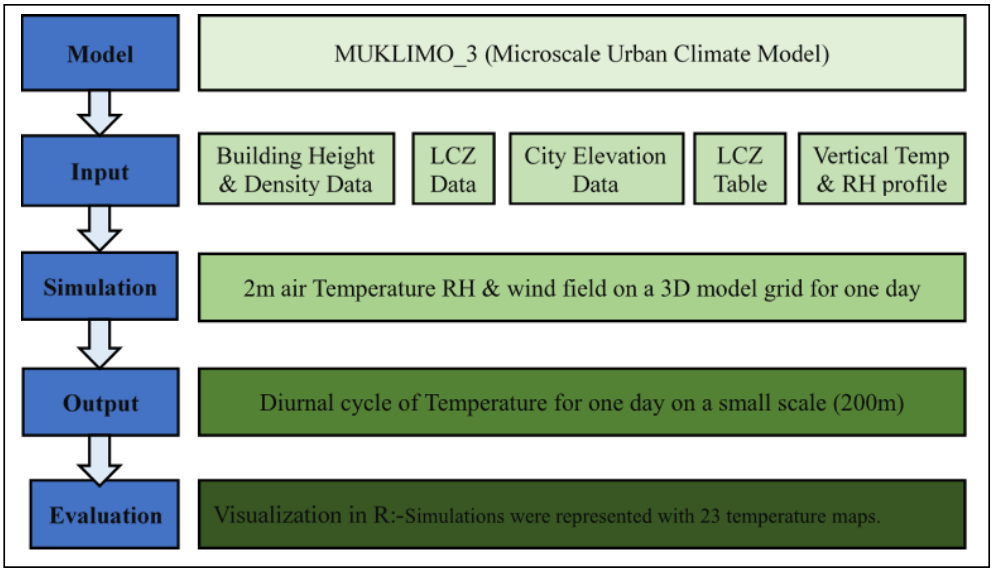

Figure 3.6: Conception framework of the MUKULIMO_3 model. Source own conceptualization

The 2 m air temperature fields for the potential warmest day (26th February 2018) condition was reproduced through idealized simulations of temperature, wind, and

relative humidity in Nairobi city based on the city's topography and LCZs data (Ochola *et al*., 2020) at a spatial resolution of 200 m. February 26, 2018, was considered in this study because it was a typical summer day, having recorded the hottest temperature with maximum thermal stress within the city. The model used LCZ data (Land use file) to describe the urban land use classes and unique thermal surfaces in Nairobi (*Figure 3.7*). Topographical data (elevation file) was used to describe the influence of city location and topology on the urban heat load within the city and its environment (*Figure 3.8*).

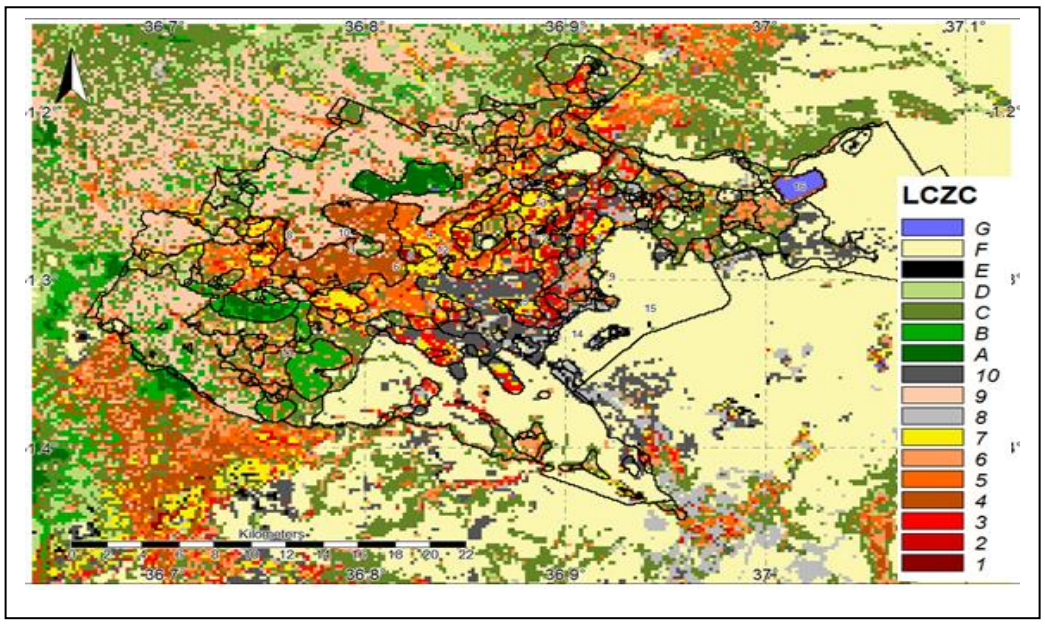

Figure 3.7: Spatial distribution of LCZs in Nairobi.Key: See Figure 3.3 for the scene ID explanation.

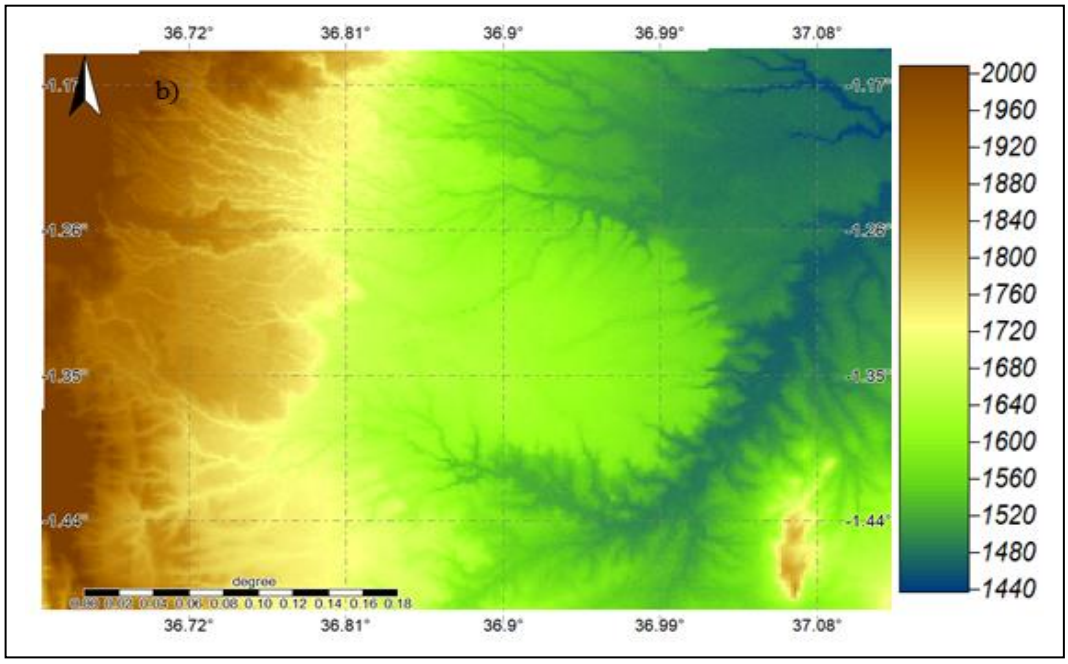

Figure 3.8: spatial distribution of topographic elevation (in metres) of Nairobi.

The five layers of meteorological data (air temperature, relative humidity, and speed of wind) in the vertical profile of the atmosphere (up to 3142 m above ground level) for the operation of the MUKLIMO_3 model was derived from the sounding data of 63741 HKNC Nairobi (Nairobi Dagoreti weather station located at latitude -1.300587^{o}E and longitude 36.759368^{o}S) observations at 00Z 28 February 2018 (*Table 3.2*).

Table 3.2: Vertical profile of the atmosphere shows various layers of temperature simulations in the Muklimo_3 model. (Source: Wyoming Weather Web - University of Wyoming).

Parameter/layers	**1**	**2**	**3**	**4**	**5**
Height above sea level (m)	1798	2106	2420	2920	3142
Temperature (^{O}C)	18.8	17.2	14.5	10.2	8.8
Relative Humidity (%)	56	68	77	95	92

One Dimension (1D) vertical atmospheric profile of time-varying atmospheric conditions (Temperature, relative humidity, and wind speed) at the Nairobi Dagoreti weather referent station was the initial boundary conditions. The 15-layered soil model and the 3-layered vegetation model were introduced (Bokva *et al*., 2014; Bokwa et al., 2015). LCZs defined land use classes according to the land use table (LU_Table), describing LCZ properties and urban structures characterized by a set of parameters for each LCZ class. The structural building properties inside a grid cell were depicted by three measurable parameters (Building fraction, Wall area index, Mean building height) to represent the interactions between the unresolved building structures and the environment (Bokwa *et al*., 2015).

MUKLIMO_3 model is a non-hydrostatic microscale model with z-coordinates (Geletič & Lehnert, 2016), which solves the Reynolds-averaged Navier-Stokes equations to simulate atmospheric flow fields in the presence of unresolved buildings (Früh et al., 2011). The model considered the friction impacts of building structures and turbulence generated because of wind stream separation to calculate turbulent fluxes of heat, moisture, and momentum (Hollosi & Zuvela-Aloise, 2017; Žuvela-Aloise, 2017; Žuvela-Aloise *et al*., 2016) at ground level, the walls and the roofs of buildings in a domain with unresolved build-up, is described in Früh et al., 2011 (Geleti *et al*., 2016). The model also considered the effects of cloud cover on radiation. However, it did not include cloud processes, precipitation, horizontal runoff, or anthropogenic heat sources. The vegetation in the canopy model has three vertical layers: tree crown, tree trunk, and low vegetation (Hollosi & Zuvela-Aloise, 2017; Žuvela-Aloise *et al*., 2016).

For the setup of the input parameters, the LCZ file was prepared according to the thresholds defined by Stewart and Oke (2012). Special attention was dedicated to the interactions between the buildings and the atmosphere. To account for the interaction between the atmosphere and the buildings, the structural properties of the buildings

within a grid cell were described by three statistical parameters: the building density, their wall area per grid volume, and their mean height (Bokwa *et al*., 2015) as shown in *(Table 3.3).*

For each LCZ class, a set of parameters were defined which described LCZ properties and urban structures: building fraction (γ_b), mean building height (h_b), wall area index (w_b), a fraction of pavement (v), a fraction of tree crown canopy (σ_t), a fraction of low vegetation (σ_c), tree height (h_t) and height of the low vegetation (h_c) surface albedo of materials (Alb). The fractions γ_b and σ_t are relative to the total grid cell area (1 km^2). The fraction v is relative to the area without buildings and trees, and σ_c is relative to the remaining surface.

Table 3.3: Parameters for Local Climate Zones in the MUKLIMO_3 model Key: 1-compact high-rise, 2-compact mid-rise, 3-compact low-rise, 4-open high-rise, 5-open mid-rise, 6-open low-rise,7-lightweight low-rise, 8-large low-rise 8-large low-rise, 9-sparsely built-up, 10-heavy industry, A- dense trees, B-scattered trees, C- bush, scrub, D-low plants, E-bare rock or paved, F-bare soil or sand; G- water.

LCZ	y_b	h_b	w_b	v	z_0	h_t	p_t	h_s	p_s	h_c	LAI_c	σ_t	σ_v	Alb
LCZ 1	0.50	80.0	29.25	0.35	0.20	0.00	0.00	0.00	0.00	0.50	1.00	0.08	0.70	0.11
LCZ 2	0.50	25.0	10.53	0.28	0.20	0.00	0.00	0.00	0.00	0.50	1.00	0.07	0.70	0.13
LCZ 3	0.49	10.0	4.49	0.25	0.20	0.00	0.00	0.00	0.00	0.50	1.00	0.08	0.70	0.15
LCZ 4	0.39	80.0	29.25	0.31	0.20	15.0	0.70	8.00	0.05	0.50	1.00	0.22	0.70	0.13
LCZ 5	0.30	25.0	10.53	0.31	0.20	15.0	0.70	8.00	0.05	0.50	1.00	0.27	0.70	0.14
LCZ 6	0.30	10.0	2.80	0.30	0.20	8.00	0.70	8.00	0.05	0.50	1.00	0.22	0.70	0.14
LCZ 7	0.90	4.00	1.50	0.05	0.20	0.00	0.00	0.00	0.00	0.50	1.00	0.01	0.70	0.14
LCZ 8	0.40	10.00	1.50	0.45	0.20	4.00	0.70	8.00	0.05	0.50	1.00	0.07	0.70	0.16
LCZ 9	0.12	8.50	2.88	0.25	0.20	4.00	0.70	8.00	0.05	0.50	1.00	0.41	0.70	0.13
LCZ 10	0.28	15.0	0.90	0.59	0.20	0.00	0.00	0.00	0.00	0.50	1.00	0.13	0.70	0.15
LCZ A	0.00	0.00	0.00	0.00	0.20	30.0	0.30	8.00	0.05	0.50	0.50	1.00	0.50	0.11
LCZ B	0.00	0.00	0.00	0.00	0.20	15.0	0.70	8.00	0.05	0.50	0.50	0.20	0.50	0.12
LCZ C	0.00	0.00	0.00	0.00	0.30	2.00	0.7.	8.00	0.05	0.50	1.50	0.20	0.90	0.14
LCZ D	0.00	0.00	0.00	0.02	0.30	0.30	0.00	0.00	0.00	0.30	1.50	0.20	0.80	0.16
LCZ E	0.00	0.00	0.00	0.95	0.03	0.00	0.00	0.00	0.00	0.20	0.50	0.00	0.40	0.17
LCZ F	0.00	0.00	0.00	0.00	0.10	0.00	0.00	0.00	0.00	0.30	1.00	0.00	0.90	0.15
LCZ G	0.00	0.00	0.00	-1.00	0.001	0.00	0.00	0.00	0.00	0.20	1.00	0.00	0.00	0.16

3.7 Measurements and Simulations of Environmental Amelioration effects of selected Plant Species on microclimate and human thermal comfort

Plant foliage thermal performance distinction and complex vegetation interaction with the built environment are challenging to achieve due to the problematic and transient criteria of the outdoor environment. The study involved actual measurements and computer simulations of the effects of different plant species and microclimate diversity.

3.7.1 Site description

The study was carried out on selected plant species in Uhuru Park and Central Park, geographically located at longitude 36.81667^{0}E, latitude -1.28333^{0}S, and altitude of 1,684 m above sea level *(Figure 3.9).* The two parks are the most popular recreational parks adjacent to the central business district of Nairobi, and they are also open to the general public.

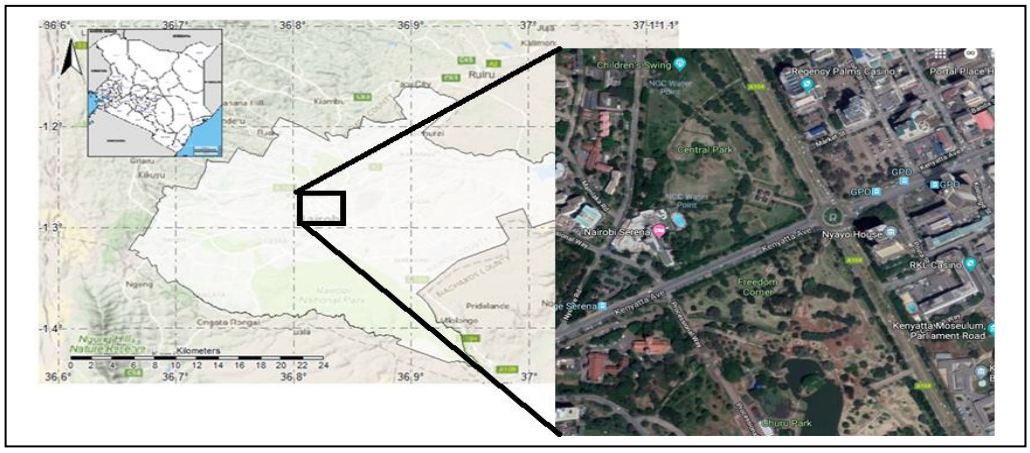

Figure 3.2: Location of Uhuru Park and central park

The climate is classified as lower Highland Tropical, with sub-humid woodland vegetation type. The city's climate favours the growth of trees. February is the hottest month in Nairobi, with an average temperature of 31°C, and the coldest is July at 17°C (Ongoma *et al*., 2016; Ongoma *et al*., 2013). The air temperature in both Uhuru and Central park during these days ranged between 22.5° C and 33.7°C, whereas the relative humidity ranged between 42.3% and 64.5%. Cloud condition was a mostly clear and partly cloudy sky.

3.7.2 Measurements and simulation of Microclimate in Different Plant Species

The microclimatic and instantaneous scales were adopted to allow analysing the *in-loco* degree of influence through mitigation of ambient temperature, globe temperature, relative humidity, infrared, and speed of wind on an individual of trees (Abreu-harbich *et al*., 2012; Abreu-Harbich *et al*., 2015). The choice of the species was based on the search of independently isolated mature plant species having different canopy sizes and shapes and plant height categories. All trees were physically described by measuring height, canopy diameter, branching length, canopy length, and crown width. The studied plant species *(Figure 3.10)* included: *Ficus benjamina* (weeping fig), *Ficus religiosa* (pippala tree), *Cassia spectabilis* (cassia, yellow shower), *Warburgia ugandensis* (East African greenheart), *Callistemon citrinus* (bottlebrush), *Bambusa vulgaris* (Bamboo), *Dypsis decaryi* (Triangle palm), *Terminalia mantaly* (Madagascar Almond), *Schinus molle* (Peruvian pepper) and *Pennisetum clandestinum* (Kikuyu grass).

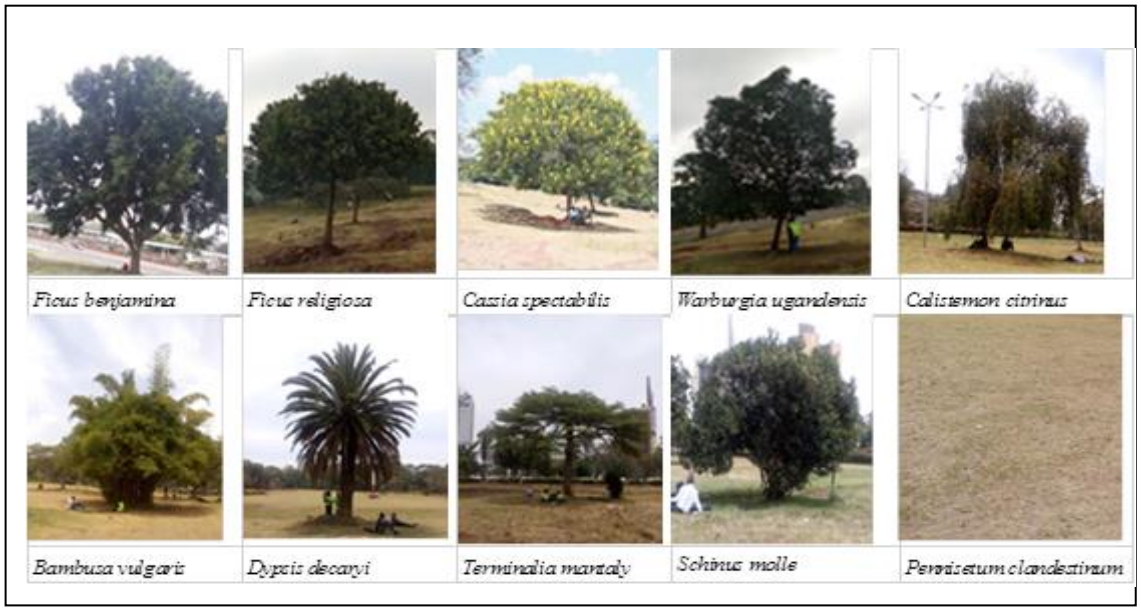

Figure 3.3: Single trees analysed.

Weather parameters were recorded every 10 minutes for 12 hours from 07.00 am to 7.00 pm in different distances (Trunk, 5m, and 10m) *(Figure 3.11)* of each of the selected plant species and the open (grass) (Abreu-harbich et al., 2012), from 16th to 28th February of the year 2017. Measurements in open (grass) were used as a control. Ambient temperatures (°C), globe temperature (°C), relative humidity (%), speed of wind (M/S), and infrared (◦C) were measured at the height of 1.1 m from the ground. In each set, there was one Wet Globe, Bulb Temperature (WGBT) recorder, model Testo 175-T2 for measurement of ambient temperature, Globe temperature, and relative humidity: One Testo 830-T1 Infrared thermometer for measurement of infrared, and one Testo 410-1 pocket-sized vane anemometer for measuring the speed of the wind. Continuous sky observation was done to record cloud conditions. Since measurements of microclimatic parameters were carried out on different days, measurements in the sun (open field covered by grass) were used as a normalisation parameter to quantify each plant species' attenuation effect.

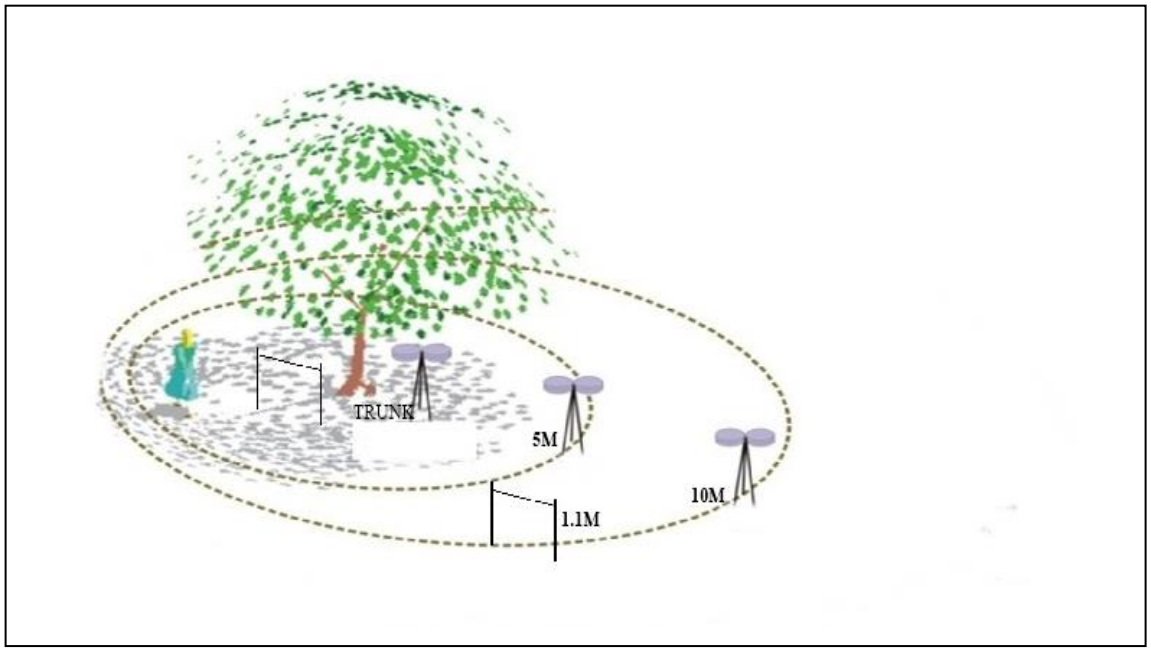

Figure 3.4: The location at which Environmental parameters are measured and the Intervals of the measurement points from the tree trunk.

The following expression (Lotufo Bueno-Bartholomei & Labaki, 2003) was used to calculate the relative variation of environmental parameters as influenced by the plant species:

$$RVtA = [(t_{Asun} - t_{Ashade})/t_{Asun}] \times 100\% \qquad \textbf{(Equation 2)}$$

Where:

RV_{tA} = relative variation of ambient temperature (%)

t_{Asun} = ambient temperature at the sun (ºC)

t_{Ashade} = ambient temperature under the canopy of the analysed tree (ºC)

Similar calculations were carried out for globe temperatures, infrared, and relative humidity (Lotufo Bueno-Bartholomei & Labaki, 2003).To calculate thermal comfort as influenced by the tree species due to specific bioclimatic conditions, thermal discomfort index (DI) as influenced by the tree species was calculated from temperature and relative humidity using the following expression:

$$DI = TEM - 0.55\,(1 - 0.01\,HUM)\,(TEM - 14.5)\ °C \quad \textbf{(Equation 3)}$$

Where:

DI = Discomfort Index DI (°C).

TEM = Air temperature (°C).

HUM = Relative humidity (%) (Georgi & Zafiriadis, 2006).

While the following equation calculated the reduction percentage of the discomfort index achieved in the shade of each tree species (Table 3.4:

$$dDI\% = [(DI_{sun} - DI_{shade})/DI_{sun}] \times 100\% \quad \textbf{(Equation 1)}$$

Where:

dDi=diviation in Discomfort index (%)

$DI_{sun=}$ Discomfort index in the sun (°C)

DI_{shade}=Discomfort index in the tree shade (°C) (Georgi & Zafiriadis, 2006).

Table 3.4: Discomfort index values (DI), in Degrees Celsius and discomfort feeling scale. (Source: Georgi & Zafiriadis, 2006).

	Discomfort Condition	**DI°C**
1	No discomfort	< 21
2	Discomfort expressed by < 50% of the population	21–24
3	Discomfort expressed by > 50% of the population	24–27
4	Discomfort expressed by the majority of the population	27–27
5	Discomfort expressed by all	29–32
6	Stages of medical alarm	> 32

The discomfort index in this study focused on comparing the index as influenced by the allometric properties of the tree species. Therefore, its use was not related to people's discomfort, but the percentage of discomfort reduction achieved as influenced by plant species (Georgi & Zafiriadis, 2006).

CHAPTER FOUR
RESULTS AND DISCUSSION

4.1 Introduction

This chapter presented results and discussions of modelling UHI and quantification of plant species' environmental amelioration effects as an adaptation strategy for Nairobi city in Kenya. The results and discussions of LCZ classification are captured in section 4.2, land surface temperature differentiation in section 4.3, Spatio-temporal variability of 2m air temperature distribution for Nairobi city MUKLIMO_3 Model in part 4.4, and attenuation effect of selected plant species on microclimate in section 4.5.

4.2 Local climate Zone classification

Using the WUDAPT methodology level 0 discussed in section 3.4, the Nairobi city area was classified into 17 LCZs for different years (*Table 3.1*) on particular days that excluded extreme weather conditions, based on processed (level 2) Landsat 8 images. There was an agreement between the spatial distribution patterns of the LCZ classes in all the six current LCZ maps generated. The details of the zones are presented in *Figure 4.1*.

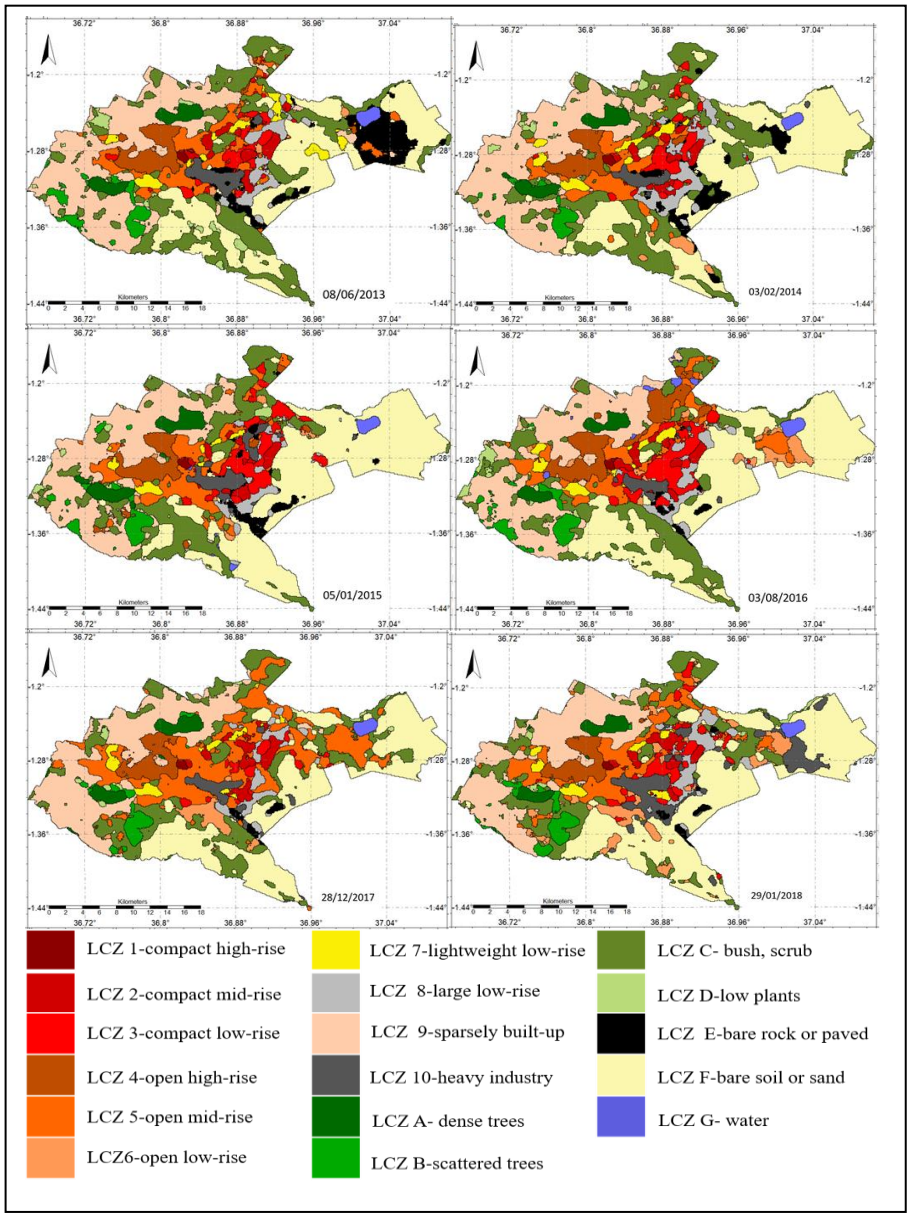

Figure 4.1: Spatial distribution of LCZs in Nairobi, based on Landsat 8 Images for different years with urban LCZ types (LCZ 1–10) and natural LCZ types (LCZ A–G).

The urbanised area (about 60%) was classified into LCZ 1-10, which potentially indicated a larger area of the apparent potential SUHI phenomenon of the city. The highest proportion (17.09%, 8.17%, 6.69%, and 5.12%) of the built-up areas (commercial and business, housing estates, residential, official, malls, and industrial buildings) belonged to LCZ 9 - Sparsely built (small or medium-sized residential buildings in a natural setting with an abundance of pervious land cover), LCZ 5 - open midrise (open arrangement of midrise buildings with 3-9 stories and abundance of pervious land cover mostly low plants and scattered trees), LCZ 10 - Heavy industry (low rise and mid-rise industrial structures and abundance of paved land cover with few on no trees), and LCZ 6 - open low-rise (open arrangement of low-rise buildings with 1-3 stories and abundance of pervious land cover mostly low plants and scattered trees), respectively.

The Central Business District (CBD) areas of Nairobi city, surrounded by the Uhuru Highway, Haile Selassie Avenue, Moi Avenue, and University Way was in the classes of LCZ 1(compact high rise) (about 0.2%) consisted of high rise density buildings with dense blocks in different heights and with different sky view factor of canyons which demonstrated that the central business centre could also form hot spot areas. Presence of LCZ 7 (Lightweight low-rise) mostly informal settlements (Kibera, Korogocho, Langata, Kangemi, Kawangware, Mathare, and Majengo slums) (about 2%) indicated high human vulnerability with adaptive capacity to urban climate impacts in Nairobi's informal settlement community.

The natural areas (about 40%) of Nairobi city belonged to land cover types LCZ A-G. Most natural areas such featureless landscapes of soil and sand with no plants in Syokimau and Mlolongo area, open arrangement of bushes, shrubs, and short woody trees mostly on bare soil or sand that cover most parts of Nairobi area, lightly wooded natural landscape Nairobi national park and areas around Ngong and Karura forests and

the heavily wooded natural landscape of Ngong and Karura forest, belonged to LCZ F - Bare soil or sand (28.31%), LCZ C -bush, scrub (15.21%) and LCZ B - scattered trees (2.44%) and LCZ A - Dense trees (2.02%) respectively. About 50.26% of the Nairobi area was built up, while about 49.74% was natural. There were limited dense trees (LCZ A) in Nairobi city, located on the outskirts (Karura and Ngong forests) of both the central business centre and residential areas (*Figure 4.2*).

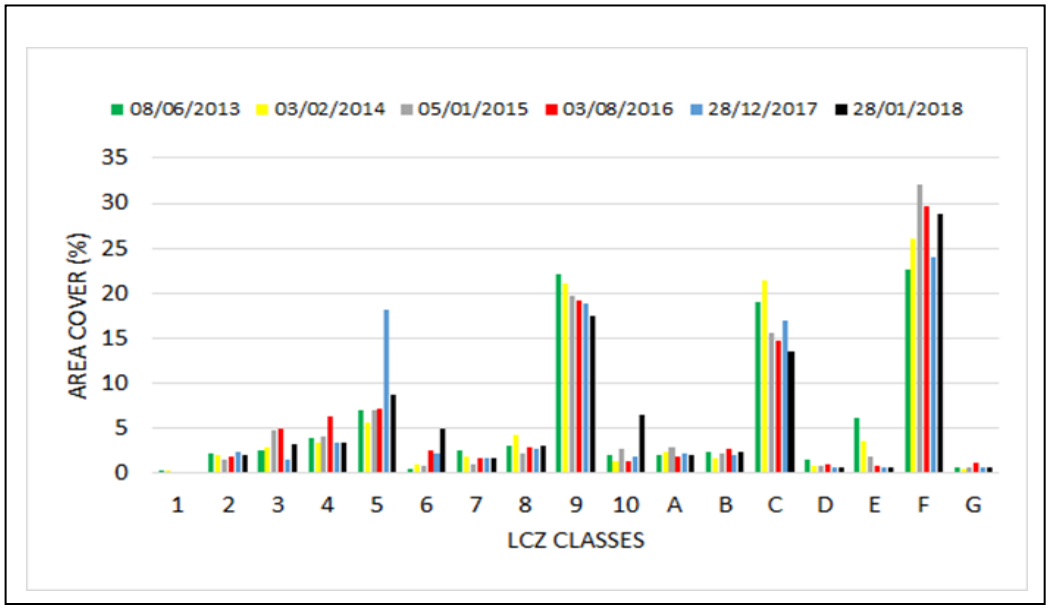

Figure 4.2: Percentage of the land cover of LCZs in Nairobi, based on Landsat 8 images. See Figure 4.1 for the scene ID explanation.

LCZ trend was similar in all the images evaluated. However, analysis of patterns was not possible since scenes were acquired in different seasons and years. The spatial distribution of urban morphological properties has approximately the same agreement with the vectorised LCZ boundaries, as seen in *Figures 4.1* and *Table 4.1*.

Table 4.1: Comparison of urban surface fractions for urban-type LCZ classes for Nairobi city and Stewart & Oke, 2012 table 1: The ratio of building plan area to total plan area (%); 2: The ratio of impervious plan area (paved, rock) to total plan area (%); 3: The ratio of pervious plan area (bare soil, vegetation, water) to total plan area (%).

LCZ	Level 1 Data Experiment				Stewart & Oke 2012			
	1 (λb)	2 (λI)	3 (λp)	Albedo	1 (λb)	2 (λI)	3 (λp)	Albedo
LCZ 1	0.5	0.35	0.15	0.11	0.4-0.6	0.4-0.6	<0.10	0.10-0.20
LCZ 2	0.5	0.28	0.22	0.13	0.4-0.7	0.3-0.5	<0.20	0.10-2.20
LCZ 3	0.49	0.28	0.23	0.15	0.4-0.7	0.2-0.5	<0.30	0.10-0.20
LCZ 4	0.39	0.31	0.3	0.13	0.2-0.4	0.3-0.5	0.3-0.4	0.12-0.25
LCZ 5	0.3	0.31	0.35	0.14	0.2-0.4	0.1-0.5	0.2-0.4	0.12-0.25
LCZ 6	0.3	0.3	0.4	0.14	0.2-0.4	0.2-0.5	0.3-0.6	0.12-0.25
LCZ 7	0.9	0.05	0.05	0.14	0.6-0.9	<0.20	<0.30	0.15-0.35
LCZ 8	0.4	0.45	0.15	0.16	0.3-0.5	0.4-0.5	<0.20	0.15-0.25
LCZ 9	0.12	0.25	0.63	0.13	0.1-0.2	<0.20	0.6-0.8	0.12-0.25
LCZ 10	0.28	0.59	0.13	0.15	0.2-0.3	0.2-0.4	0.4-0.5	0.12.0.20
LCZ A	0	0	1	0.11	<0.10	<0.10	>0.90	0.10-0.20
LCZ B	0	0	1	0.12	<0.10	<0.10	>0.90	0.15-0.25
LCZ C	0	0	1	0.14	<0.10	<0.10	>0.90	0.15-0.30
LCZ D	0	0.02	0.98	0.16	<0.10	>0.90	>0.90	0.15-0.25
LCZ E	0	0.95	0.05	0.17	>0.90	<0.10	<0.10	0.15-0.30
LCZ F	0	0	1	0.15	<0.10	>0.90	>0.90	0.20-0.35
LCZ G	0	-1	1	0.16	<0.10	<0.10	>0.90	0.02-0.10

The overall accuracy was 98.17%, and the Kappa Coefficient was 98.0 %. The accuracy assessment demonstrated satisfying results for the WUDAPT level 0 classification. The confusion matrix also indicates that all the LCZs classification a relatively higher accuracy of over 90% for Nairobi city. The misclassification was mainly in built-up types LCZs 2, 6, 8, 9 & 10 (compact midrise, open low rise, large low-rise sparsely built, and heavy industry) and land cover types LCZs B, C&G (scattered trees, bush, and water) respectively (*Table 4.2*).

Table 4.2 Confusion Matrix of LCZ Map in Nairobi City.

LCZ CLASS	LCZ 1	LCZ 2	LCZ 3	LCZ 4	LCZ 5	LCZ 6	LCZ 7	LCZ 8	LCZ 9	LCZ 10	LCZ A	LCZ B	LCZ C	LCZ D	LCZ E	LCZ F	LCZ G	Number of Predicted Pixels	User' Accuracy (%)
LCZ 1	14	0	0	0	0	0	0	0	0	0	0	0	0	0	0	0	0	14	100
LCZ 2	0	32	0	0	0	0	0	0	0	2	0	0	0	0	0	0	0	34	94.1
LCZ 3	0	0	42	0	0	0	0	0	0	0	0	0	0	0	0	0	0	42	100
LCZ 4	0	0	0	44	0	0	0	0	0	0	0	0	0	0	0	0	0	44	100
LCZ 5	0	0	0	0	40	0	0	0	0	0	0	0	0	0	0	0	0	40	100
LCZ 6	0	0	0	0	1	52	0	0	0	0	0	0	0	0	0	0	0	53	98.1
LCZ 7	0	0	0	0	0	0	13	0	0	0	0	0	0	0	0	0	0	13	100
LCZ 8	0	0	0	0	0	0	0	80	0	0	0	0	0	0	1	0	0	81	98.8
LCZ 9	0	0	0	0	0	0	1	0	103	0	0	0	0	0	0	0	0	104	99
LCZ 10	0	0	5	0	0	0	0	0	0	48	0	0	0	0	2	0	0	55	87.3
LCZ A	0	0	0	0	0	0	0	0	0	0	54	0	0	0	0	0	0	54	100
LCZ B	0	0	0	0	0	0	0	0	0	0	0	83	0	0	0	0	4	87	95.4
LCZ C	0	0	0	1	0	0	0	0	0	0	0	0	130	0	0	0	2	133	97.7
LCZ D	0	0	0	0	0	0	0	0	0	0	0	0	0	177	0	0	0	177	100
LCZ E	0	0	0	0	0	0	0	0	0	0	0	0	0	0	7	0	0	7	100
LCZ F	0	0	0	0	0	0	0	0	0	0	0	0	0	0	0	112	0	112	100
LCZ G	0	0	0	0	0	0	0	0	0	0	0	0	0	0	1	0	44	45	97.8
Number of Actual pixels	14	32	47	45	41	52	14	80	103	50	54	83	130	177	11	112	50		
Producer's Accuracy (%)	100	100	89	98	98	100	93	100	100	96	100	100	100	100	63.6	100	88		
Overall Accuracy (%)	98																		
Kapa Coefficient	0.98																		

The results of building fractions, impervious fractions, pervious fractions. Building heights and albedo of materials *Table 4.1* showed a similar trend as Stewart & Oke, 2012, *Table 3 and 4* (Bechtel *et al*., 2015b; Stewart & Oke, 2012). It was found that all the LCZs were accurately detected and classified. The WUDAPT Level 0 data is coarse but provides comprehensive and consistent coverage for Nairobi city. These data described the urban landscape regarding neighbourhood-scale using the LCZ scheme as spatial units (Bechtel *et al*., 2015; Bechtel & Daneke, 2012; Stewart & Oke, 2012) using available multi-spectral satellite imagery (Landsat8) and free SAGA and Google Earth software. Nairobi city urban domain was categorised into 10 urban and 7 natural surface cover types. Each LCZ type was described regarding each in ground-based and aerial photographs' typical appearance and was linked to some urban parameter values.

The LCZ classification result of Nairobi city is more reliable and accurate due to the Landsat 8 scenes with less than 10% cloud cover, acquired immediately after the rainy seasons in the Nairobi area that eliminated the solar and atmosphere influence. However, the miscalculation in classification could have occurred due to limited information provided by the buildings and vegetation in the Landsat images. The Google Earth image was regarded as the reference data in this study, accurate enough to reflect the true land cover to validate the classification result. It is important to note that, since Nairobi metropolitan is experiencing fast urbanisation, the land cover and built-up types of cities are complex. They have their unique urban morphology characteristics as indicated by the LCZ map, which implies the potentially high UHI intensity and poor thermal environment.

Availability of LCZs for Nairobi could open opportunities for domestic and global inter and intra LCZ comparisons between cities to ensure comprehensive planning and compilation of feasible urban plans. Moreover, the study offers the meaning of the term urban on a measurable basis defined as a ‘Local Climate Zone’ for standardised

assessments to gain further insight into the interweaving dynamism of urban morphology of Nairobi city.

4.3 Land Surface Temperature Estimation

The six Landsat 8 images showed a similar spatial distribution of surface temperatures that agreed with the vectorised LCZ boundaries. LST patterns were sensitive to building densities and heights, land cover types, and surface wetness. Dry and natural zones were more thermally responsive (over 45^{o}C) than wet and built-up zones with vegetation (30^{o}C - 40^{o}C). In built-up zones of the city, warmer LSTs (about 45^{o}C) were very often associated with heavy industry, compact buildings, lightweight low-rise (slums), large low-rise buildings, and paved areas (which are quite extensive). Natural LCZs with water bodies, dense trees, and sparsely built classes were associated with low LSTs (less than 30^{o}C) regardless of whether they lay in the core of the city or the countryside. Away from the densely built-up areas, the warm parts (about 58^{o}C) of the cities also occurred near large patches of relatively flat, pervious surfaces (bare soil and sand) in the eastern part of Nairobi, which is lying in semi-arid areas of Nairobi. In contrast, low LSTs (about 22^{o}C) occurred at the northern, western, and southwestern Nairobi, where the forestry areas prevailed. The coolest LST (22^{o}C) was also correspondent with the water body coverage (e.g., Ruai sewerage treatment dams) (*Figure 4.3*).

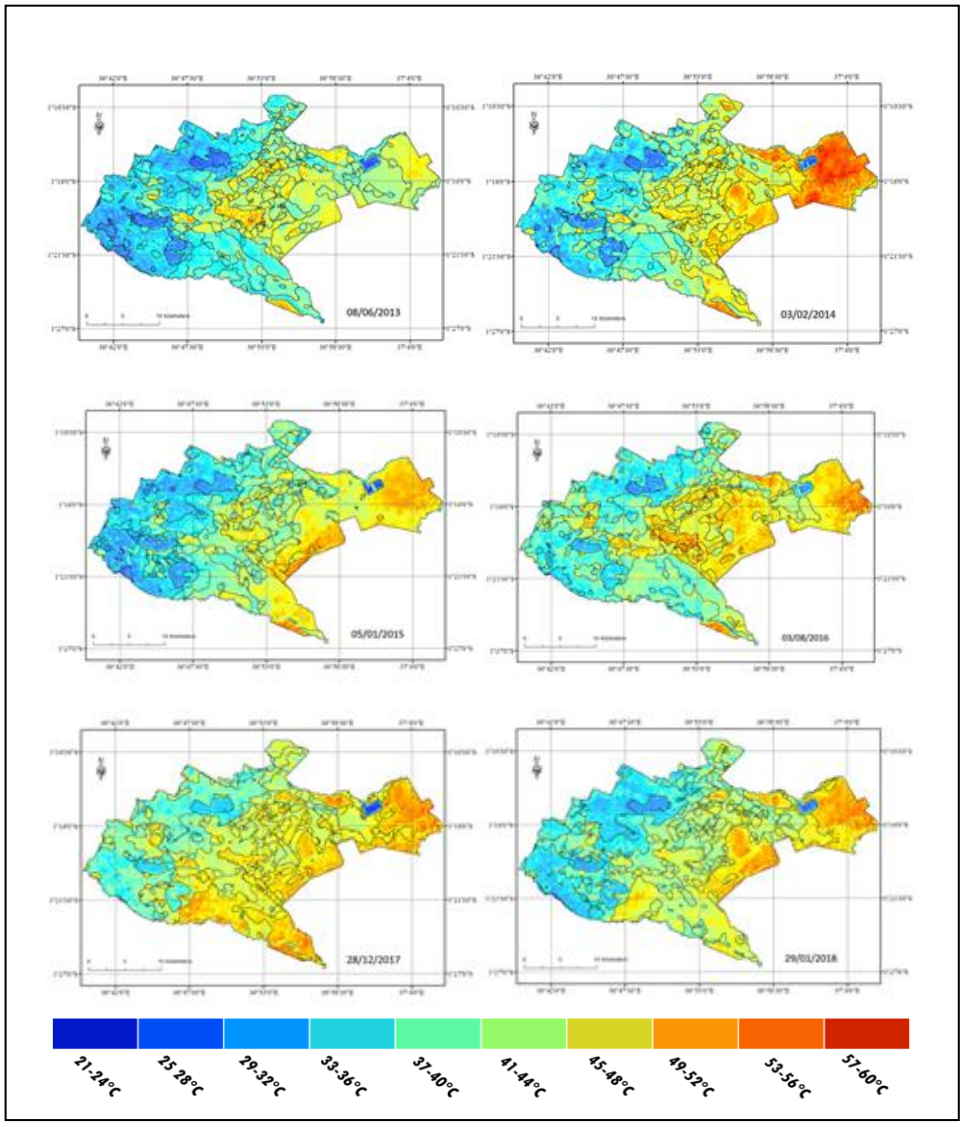

Figure 4.3: Spatial distribution and Variability of LST in Nairobi City based on Landsat 8 images for different years. See table 3.1 and figure 4.1.

4.3.1 Local climate zones and Land Surface Temperature

The spatial distributions of LCZs and LSTs indicated that there was a positive degree of correspondence. Therefore, further investigations were performed to assess their relations. Box plots exploring typical LSTs for individual LCZs showed relatively consistent results for all the six Landsat 8 images considered in this study (*Figure 4.3*).

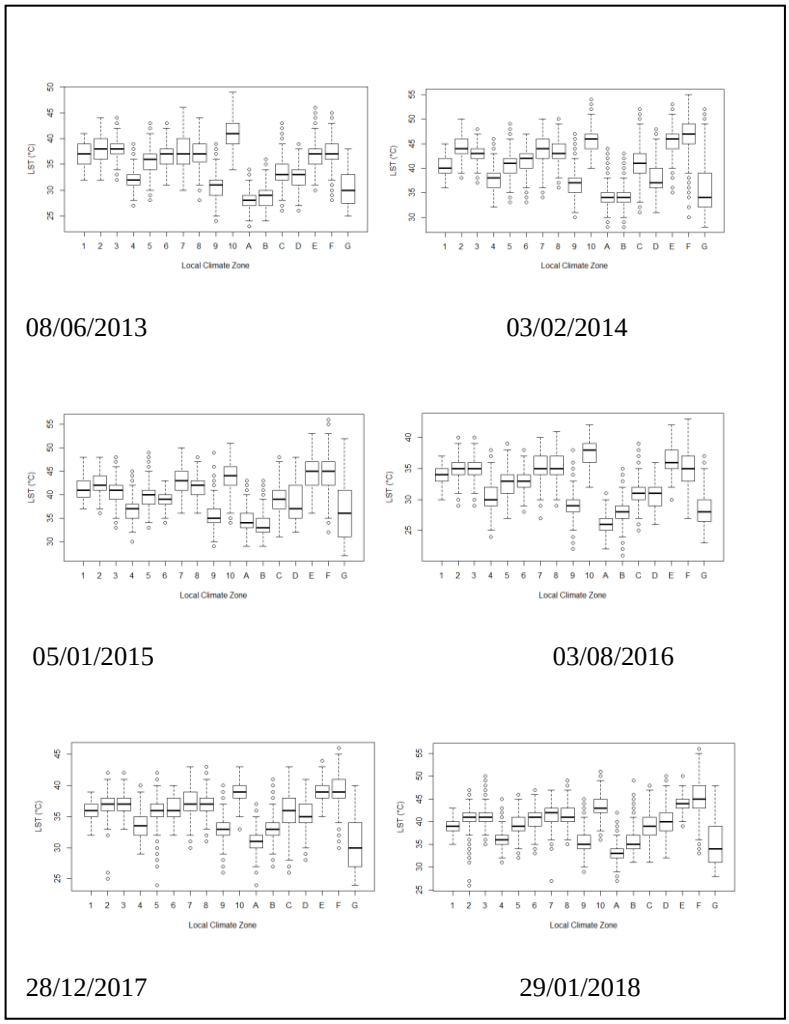

Figure 4.2: Boxplots with LSTs in LCZ classes for Nairobi city based on Landsat 8 images for different years with urban LCZ types (LCZ 1–10) and natural LCZ types (LCZ A–G). The line within the box indicates the median. The bottom of the box is the first quartile; black boxes crosses indicate outliers.

The LSTs for individual LCZs could not be further compared directly across the different Landsat 8 images. They represented different days of the years spanning from June 2013 to January 2018 (see *Table 4.1*). Particular LSTs differences arose from

dynamic factors such as land cover change and the synoptic situation on a given day. The statistical summary indicated considerable differences among LCZs regarding the mean LSTs of each six Landsat 8 images. LSTs at LCZs 1-10 “built-up cover” types were generally higher than LCZs A-G “natural” cover types for the entire city.

Regarding the LST variation among LCZs with contrasting urban morphology, LCZ 10 (Heavy industry), which is characterised with low rise and midrise (metal, steel, and concrete) structures with few or no plants and land cover that is mostly paved and hard parked demonstrated the highest mean LST variation in all the six Landsat 8 images compared to other built-up LCZs. It was followed by LCZ 3 (dense mix of low-rise buildings) and LCZ 2 (compact mid-rise buildings) as the second- and third-warmest LCZs. Additionally, higher mean LSTs were also associated with LCZ 8 (large low-rise) and LCZ 7 (lightweight, low rise), mostly slum or surrounded by slum areas whose residents are most vulnerable to the effect of urban climate change. The coolest built-up type LCZ was LCZ 9 (sparsely built with sparse arrangement of small or medium-sized buildings in natural setting and abundance of a pervious land cover comprising of both low plants and scattered trees) and LCZ 4 (open high-rise buildings with an abundance of pervious land cover constituting of both low plants and scattered trees), due to the vegetation cooling effect.

Regarding the LST variation among natural LCZ types, LCZ A (dense trees in a pervious land cover of low plants) and LCZ G (large open water bodies) demonstrated the lowest mean LSTs. This was followed by LCZ B (scattered trees and pervious land cover of low plants), LCZ C (open arrangements of bushes, scrubs, and short woody trees with pervious land cover that is made up of bare soil or sand), and LCZ D (low plants mostly featureless landscape of grass or herbaceous plants, or crops with few or no trees). The natural LCZs functioned as natural forests, tree cultivations, urban parks,

natural scabland, grassland or. Generally, water bodies and forested areas recorded the lowest mean LSTs in all the six Landsat 8 images (*Figure 4.4*).

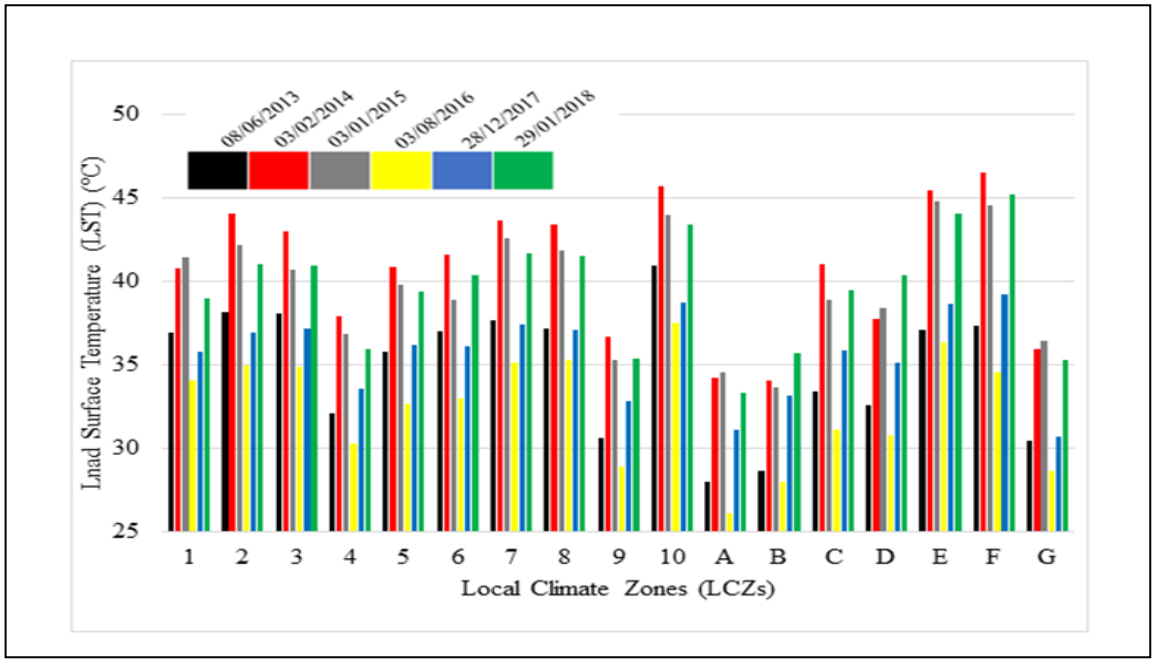

Figure 4.3: Mean LST distribution of LCZ classes for Nairobi city based on Landsat 8 images for different Years with urban LCZ types (LCZ 1–10) and natural LCZ types (LCZ A–G). See Table 3.1 for the scene ID explanation.

The t-test results presented in Table 3 showed statistically significant differences ($P<0.05$) among mean LSTs between the LCZs in all the six Landsat 8 images. Significant differences in mean LSTs represent positive results in this analysis. This result strongly supports the WUDAPT level 0 methodology used for LCZ classification (Bechtel *et al.*, 2017; Buyantuyev & Wu, 2010; Connor *et al.*, 2015; Perger *et al.*, 2015; Voogt & Oke, 2003) in Nairobi city. LCZs are differentiated based on variability in the urban structure, urban surface cover, urban fabric, and human activity. However,

considering the nadir view position of the sensors, the effect of vertical surfaces on apparent surface temperature is neglected, and simultaneously, dense development significantly reduces the increase in a shaded area with building height.

Table 4.3: Results for t-test analysis showing mean significant differences of LSTs between individual LCZs in different Landsat 8 scenes. See Table 3.1 for the scene ID explanation.

Image Date	t-statistic	P-value	Conf.int
08/06/2013	-7.5683	5.373775e-13	-2.71 - 1.59
03/02/2014	-4.4191	1.433734e-05	-2.542 – 0.975
03/01/2015	-4.3615	1.574107e-05	-2.84 – 1.08
03/08/2016	-12.1647	5.33341e-31	-2.51 – 1.81
28/12/2017	-13.0012	8.596511e-31	-5.07 – 3.73
29/01/2018	-13.0155	1.737407e31	-5.83 – 4.30

This analysis indicated specific differences between six Landsat 8 images. Each image leads to different LSTs using the same Split window retrieval algorithm for Landsat 8. The differences could result from different environmental parameters scene viewing geometry, time, distance from the sun, and solar azimuth angle (Krayenhoff & Voogt, 2016), as shown in *Table 3.1*. A higher proportion of vertically-oriented surfaces in urban areas than rural environments causes uneven solar heating of those surfaces and induces a thermal anisotropy effect (Lelovics & Unger, 2013; Unger, 2004). It is important to stress that both scenes identified the same sets of warmest (coldest) LCZs. Last but not least, an essential precondition for LST comparison between different zones is the mutual independence of LCZ classification and the LST fields. Consequently, this is an essential methodological aspect of this study concerning widely-used imagery-based methods (Bechtel *et al*., 2015; Brousse *et al*., 2016; Cai *et al*., 2016; Danylo *et al*., 2016; Ren *et al*., 2016; Ren *et al*., 2017; See *et al*., 2015; Wang *et al*., 2018), including thermal bands for LCZ delimitation.

Overlaying a temporal series of thermal satellite imagery with the LCZ boundaries was essential to understand the spatial locations of hotspots in Nairobi city to allow further examination. The study results provided a partial but coherent insight into the nature of morning hour (around 07.00 hours) spatial distribution of LSTs in LCZs as the vertical surfaces were neglected. Knowledge of LSTs as an essential climate parameter related to surface energy balance is critical in the management of SUHI in Nairobi city.

The characteristics of UHI are related to both the intrinsic nature of a city, such as increased roughness due to building geometries, drier and more impervious surfaces, and anthropogenic heat and moisture releases (Stewart & Oke, 2012; Bechtel *et al*., 2015), as well as to external influences which originate from climate, prevailing weather circumstances and seasons (Bechtel *et al*., 2015; Connor *et al*., 2015; See *et al*., 2015; Stewart & Oke, 2006; Stewart *et al*., 2014). While it is primarily a nocturnal phenomenon, SUHI occurs during the daytime with a spatial and temporal pattern actively controlled by the unique characteristics of each LCZs (Bokva *et al*., 2014; Gulyás *et al*., 2006; Ragheb *et al*., 2016; Unger *et al*., 2014). It is typically developed during clear skies and is ordinarily an aftereffect of the dominant reflective surfaces of the city compared to surrounding rural areas (Ching *et al*., 2016; Stewart *et al*., 2014; Stone & Rodgers, 2001). Thus, LSTs retrieved from Landsat 8 (which has a Thermal Infrared Sensor (TIRS) that captures the temperatures of the Earth's surface in bands 10 and 11 with a spatial resolution of 100m) may be a suitable alternative, as their spatial coverage is complete.

Even though surface temperature influences the air temperature of the boundary layer atmosphere (Unger, 2004), the interaction between the two types of temperatures is quite complicated in urban settings (Schwarz *et al*., 2012). The spatial extent of LSTs is modified by several static factors (for example, LULC types, urban morphology, topography) as defined by the LCZ classification and dynamic factors (for example, the

geometry of thermal imagery acquisition, solar elevation) as defined by the sensor. These factors modify the energy balance of urban areas and also generate thermal anisotropy effects (Bechtel *et al*., 2012).

When interpreting the thermal behaviour of LCZ 10, it must be taken into account that the LCZ 10 delineation was based on the Nevertheless, the higher LSTs of industrial areas in the daytime, which many authors have previously described (Stewart *et al*., 2014; Taubenböck *et al*., 2010; Voogt & Oke, 2003). Unexpectedly, the LSTs of LCZ 8 (large low-rise) were in all the scenes considerably lower than the LSTs of LCZ 10. This may correspond to the different thermal properties implicit in the large roof surfaces that often occur in LCZ 8 (Akbari & Levinson, 2008; Bechtel *et al*., 2015; Parlow *et al*., 2014).

LCZ A (dense trees) was identified as a lower LST zone, but many positive outliers are evident (i.e., highest LST). This is a reaction to the relatively high number of patches, mainly consisting of clear-cuts of areas that are often below the spatial resolution of the data used for LCZ classification. On the other hand, the low LST of LCZ G (water) should be considered realistic since temperature differences reflect the different characters of individual bodies of water. Therefore, several criteria could be used to identify and control urban heat loads in Nairobi city which should be investigated: the (H/W) ratio between the height of the buildings (H) and the width of the adjacent street (W), the orientation, reflectivity, conductivity, plot coverage, balconies and vegetation building heights, and human activities (Bechtel et al., 2019; H. Li et al., 2018; Taslim, Parapari, & Shafaghat, 2015).

Emission from heat sources, together with heat accumulated and reradiated back into the environment, leads to higher LSTs in built-up LCZs such as industrial areas LCZ 10 (heavy industry). The increased temperatures are anticipated to bring significant heat

waves throughout urban areas in Nairobi. Most affected will be areas with vegetation removed and in places of dark surfaces such as asphalt roads and black roofs. Other factors contributing to the SUHI include reduced porous surfaces, tall buildings and narrow streets, decreased surface waters, and concentrated heat-generating activities in urban areas, e.g., motor vehicles, factories, and homes. Therefore, mitigation and adaptation strategies that increase urban green cover (dense trees), pervious land cover (low plants and grasslands), the low albedo of materials (light coloured surfaces), and reducing dense development (to significantly reduce the increase in a shaded area with building height) (Bechtel *et al*., 2017; Buyantuyev & Wu, 2010; Connor *et al*., 2015; See *et al*., 2015; Voogt & Oke, 2003) is critical for Nairobi city.

4.4 Spatio-Temporal Variability of 2m Air Temperature Distribution for Nairobi city

The MUKLIMO_3 model output revealed intricate spatial and temporal patterns represented with 24 2 m air temperature maps at a horizontal resolution of 200 m across Nairobi city and its environment. The time step between two successive modelled fields was 60 minutes. The results indicated a complex spatial structure of the simulated 2 m air temperature and urban heat load in Nairobi City. High-density built-up areas in the city center and residential areas with flat terrain north-east of Nairobi city recorded possible maximum urban cooling during the daytime and maximum urban heating patterns at night compared to sparsely built areas covered with vegetation. The spatial pattern of simulated 2 m air temperature confirmed the presence of canopy layer UHI across Nairobi city. The variation in simulated warmer 2 m air temperature in parts of the town accrued from terrain-induced flows and land surface heterogeneity as described by the LCZ parameters (*Figure 4.5*).

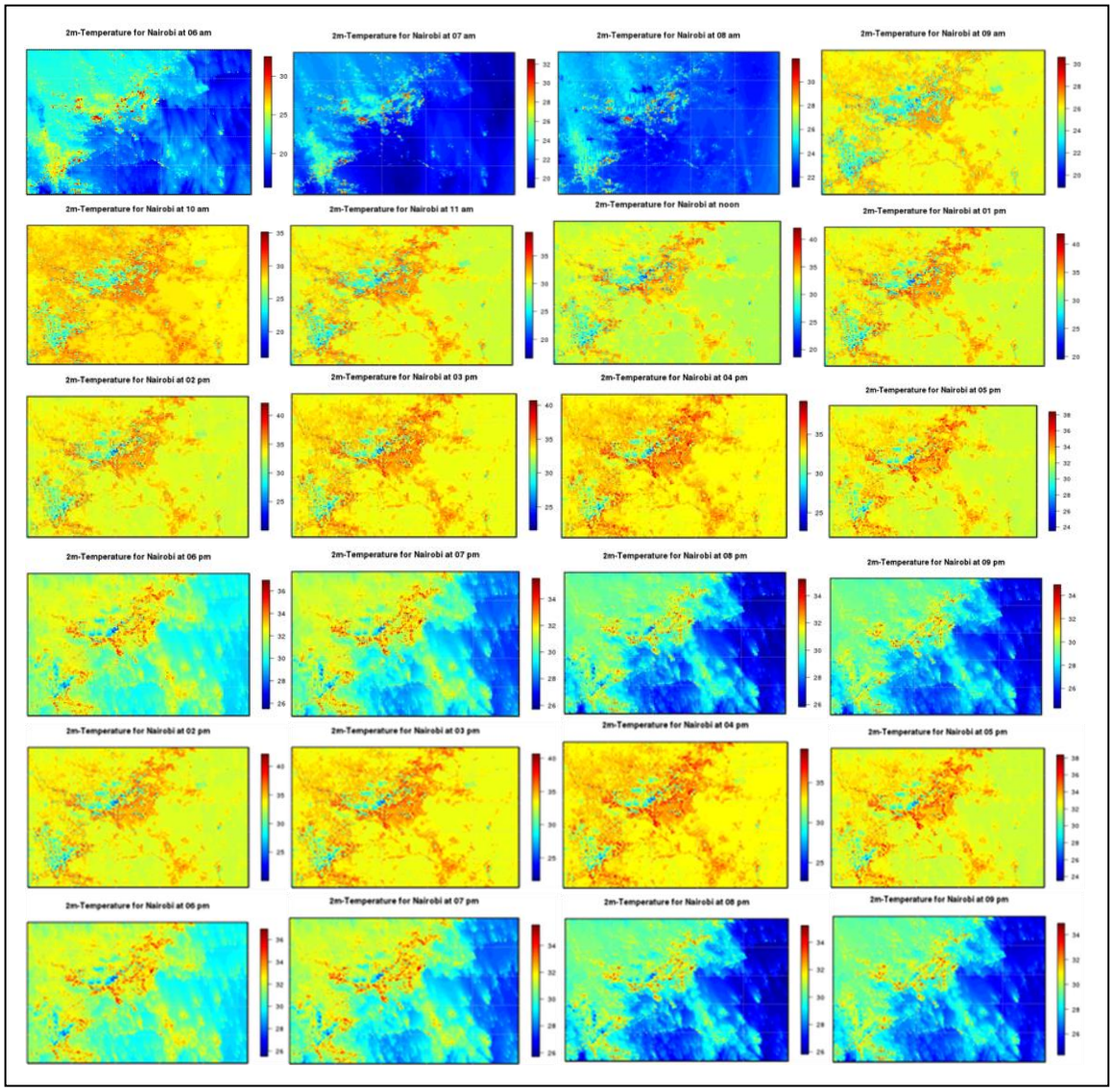

Figure 4.4: Modelled Spatio-temporal variability of the 2m air temperature (°C) in Nairobi city on 26th February 2018

Lower 2 m air temperature early in the morning was typical of natural LCZ types, while the warmer 2 m air temperature was typical of built-up LCZ types. Places with the lowest air temperature in the early morning hours before sunrise was located in areas

dominated by the featureless landscape of soil or sand cover with few or no plants (LCZ-F) in the south-eastern (Mlolongo, Syiokimau, Athi River, and some parts of Emabakasi) parts of Nairobi. After the sunrise, Lower 2 m air temperature is typical to natural landscapes with forests, scattered trees, bushes, low plants, and water bodies (LCZs A, B, and G).

In comparison, warmer 2 m air temperature are typical to both open and high-density built-up areas considerable low rise and heavy industrial buildings (LCZs 1- 10), and open natural with bushes and scrubs, low plants (mostly grasslands, agricultural fields, and parks), and paved allotment areas, and bare soils and sand (LCZs C, D, E, and F) as illustrated by 2 m air temperature for Nairobi from 09 am to 05 pm. As the air gets warmer (from 11 am to 05 pm), the model gradually generates areas with a higher proportion of LCZ 2, 3,7,8,9, and 10 warmer than their surroundings, including areas outside the compact urban development. However, the distinct UHI is not formed until noon to 03 pm. At 03 pm, the UHI is formed over most of the city center. After sunset, the 2 m air temperature distribution was predominantly influenced by the spatial distribution of wind fields within LCZs. Areas with lower temperature were located in high-density built-up areas, very large low rise and heavy industrial buildings (LCZs 1-10) as illustrated by 2 m air temperature for Nairobi at 06 pm to 05 am.

However, the warmer air temperature was located in build-up LCZ types. As the air gets colder (from 06 pm to 05 pm), the model gradually generated areas with a lower proportion of hot spots (build-up areas) warmer than their surroundings, including areas outside the compact urban development. The distinct nocturnal UHI formed only in built-up areas of the city center and reduced gradually after the sunset. Hotspots within the city were formed in areas with a higher proportion of high-density built-up classes (LCZ 2, 3, 7 and 10), with 2 m air temperature range of 30 °C to 40 °C during daytime and 28 °C to 34°C at night.

On the contrary, relatively cooler spots within the city correspond to larger areas of LCZ A, B, and G during the daytime where 2 m air temperature reached 20 °C, LCZ A, B, C, D, F and G during night time where air temperature reaches about 18 °C at 04 am. The lowest temperature predicted for forested areas (LCZ A) in the city center was about 25 °C. Thus the model simulated temperature differences of up to 15 °C between the warmest part of the city and the most cooling forests at 1200 noon to 03 pm (figure 5 and 6). The model, however, forecasts a relatively higher intensity of canopy layer UHI during the evening and night hours. At 9 p.m., the warmest parts of the city are only about 12 °C warmer than the natural landscape (predominantly LCZ D) and up to 10 °C warmer than the forested areas. Spatial analysis of simulated of 2 m temperature fields and the increase of heat load in the high-density built-up areas demonstrated canopy layer UHI in Nairobi city as a joined impact of both terrain (for example, terrain sheltering and the unfavorable location of the city), or local land surface heating (due to a high percentage of water-resistant, non-reflective surfaces, building structure type and density, a high fraction of asphalt and a small amount of vegetation cover) which add to the formation of excessive urban heat load.

During the day, the heat load in high altitude vegetated areas was locally reduced compared to the lowland high built-up areas visible in the vertical temperature profile (*Table 3.3*) due to the temperature inversion, which makes the elevated and natural areas warmer. The location of the city and the building type, consisting of high density, a high fraction of pavement, and a small amount of vegetation, contributed to the formation of excessive heat load at night. During the night, robust and reliable cooling of the free surface results in a temperature inversion, and therefore MUKLIMO_3 model assumed a temperature that was just 1 °C higher in the high-density built-up areas than in the rural natural surroundings and temperature that was about 10 °C higher in the built-up areas than in the coldest forests.

MUKLIMO_3 model primarily reflected the effect of elevation and land cover on UHI distribution evident during the daytime and at night. The model predicts higher temperature at lower elevations globally, and it can be considered a simplification (Bokva *et al*., 2014; Bokwa *et al*., 2015). On the other hand, the model did not reflect the extent of the variability of building density (i.e., the amount and effect of accumulated heat). It is anticipated that for a more accurate simulation of the spatiotemporal temperature field, it is necessary to focus on the LCZ table. Moreover, it is possible that the concept of LCZ is too general for modelling on a detailed level and may have caused incorrect settings of the thermal capacity of individual surfaces. However, the use of LCZ classes to describe urban features decreased model uncertainties related to selection choice by limiting and standardizing the parameterization of the unresolved buildings in the MUKLIMO_3 model. Generally, the MUKLIMO_3 model considered the physical features of the unresolved urban structure and the elevation and advection of the air masses between the surrounding surfaces computing atmospheric processes in the urban condition. The heat load for an individual city relied upon relief, the surrounding land use types, and location in the city.

The comparison of the real station measurements and MUKLIMO_3 simulations in Nairobi city and its surroundings was impossible because of a lack of access to the hourly 2 m air temperature data from the metrological stations. However, the model prediction was consistent and could correspond best with the situation on 28 February 2018; this may be related to more stable atmospheric conditions very close to climatological warm days. However, Individual problems with the accuracy of the model simulation could be primarily related to the starting phase of the modelling (at 10.00 am and 11.00 am). Additionally, the MUKLIMO _3 model should simulate future projections of the UHI phenomenon and create spatial configurations of planting designs with more cooling and fewer energy demands and their application to the whole in Nairobi city.

4.5 Environmental Amelioration Effects of Different Plant Species on Microclimate and human thermal comfort

The allometric properties of the measured plant species are shown in *Table 4.4*. Results of relative diurnal variation of ambient temperature, globe temperature, surface temperature, relative humidity, and discomfort index as influenced by single isolated tree species in both Uhuru Park and Central Park based on average of data from field measurement from day 47 to day 59 of the year 2017.

Table 4.4: Allometric properties of the measured tree species

Species Name	Adult Status	DBH (m)	Tree height (m)	Branching length(m)	Crown length(m)	Crown width(m)
Ficus benjamina	Mature	0.86	21.2	3.7	17.5	17.6
Ficus religiosa	Mature	0.27	6.9	3.5	3.4	4.8
Cassia spectabilis	Mature	0.49	12.5	4.5	8.5	14.8
Warburgia ugandensis	Mature	0.44	16.1	4	12.1	7.2
Calistemon citrinus	Mature	0.31	6.6	1.2	5.4	6.8
Bambusa vulgaris	Mature	3.4	8.5	1.7	6.8	13.6
Dypsis decaryi	Mature	0.6	8.5	5.1	3.4	6.8
Terminalia mantaly	Mature	0.56	5.7	3.8	1.9	7.6
Schinus molle	Mature	0.61	3.4	0.5	2.9	3.4

Ficus benjamina had the most effective diameter at breast height, tree height, crown width, *Cassia spectabilis*, *Warburgia ugandensis,* and *Ficus religiosa*, respectively. However, the crown height of *Ficus benjamina* had the most attenuating effect, followed by *Warburgia ugandensis*, *Cassia spectabilis*, and *Ficus religiosa*, respectively. *Bambusa vulgaris* had the most significant tree height, while *Schinus molle* was the shortest plant. *Terminalia mantaly* had the smallest crown height. The globe

temperatures, surface temperature, relative humidity, and discomfort index variations were similar to ambient temperature attenuations' values. It can be seen that trunk temperatures were the smallest, followed by the 5 m and 10 m temperatures in all the single isolated trees.

The four plants measured in Uhuru Park presented results: *Ficus benjamina* yielded the highest values for the attenuation of ambient temperature (20.07%), followed *by Cassia spectabilis* (17.77%). *Ficus religiosa* and *Warburgia ugandensis* produced the lowest ambient temperature attenuation (15.2% and 14.62%), respectively. The five plants measured in central park produced the following results: *Callistemon citrinus* (9.01%), followed by *Dypsis decaryi* (7.02%), *Bambusa vulgaris* (6.78%), *Terminalia mantaly* (5.91%), and *Schinus molle* (4.77%) as illustrated by Mean diurnal Relative variation of ambient temperature in *Figure 4.6.*

Ficus benjamina presented the highest mean relative attenuation of globe temperature (22.17%), followed *by Cassia spectabilis* (19.03%), *Ficus religiosa* (16.25%), and *Warburgia ugandensis* (12.60%). *Callistemon citrinus* produced a mean relative attenuation effect of 8.73%, followed by *Dypsis decaryi*(6.84%), *Bambusa vulgaris* (5.98%) *Terminalia mantaly* (5.94%), and *Schinus molle* (3.06%) as illustrated by Mean diurnal Globe Temperature in *Figure 4.7.*

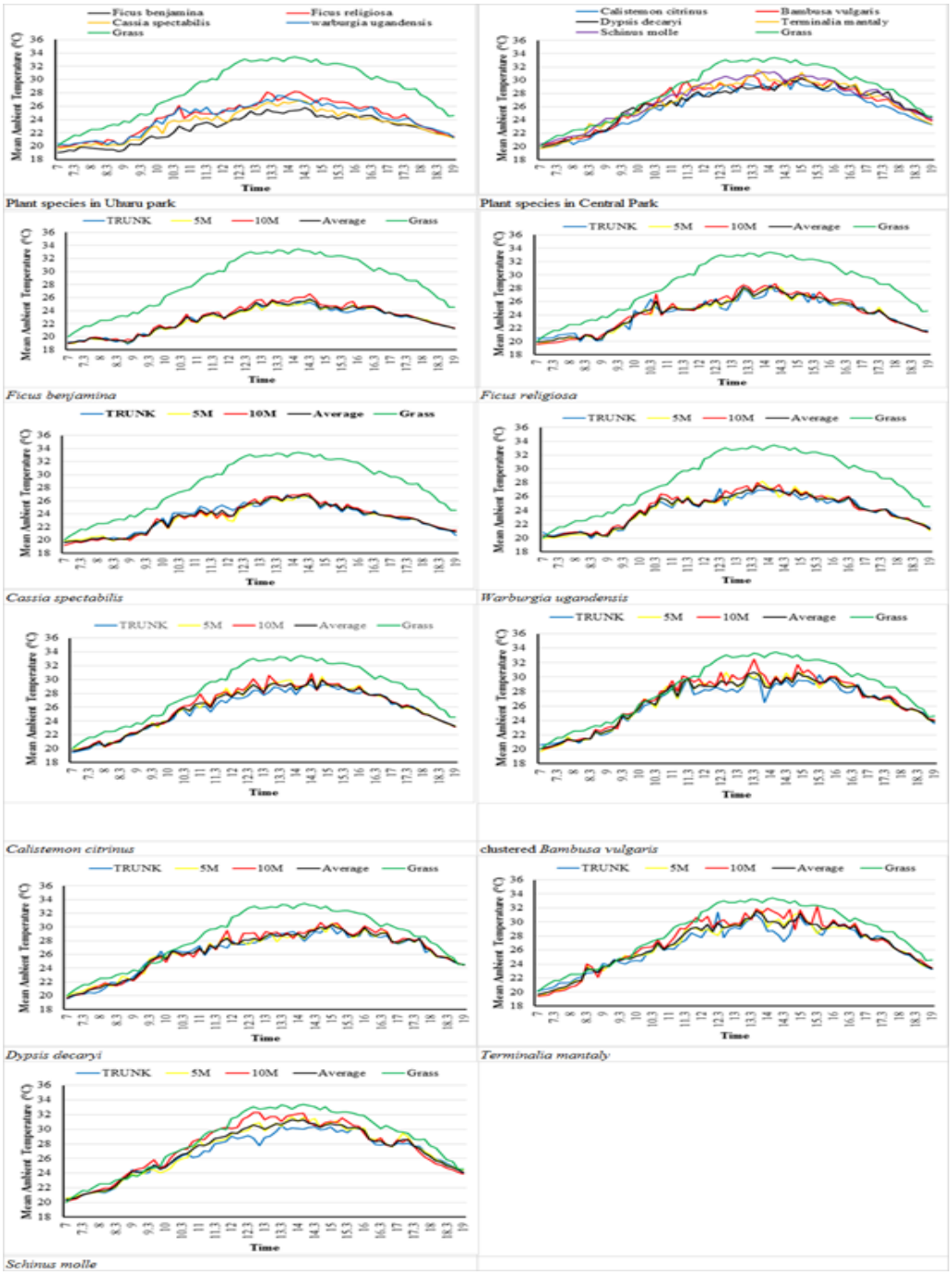

Figure 4.6: Mean diurnal Relative variation of ambient temperature

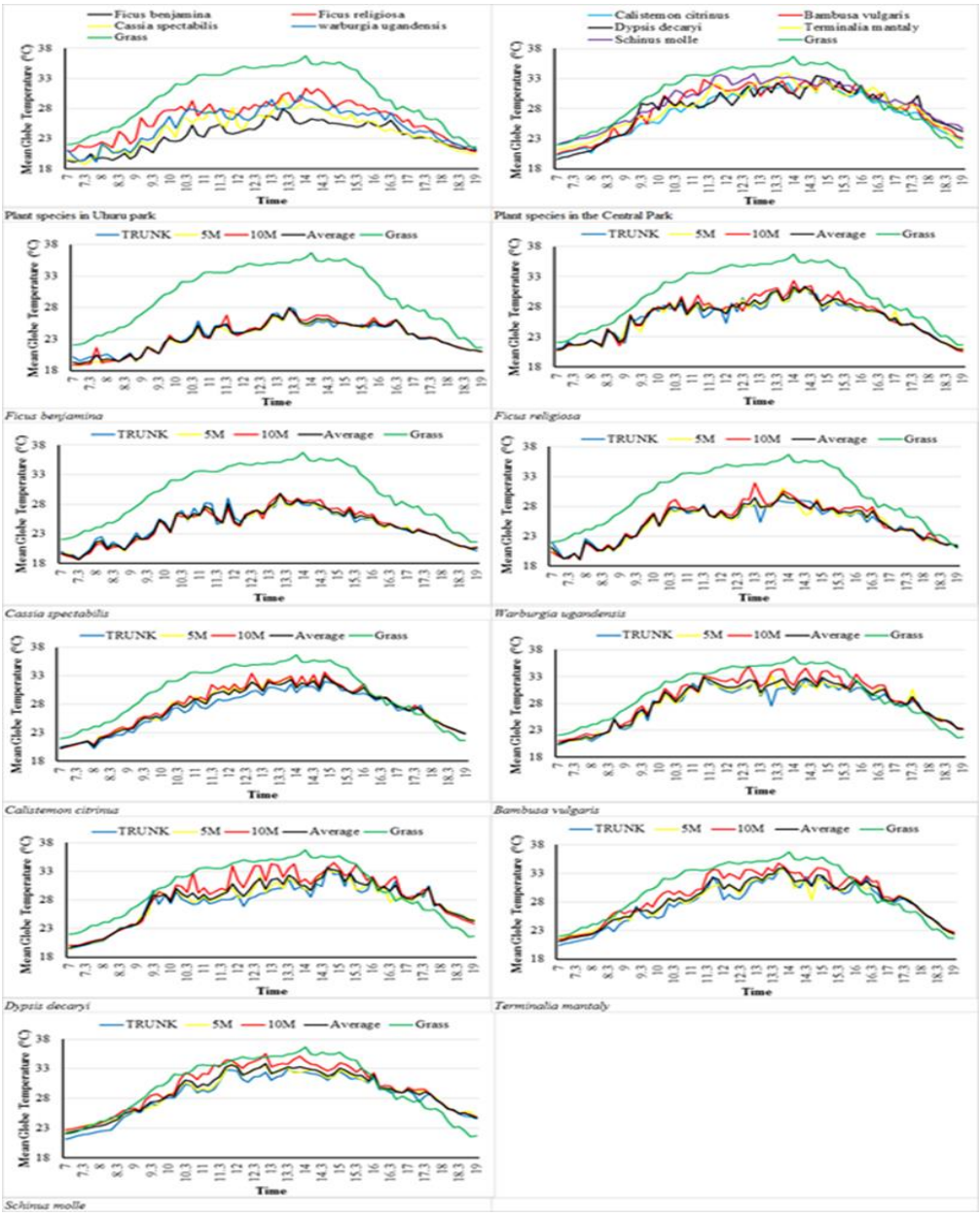

Figure 4.7: Mean diurnal Globe Temperature

Ficus benjamina presented the highest relative attenuation of surface temperature *(Figure 4.8)* with a mean variation value of 40.26%, followed *by Cassia spectabilis* (33.86%), *Ficus religiosa* (28.50%), and *Warburgia ugandensis* (23.13%). In the central park, *Callistemon citrinus* produced a relative attenuation effect of 16.01%, followed by *Dypsis decaryi* (12.66%), *Bambusa vulgaris*(11.80%), *Schinus molle* (10.0%), and *Terminalia mantaly* (4.7%).

The mean diurnal relative humidity *(Figure 4.9)* for different plant species presented results as follows: *Ficus benjamina* produced the highest relative attenuation of relative humidity with a mean variation value of 54.02%, followed *by Cassia spectabilis* (50.21%), *Ficus religiosa* (44.75%) and *Warburgia ugandensis* (44.50%). *Callistemon citrinus* (17.05%), *Dypsis decaryii* (12.70%), *Bambusa vulgaris* (12.43%), *Schinus molle*(10.58%) and *Terminalia mantaly* (10.19%).

It can be observed that *Ficus benjamina* showed the highest reduction percentage of thermal discomfort index (12.00%), followed by *Cassia spectabilis* (10.19%), *Warburgia ugandensis* (8.37%), and *Ficus religiosa* (7.86%). Plants in Central park showed the lowest relative variation of reduction percentage of discomfort index as follows; *Callistemon citrinus* (5.72%), *Dypsis decaryi* (4.48%), *Bambusa vulgaris*(3.87%), *Terminalia mantaly* (3.91%), and *Schinus molle*(2.91%) *(Figure 4.10).*

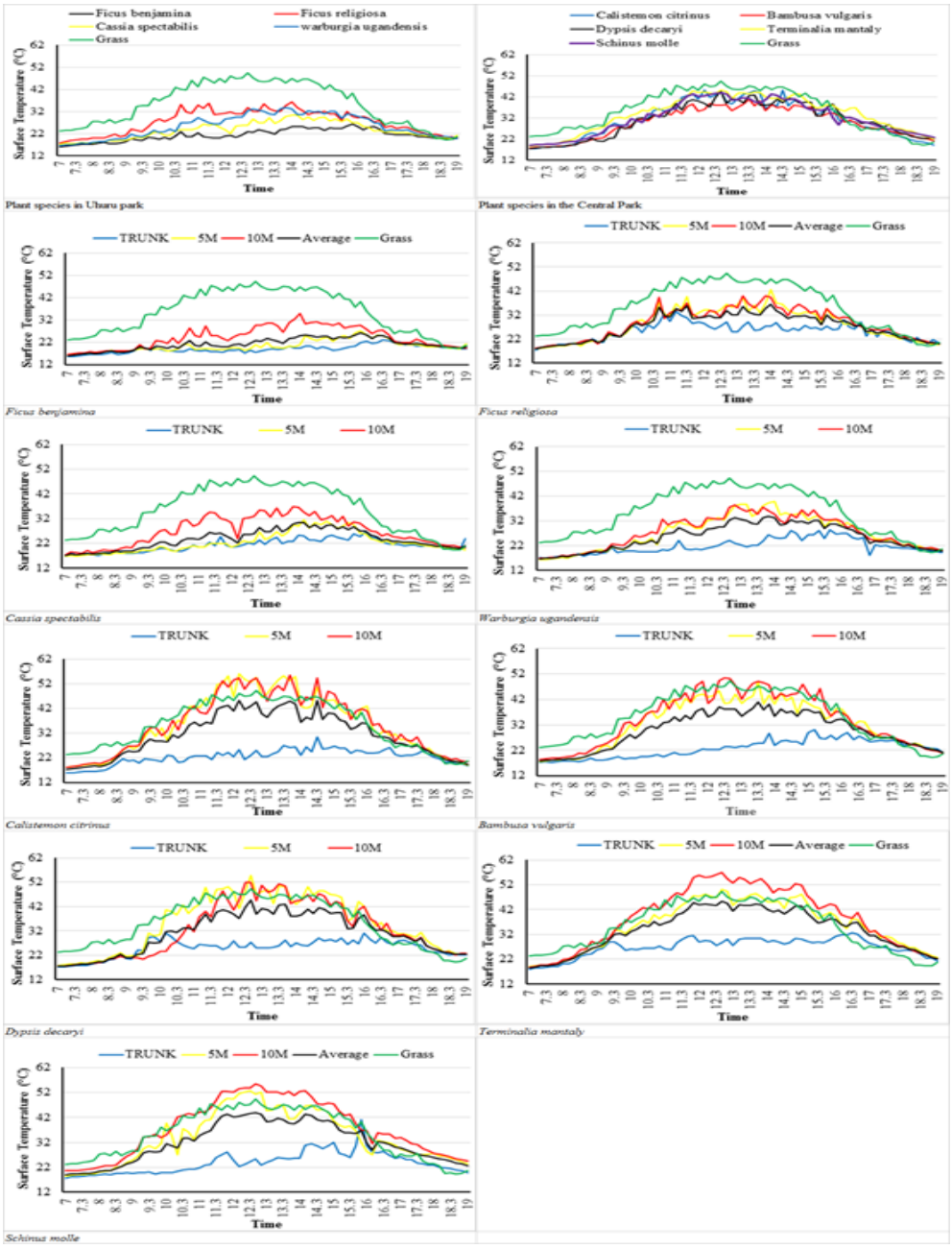

Figure 4.8: Mean diurnal Surface Temperature.

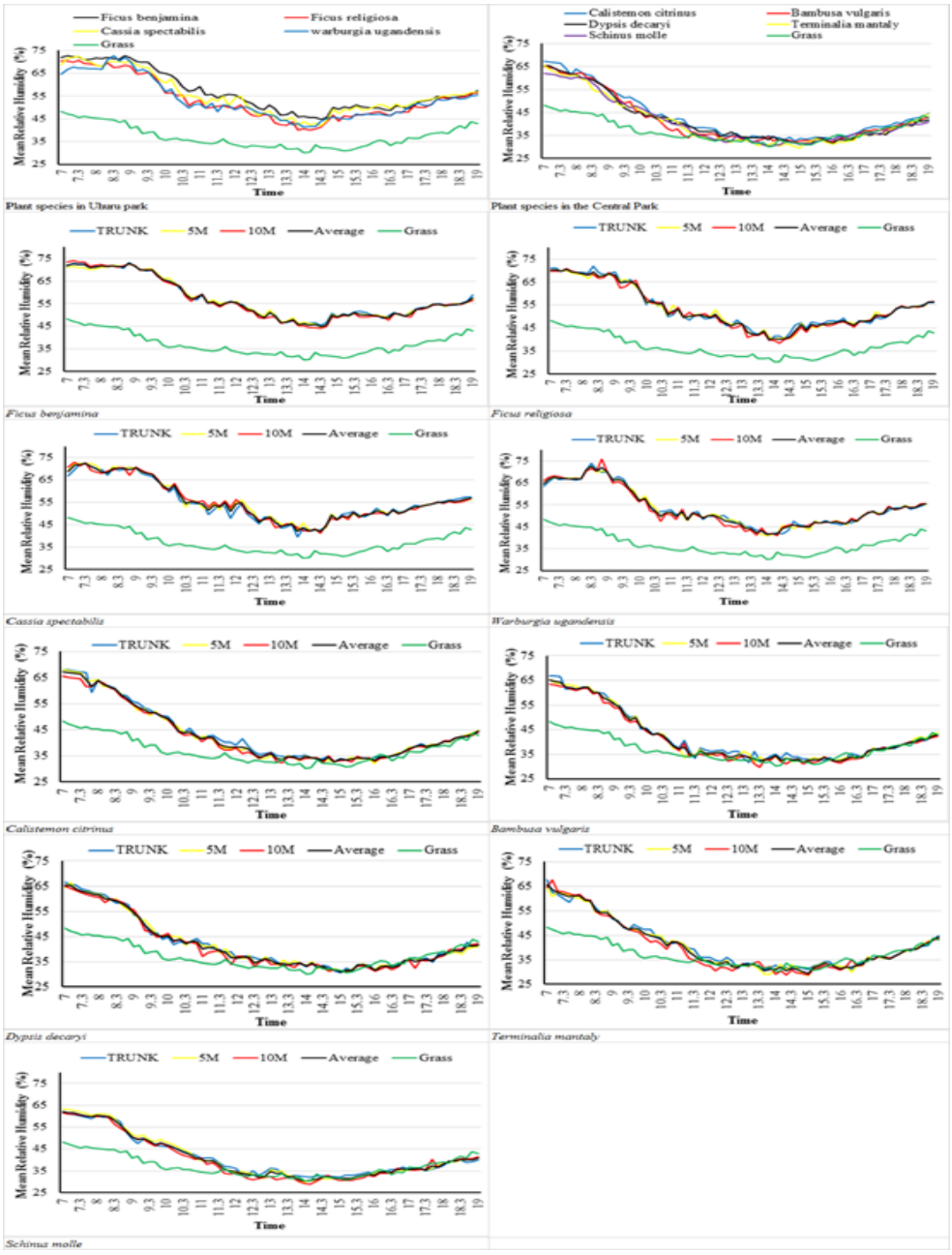

Figure 4.9: Mean diurnal Relative Humidity.

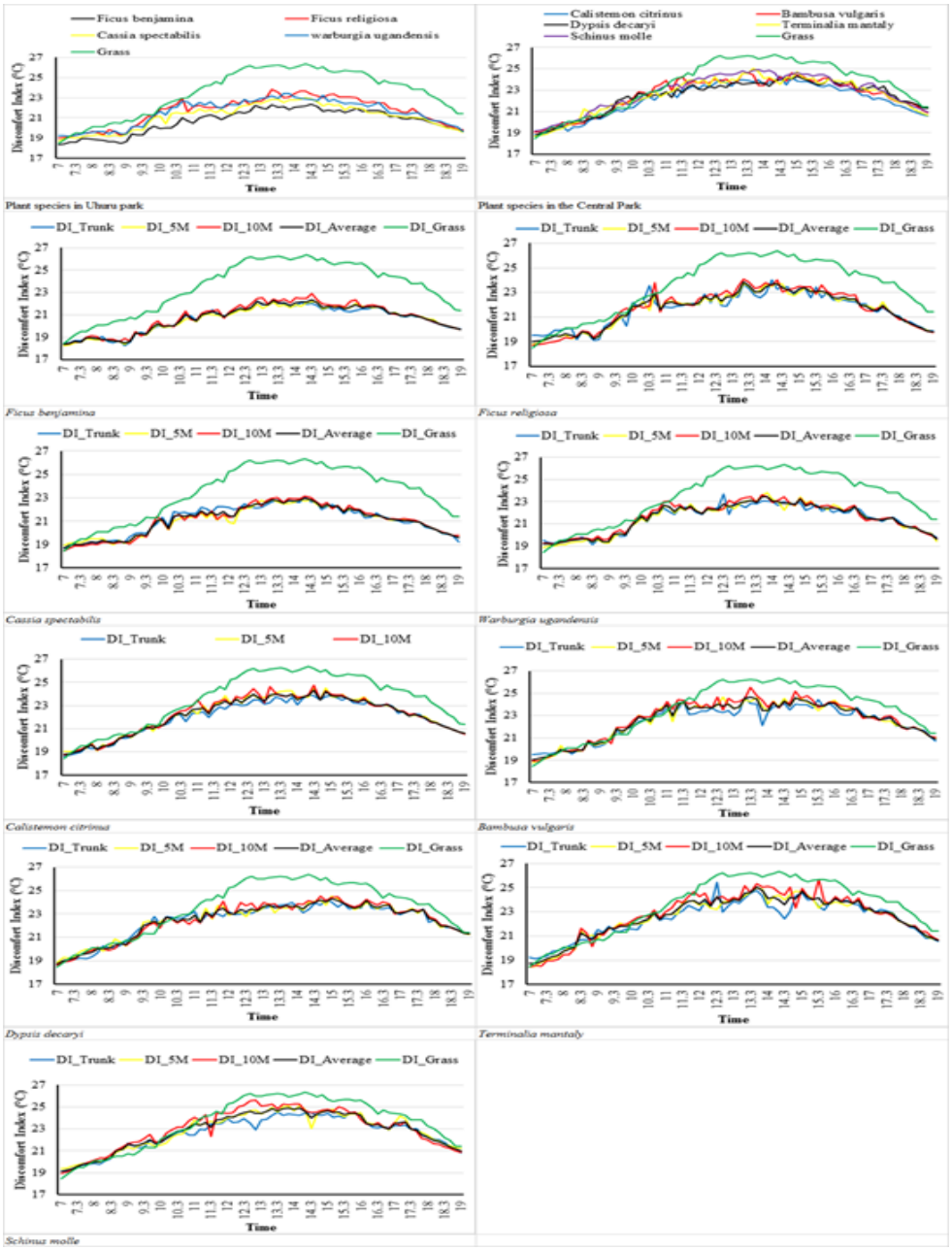

Figure 4.5: Diurnal courses of Relative variation of discomfort index.

The diurnal discomfort index of all the analysed tree species in Uhuru Park ranged from 20°C to 25°C from 11.00 am to 6.00 pm, which meant that discomfort was expressed by < 50% of the population who sat in the shades of the individual plant species (Georgi & Zafiriadis, 2006). There was no significant difference between the discomfort index at the trunk, 5m, and 10 m. However, different plant species expressed specific differences. However, there was thermal discomfort index variation amongst the studied plant species.

These results confirmed variation in microclimate and thermal comfort by different tree species. Plants with massive canopy structures and dense leaves attenuated environmental parameters more effectively. They improved thermal comfort via higher rates of transpiration and synergistic thermal effects of leaf physical traits. These findings confirm Lotufo Bueno-Bartholomei & Labaki (2003). The variation in performance could be attributed to interspecific variation in the crown dimensions, mainly by crown width and crown area, and specific allometric characteristics of the analysed tree species like structure and density of the treetop, size, shape, and colour of leaves, tree age, and growth (Masson *et al*., 2014).

Tree canopy temperature is a proxy for the energy balance between the leaf interior and the ambient environment. Incoming solar radiation absorbed by a leaf is partly used for biochemical reactions such as photosynthesis, but a more substantial proportion is converted to leaves' thermal energy. Plant canopy temperature is predominately

determined by ambient temperature but also regulated by leaf physical traits and transpiration. When plants are exposed to hot conditions, they can reduce the amount of accepted radiation through reflection and movement and dissipate excessive heat via radiation emission, heat convection, and transpiration. However, each of these processes' relative contributions differs significantly among different plant species (Zhongli & Xu Hanqiu, 2016).

Tree canopies create microclimates through the interception of solar radiation and evapotranspiration, thereby modifying the heat balance of the surrounding environment. Radiation interception is owed to shade counteractive short and long-wave radiation from the upper half of the globe. In contrast, evapotranspiration is owed to the water content conveying limit of the soil–tree-air framework. Plant leaves and branches reduce the amount of solar radiation that reaches the area below the canopy of a tree or plant (Fahmy et al., 2010). Plants also cause the diurnal patterns of cooler daytime temperatures and warmer nighttime temperatures due to trapped heat and humidity within the urban canopy layer compared with the rapid nocturnal cooling of open areas (Coutts *et al*., 2016). The amount of sunlight transmitted through the canopy varies based on plant species.

Large tree species with thicker trunks support broader and less deep crowns with greater branching height than smaller ones. Trees with large canopies and dark green leaves such as *Ficus benjamina* presented the highest attenuation of environmental parameters.

In contrast, small canopy sizes such as *Ficus religiosa* produced the lowest attenuation effect. Medium-sized tree canopies such as *Cassia spectabilis* and *Warburgia ugandensis* presented relatively medium attenuation of environmental parameters. *Ficus benjamina* has a plagiotropic trunk and large spherical-shaped canopy that offers a large surface area to solar radiation during transpiration and produces a significant shading effect underneath, compared to *Ficus religiosa*, which has a small spherical shaped canopy. However, the interaction between canopy allometric properties makes it difficult to measure the thermal impact of trees' physical traits and transpiration separately for individual plants. Some previous studies only analysed the effects of one or several leaf physical traits on leaf temperature (Shashua-Bar *et al*., 2011), while many physical characteristics could be associated with leaf temperature. Also, the thermal effects of all the physical traits may differ from the individual contribution.

Ambient temperatures must be neither too low nor too high to reduce individual vulnerability and maintain a comfortable thermal environment. Body temperature, approximately 37°C, is kept by consuming calories from food and heat exchanges with the immediate surroundings according to the heat transmission mechanisms (Fröhlich & Matzarakis, 2013). Human thermal comfort is subjective and based on contextual parameters such as activity level, physiological and psychological acclimatisation to heat, clothing worn, air temperature, the temperature of the surrounding surfaces, solar radiation, and airflow and relative humidity of the air. Therefore, thermal comfort is

unique, and it is impossible to define a type of thermal environment that meets everyone's requirements. However, the acceptable temperature range for a high percentage of people is between 20°C and 27°C, with an optimal humidity rate of 35% to 60% (Shooshtarian & Ridley, 2017).

CHAPTER FIVE
SUMMARY, CONCLUSIONS & RECOMMENDATIONS

5.1 Introduction

The concept of LCZs was used to study the combined effect of Urbanization and climate variability and quantify different plant species as an adaption strategy to the UHI phenomenon for Nairobi city. This chapter summarises fundamental concepts important to understanding and adapting the phenomenon, conclusions, and recommendations of the findings.

5.2 Summary

The research study simulated UHI and quantified plant species' benefits as an adaptation strategy for Nairobi city. The study aimed to evaluate the relationship between LCZs and UHI's spatial distribution and quantify diverse plant species' environmental amelioration effects on urban microclimate and human thermal comfort. Specifically, the study generated of the LCZs for Nairobi city Urban Temperature studies using the WUDAPT methodologies; simulated the LSTs using the spit window tool algorithm and then differentiated using the LCZ as classification units for surface urban heat island (SUHI) management in Nairobi city; simulated the Spatio-Temporal variability of Canopy Layer Urban Heat Island (CLUHI) distribution in Nairobi City using MUKLIMO_3 model and; Quantified the attenuation effects of different plant species on microclimate and human thermal comfort.

The results confirmed that the concept of the Local Climate Zone (LCZ) scheme classified natural and urban landscapes based on climate-relevant surface properties that captured the forms and functions of Nairobi city. All 17 LCZs are present. The classification was quantitatively delineated by scored urban morphological properties of built-up (LCZ 1-10) areas and natural areas (LCZ A-G), which indicated the potential

UHI distribution pattern of Nairobi city. About 50.26% of the Nairobi area was built up, while about 49.74% was natural. The study revealed the gradations of morphological properties of LCZs and the geographical space, which had the potentials to enable quantitative comparisons of Nairobi City domestically and internationally.

Downtown areas of Nairobi city were mainly classified into the compact built-up classes (LCZs 1, 2 &3) and LCZ E (bare rock or paved), which demonstrated that the central business centre could form hot spot areas with potentially high UHI intensity. LCZ 7 (Lightweight low-rise), mostly informal settlements potentially highly vulnerable to climate change effects, took up the areas around residential high-rise buildings in the city. There were limited dense trees (LCZ A), which were also located on the outskirts of both the central business centre and residential areas.

There was both surface and canopy layer UHI phenomenon in Nairobi city characterised by an increase in urban areas' temperature compared to the surrounding rural areas. UHI was present in areas with a high percentage of water-resistant, non-reflective surfaces and low vegetation. Materials such as stone, concrete, and asphalt trap heat at the surface, while the lack of vegetation reduces heat loss due to evapotranspiration. Also, anthropogenic heat and atmospheric pollutants could have contributed to the increase of UHI intensity. The UHI effect varied in different LCZ and depended on city size, land use, topographic factors, vegetation, urbanisation, and industrialisation of the area, the season of the year and time of day, and prevailing meteorological conditions.

The results here were the first to compare the spatial distribution of land surface temperatures with local climate zones for Nairobi's cities in the Republic of Kenya. Statistical analysis of LST showed significant differences among typical LCZs. The warmest zones were LCZ 10 (heavy industry), LCZ 3 (compact low-rise buildings), LCZ 2 (compact mid-rise buildings), LCZ 7 (lightweight low-rise), and LCZ 8 (large

low-rise), while the coldest (LCZ G (water bodies), LCZ A (dense trees) and LCZ 9 (sparsely built). These findings generally support the concept of LCZs and the GIS-based method used for their delimitation and investigation of the influence of complex urban morphology on local climate formation in Nairobi city for better climatic-spatial planning in the future. Specific questions remain open to future research, such as seasonality in LST differences and thermal anisotropy (complete surface temperature differences).

The MUKLIMO _3 model identified thermally sensitive areas within the city through idealised simulations of temperature, wind, and relative humidity in the urban area based on the orography and LCZs data with 200 m resolution for the potential warmest (26th February) day conditions in Nairobi city. Analysis of spatiotemporal gradients of temperature fields of Nairobi City showed increased heat load in the built-up areas and informal settlements as a combined effect of natural and anthropogenic factors. The unfavourable location in the city and the building type, consisting of high density, low housing with a high fraction of pavement, and a small amount of vegetation, contribute to the excessive heat load.

On the other hand, quantification of the environmental amelioration effects of diversity of plant species on microclimate and human thermal comfort in Nairobi city showed differences in performance. *Ficus benjamina* (12.00%) presented the highest ability to attenuate air temperature, relative humidity, globe temperature, and reduce thermal discomfort index, followed by *Cassia spectabilis* (10.19%), *Warburgia ugandensis* (8.37%), *Ficus religiosa* (7.86%), *Callistemon citrinus* (5.72%), followed by *Dypsis decaryi* (4.48%), *Bambusa vulgaris* (3.87%), *Terminalia mantaly* (3.91%) and *Schinus molle* (2.82%). The diurnal discomfort index of all the analysed tree species ranged from 20°C to 25°C from 11.00 am to 6.00 pm, which meant that discomfort was expressed by < 50% of the population who sat under the shade. Microclimate control differences were

attributed to specific tree allometric properties of the analysed and the individual sample species, like structure and density of the treetop, size, shape, and colour of leaves, tree age, and growth.

Therefore, total height and canopy geometry are important to consider when selecting plants to accomplish specific urban designs, such as thermal performance. Plant species have a varied cooling effect as influenced by plant canopy size, structure, and density. Leaf temperature depends on anatomical structure (leaf mass, size, shape, angle, reflectance), physical (incoming energy, air temperature, the wind), and physiological (transpiration, stomatal conductance) factors and are intimately coupled with the water status of the plant.

5.3 Conclusions

The study was the first to compare the inter LCZ differentiation of LST distribution in Nairobi, a tropical city, employing the Landsat 8 sensor data. There was a positive correspondence in the spatial distributions of LCZs and LSTs under the limited relief and weather conditions tested in this study. The division of urban and rural landscapes into LCZs is therefore justified on both physical and empirical grounds. LSTs show typical surface temperatures that differ significantly between LCZs. These findings generally support the concept of LCZs as a classification unit for urban studies and future spatial planning in Nairobi city. Although the concept of LCZs was developed to classify air temperature measurements, individual LCZ also prove characteristic features of LSTs. Specific questions remain open to future research, such as seasonality in LST differences and thermal anisotropy (complete surface temperature differences).

The variations in simulated 2 m air temperature patterns accrued from terrain-induced flows and land surface heterogeneity, as described by the urban parameters. Therefore, the enhancement of urban heat load in Nairobi could be linked to the rapid urbanization

process and its historical development. The results were the first to provide the relationship between LCZs and the spatial distribution of UHI for Nairobi city using the MUKLIMO_3 model. The MUKLIMO_3 model outputs could be used to study the development of urban microclimates within Nairobi city. The results could also be useful for evaluating the influence of location, urban parameters, and weather conditions on urban microclimatic within Nairobi city.

In urban green spaces, different plant species can improve thermal comfort, mitigate air temperature, and control relative humidity, thereby ensuring a better quality of life for people. The tree canopy type is a significant component contributing to thermal comfort by attenuating solar radiation and controlling wind speed. Tree microclimate depends on canopy anatomical structure (leaf mass, size, shape, angle, reflectance), physical (incoming energy, air temperature, the wind), and physiological (transpiration, stomatal conductance) factors. Trees with larger canopies tend to cast more shade and deliver greater thermal comfort than smaller ornamental species. The diversified effects of plant species on urban microclimate can be used efficiently to improve thermal comfort in urban green spaces (Lotufo Bueno-Bartholomei & Labaki, 2003) of tropical cities such as Nairobi. Studying the strategies of tree temperature regulation in different plant species could improve the understanding of urban planting design and the adaptation of plants to various environmental functions. Since tree planting is a practical and inexpensive solution to UHI, the species used for urban planting must be chosen cautiously to ensure good foliage density. When the tree is mature, it will filter out at least 60% of solar radiation.

5.4 Recommendations

This study was carried out for one year. The measurements and simulation of UHI, microclimates and human thermal comforts in different plant species were based on historical and current data. It is therefore recommended that;

1. Proposals for urban planning and design strategies to manage urban heat in Nairobi City can focus on: improving the efficiency of urban systems, both in energy and transportation; optimising the form and layout of urban LCZs to enhance ventilation; promoting appropriate building materials with high reflectivity and; Increasing the use of green and blue urban infrastructure.
2. The data generated from LCZ classification and UHI mapping can be applied in numerical modelling and local climate change planning implementation in Nairobi for better climatic-spatial planning in the future.
3. MUKLIMO _3 model canbe used to simulate future projections of the UHI phenomenon in Nairobi city. However, the MUKLIMO_3 model must be validated for Nairobi city to reach a better performance and to understand the model settings and optimal input data preparations.
4. Planting trees such as *Ficus benjamina*, *Cassia spectabilis* and *Warburbugia ugandensis* can be adopted to attenuate microclimate and improve thermal comfort in Nairobi city. However, Further research study on spatial configurations of planting designs with more cooling and fewer energy demands and their application to the whole city is needed.

REFERENCES

Abreu-harbich, L. V. De, Labaki, L. C., Matzarakis, A., Vieira De Abreu-Harbich, L., Labaki, L. C., Matzarakis, A., … Matzarakis, A. (2012). Different Trees and configuration as microclimate control strategy in Tropics. *International Conference on Urban Climates*, 8–11. Retrieved from https://www.researchgate.net/profile/Andreas_Matzarakis/publication/262560304_Different_Trees_and_configuration_as_microclimate_control_strategy_in_Tropics/links/00b49537f967750c57000000.pdf

Aguilar, E., Peterson, T. C., Obando, P. R., Frutos, R., Retana, J. A., Solera, M., Mayorga, R. (2005). Changes in precipitation and temperature extremes in Central America and northern South America, 1961?2003. *Journal of Geophysical Research*, *110*(D23), D23107. https://doi.org/10.1029/2005JD006119

Akbari, H., & Levinson, R. (2008). Evolution of Cool-Roof Standards in the US. *Advances in Building Energy Research*, *2*(1), 1–32. https://doi.org/10.3763/aber.2008.0201

Alavipanah, S., Wegmann, M., Qureshi, S., Weng, Q., & Koellner, T. (2015). The role of vegetation in mitigating urban land surface temperatures: A case study of Munich, Germany during the warm season. *Sustainability (Switzerland)*, *7*(4), 4689–4706. https://doi.org/10.3390/su7044689

Ali, S. B., Patnaik, S., & Madguni, O. (2017). Microclimate land surface temperatures across urban land use/ land cover forms. *Global J. Environ. Sci. Manage*, *3*(3), 231–242. https://doi.org/10.22034/gjesm.2017.03.03.001

Angel, S., Sheppard, S. C., Civco With Robert Buckley, D. L., Chabaeva, A., Gitlin, L., Kraley, A., … Perlin, M. (2005). *The Dynamics of Global Urban Expansion*. Retrieved from http://www.williams.edu/Economics/UrbanGrowth/DataEntry.htm.

Bechtel, B., Alexander, P., Böhner, J., Ching, J., Conrad, O., Feddema, J., … Stewart, I. (2015). Mapping Local Climate Zones for a Worldwide Database of the Form and Function of Cities. *ISPRS International Journal of Geo-Information*, *4*(4), 199–219. https://doi.org/10.3390/ijgi4010199

Bechtel, B., Alexander, P., & Earth, G. (2012). Software Required : Part 1 : Google Earth.

Bechtel, B., & Daneke, C. (2012). Classification of local climate zones based on multiple earth observation data. *IEEE Journal of Selected Topics in Applied Earth Observations and Remote Sensing*, *5*(4), 1191–1202. https://doi.org/10.1109/JSTARS.2012.2189873

Bechtel, B., Demuzere, M., Sismanidis, P., Fenner, D., Brousse, O., Beck, C., … Verdonck, M.-L. (2017). Quality of Crowdsourced Data on Urban Morphology—The Human Influence Experiment (HUMINEX). *Urban Science*, *1*(2), 15. https://doi.org/10.3390/urbansci1020015

Bechtel, B., Zakšek, K., & Hoshyaripour, G. (2012). Downscaling Land Surface Temperature in an Urban Area: A Case Study for Hamburg, Germany. *Remote Sensing*, *4*(10), 3184–3200. https://doi.org/10.3390/rs4103184

Boice, D. C., Huebner, W. F., & Garcia, N. (1970). The Urban Heat Island Of San Antonio, Texas (USA). *WIT Transactions on Ecology and the Environment*, *14*.

https://doi.org/10.2495/AIR960661

Bokva, A., Dobrovolny, P., Gál, T., Geletic, J., Gulyás, Á., Hajtó, M., … Zuvela-Aloise, M. (2014). Modelling the impact of climate change on heat load increase in Central European cities, (Sievers 1995), 6–10. Retrieved from http://real.mtak.hu/28567/1/CCMA2-5-3151332_a.pdf

Bokwa, A., Hajto, M. J., Walawender, J. P., & Szymanowski, M. (2015). Influence of diversified relief on the urban heat island in the city of Kraków, Poland. *Theoretical and Applied Climatology*, *122*(1–2), 365–382. https://doi.org/10.1007/s00704-015-1577-9

Brazel, A., Selover, N., Vose, R., & Heisler, G. (2000). The tale of two climates-Baltimore and Phoenix urban LTER sites. *Climate Research*, *15*(2), 123–135. https://doi.org/10.3354/cr015123

Briscoe, D. (2017). transPLANTing Heat Island Effects in Tokyo. *UPLanD - Journal of Urban Planning, Landscape & Environmental Design*, *2*(1), 153–163. https://doi.org/10.6092/2531-9906/5145

Brousse, O., Martilli, A., Foley, M., Mills, G., & Bechtel, B. (2016). WUDAPT, an efficient land use producing data tool for mesoscale models? Integration of urban LCZ in WRF over Madrid. *Urban Climate*, *17*, 116–134. https://doi.org/10.1016/j.uclim.2016.04.001

Brown, M. (2004). Urban morphological analysis for mesoscale meteorological and dispersion modelling applications: Current issues. *Researchgate.Net*. Retrieved from http://library.lanl.gov/cgi-bin/getfile?01000060.pdf

Buyantuyev, A., & Wu, J. (2010). Urban heat islands and landscape heterogeneity: linking spatiotemporal variations in surface temperatures to land-cover and socioeconomic patterns. *Landscape Ecology*, *25*(1), 17–33. https://doi.org/10.1007/s10980-009-9402-4

Cai, G., Du, M., & Xue, Y. (2011). Monitoring of urban heat island effect in Beijing combining ASTER and TM data. *International Journal of Remote Sensing*, *32*(5), 1213–1232. https://doi.org/10.1080/01431160903469079

Cai, M., Ren, C., Xu, Y., Dai, W., & Wang, X. M. (2016). ScienceDirect Local Climate Zone Study for Sustainable Megacities Development by Using Improved WUDAPT Methodology – A Case Study in Guangzhou. *Procedia Environmental Sciences*, *36*, 82–89. https://doi.org/10.1016/j.proenv.2016.09.017

Cellura, M., Culotta, S., Brano, V. Lo, & Marvuglia, A. (2011). Nonlinear Black-Box Models for Short-Term Forecasting of Air Temperature in the Town of Palermo (pp. 183–204). Springer, Berlin, Heidelberg. https://doi.org/10.1007/978-3-642-19733-8_11

Charabi, Y., & Bakhit, A. (2011). Assessment of the canopy urban heat island of a coastal arid tropical city: The case of Muscat, Oman. *Atmospheric Research*, *101*(1–2), 215–227. https://doi.org/10.1016/J.ATMOSRES.2011.02.010

Chen, F., Yang, X., & Zhu, W. (2014). WRF simulations of urban heat island under hot-weather synoptic conditions: The case study of Hangzhou City, China. *Atmospheric Research*, *138*, 364–377. https://doi.org/10.1016/J.ATMOSRES.2013.12.005

Chen, J., Zhu, W., Tian, Y. Q., Yu, Q., Zheng, Y., & Huang, L. (2017). Remote

estimation of coloured dissolved organic matter and chlorophyll-a in Lake Huron using Sentinel-2 measurements. *J. Appl. Remote Sens*, *11*(4), 36007–36015. https://doi.org/10.1117/1.JRS.11

Ching, J., Mills, G., See, L., Bechtel, B., Feddema, J., Stewart, I., … Masson, V. (2016). Wudapt (World Urban Database and Access Portal Tools): an International Collaborative Project for Climate-Relevant Physical Geography Data for the World ' S Cities, 1–7.

Comrie, A. C., & Comrie, A. C. (2000). Mapping a Wind–Modified Urban Heat Island in Tucson, Arizona (with Comments on Integrating Research and Undergraduate Learning). *Bulletin of the American Meteorological Society*, *81*(10), 2417–2431. https://doi.org/10.1175/1520-0477(2000)081<2417: MAWMUH>2.3.CO;2

Connor, O., Fatima, M. De, Bechtel, B., Foley, M., Mills, G., Ching, J., … Gál, T. (2015). CENSUS of Cities: LCZ Classification of Cities (Level 0) – Workflow and Initial Results from Various Cities. *ICUC9, Toulouse, France (20-24 July)*, (Level 0), 8–13. https://doi.org/10.13140/RG.2.1.4028.5206

Coseo, P., & Larsen, L. (2014). How factors of land use/land cover, building configuration, and adjacent heat sources and sinks explain Urban Heat Islands in Chicago. *Landscape and Urban Planning*, *125*, 117–129. https://doi.org/10.1016/J.LANDURBPLAN.2014.02.019

Coutts, A. M., White, E. C., Tapper, N. J., Beringer, J., & Livesley, S. J. (2016). Temperature and human thermal comfort effects of street trees across three contrasting street canyon environments. *Theoretical and Applied Climatology*, *124*(1–2), 55–68. https://doi.org/10.1007/s00704-015-1409-y

Crawford, B., & Christen, A. (2014). Spatial variability of carbon dioxide in the urban canopy layer and implications for flux measurements. *Atmospheric Environment*, *98*, 308–322. https://doi.org/10.1016/J.ATMOSENV.2014.08.052

Danodia, A., Nikam, B. R., & Kumar, S. (2017). Land Surface Temperature Retrieval By Radiative Transfer Equation And Single Channel Algorithms Using Landsat-8 Satellite Data Land Surface Temperature Retrieval By Radiative Transfer Equation And Single Channel Algorithms Using Landsat-8 Satellite, (October).

Danylo, O., See, L., Bechtel, B., Schepaschenko, D., & Fritz, S. (2016). Contributing to WUDAPT: A Local Climate Zone Classification of Two Cities in Ukraine. *IEEE Journal of Selected Topics in Applied Earth Observations and Remote Sensing*, *9*(5), 1841–1853. https://doi.org/10.1109/JSTARS.2016.2539977

Deng, R., Tian, G., Wuang, X., & Cheng, X. (2003). Quantitative remote sensing for synthetic aerosol and its application in the Shanghai district. In H.-L. Huang, D. Lu, & Y. Sasano (Eds.) (Vol. 4891, p. 370). International Society for Optics and Photonics. https://doi.org/10.1117/12.466036

Dobrovolný, P., & Krahula, L. (2015). The spatial variability of air temperature and nocturnal urban heat island intensity in the city of Brno, Czech Republic, *23*. https://doi.org/10.1515/mgr-2015-0013

Ezber, Y., Lutfi Sen, O., Kindap, T., & Karaca, M. (2007). Climatic effects of urbanisation in Istanbul: a statistical and modelling analysis. *International Journal of Climatology*, *27*(5), 667–679. https://doi.org/10.1002/joc.1420

Fabbri, K. (2015). The Thermal Comfort and Child Development Psychology. In *Indoor Thermal Comfort Perception* (pp. 149–178). Cham: Springer International

Publishing. https://doi.org/10.1007/978-3-319-18651-1_6

Fahmy, M., Sharples, S., & Yahiya, M. (2010). LAI based trees selection for mid-latitude urban developments: A microclimatic study in Cairo, Egypt. *Building and Environment*, *45*(2), 345–357. https://doi.org/10.1016/j.buildenv.2009.06.014

Fröhlich, D., & Matzarakis, A. (2013). Modelling of changes in thermal bioclimate: Examples based on urban spaces in Freiburg, Germany. *Theoretical and Applied Climatology*. https://doi.org/10.1007/s00704-012-0678-y

Früh, B., Becker, P., Deutschländer, T., Hessel, J.-D., Kossmann, M., Mieskes, I., … Wienert, U. (2011). Estimation of Climate-Change Impacts on the Urban Heat Load Using an Urban Climate Model and Regional Climate Projections. *Journal of Applied Meteorology and Climatology*, *50*(1), 167–184. https://doi.org/10.1175/2010JAMC2377.1

Gartland, L. (2012). *Heat islands: understanding and mitigating heat in urban areas*. Retrieved from https://www.taylorfrancis.com/books/9781136564215

Gartland, L. M. (2008). *Heat Islands*. Routledge. https://doi.org/10.4324/9781849771559

Geleti, J. Č., Lehnert, M., Dobrovolný, P., & Bulletin, H. G. (2016). Modelled spatio-temporal variability of air temperature in an urban climate and its validation : a case study of Brno, Czech Republic, *65*, 169–180. https://doi.org/10.15201/hungeobull.65.2.7

Geletič, J., & Lehnert, M. (2016). GIS-based delineation of local climate zones: The

case of medium-sized Central European cities. *Moravian Geographical Reports*, *24*(3), 2–12. https://doi.org/10.1515/mgr-2016-0012

Geletič, J., Lehnert, M., Savić, S., Milošević, D., Geleti, J., Lehnert, M., … Milo, D. (2018). Modelled spatiotemporal variability of outdoor thermal comfort in local climate zones of the city of Brno, Czech Republic. *Science of the Total Environment*, *624*, 385–395. https://doi.org/10.1016/j.scitotenv.2017.12.076

Georgi, N. J., & Zafiriadis, K. (2006). The impact of park trees on microclimate in urban areas. *Urban Ecosystems*, *9*(3), 195–209. https://doi.org/10.1007/s11252-006-8590-9

Giridharan, R., Ganesan, S., & Lau, S. S.. (2004). Daytime urban heat island effect in high-rise and high-density residential developments in Hong Kong. *Energy and Buildings*, *36*(6), 525–534. https://doi.org/10.1016/J.ENBUILD.2003.12.016

Golden, J. S. (2004). The Built Environment Induced Urban Heat Island Effect in Rapidly Urbanizing Arid Regions – A Sustainable Urban Engineering Complexity. *Environmental Sciences*, *1*(4), 321–349. https://doi.org/10.1080/15693430412331291698

Gulyás, Á., Unger, J., & Matzarakis, A. (2006). Assessment of the microclimatic and human comfort conditions in a complex urban environment: Modelling and measurements. *Building and Environment*, *41*(12), 1713–1722. https://doi.org/10.1016/J.BUILDENV.2005.07.001

Hansen, J., Ruedy, R., Sato, M., Imhoff, M., Lawrence, W., Easterling, D., … Karl, T. (2001). A closer look at United States and global surface temperature change. *Journal of Geophysical Research: Atmospheres*, *106*(D20), 23947–23963.

https://doi.org/10.1029/2001JD000354

Hashim, J. H., & Hashim, Z. (2016). Climate Change, Extreme Weather Events, and Human Health Implications in the Asia Pacific Region. *Asia Pacific Journal of Public Health*, *28*(2_suppl), 8S–14S. https://doi.org/10.1177/1010539515599030

Hollosi, B., & Zuvela-aloise, M. (2017). Urban climate model MUKLIMO _ 3 in prediction mode – evaluation of model performance based on the case study of Vienna, *19*, 16455.

Jones, P. D., Groisman, P. Y., Coughlan, M., Plummer, N., Wang, W.-C., & Karl, T. R. (1990). Assessment of urbanisation effects in time series of surface air temperature over land. *Nature*, *347*(6289), 169–172. https://doi.org/10.1038/347169a0

Jones, P. D., & Jones, P. D. (1994). Hemispheric Surface Air Temperature Variations: A Reanalysis and an Update to 1993. *Journal of Climate*, *7*(11), 1794–1802. https://doi.org/10.1175/1520-0442(1994)007<1794:HSATVA>2.0.CO;2

Karl, T. R., Diaz, H. F., Kukla, G., Karl, T. R., Diaz, H. F., & Kukla, G. (1988). Urbanisation: Its Detection and Effect in the United States Climate Record. *Journal of Climate*, *1*(11), 1099–1123. https://doi.org/10.1175/1520-0442(1988)001<1099:UIDAEI>2.0.CO;2

King, V., & Davis, C. (2007). A case study of urban heat islands in the Carolinas. *Environmental Hazards*. https://doi.org/10.1016/j.envhaz.2007.09.005

Koç, A., Yilmaz, S., Akif Irmak, M., & Matzarakis, A. (2015). The role of trees in urban thermal comfort and SkyView Factor. Retrieved from

http://www.meteo.fr/icuc9/LongAbstracts/bph1-1-2751290_a.pdf

Kolokotroni, M., Giannitsaris, I., & Watkins, R. (2006). The effect of the London urban heat island on building summer cooling demand and night ventilation strategies. *Solar Energy*, *80*(4), 383–392. https://doi.org/10.1016/J.SOLENER.2005.03.010

Kolokotroni, M., & Giridharan, R. (2008). Urban heat island intensity in London: An investigation of the impact of physical characteristics on changes in outdoor air temperature during summer. *Solar Energy*, *82*(11), 986–998. https://doi.org/10.1016/J.SOLENER.2008.05.004

Lehnert, M., & Geletiˇ, J. (2016). Land Surface Temperature Differences within Local Climate Zones, Based on Two Central European Cities Land Surface Temperature Differences within Local Climate Zones, Based on Two Central European Cities, (September). https://doi.org/10.3390/rs8100788

Lehnert, M., Geletič, J., Husák, J., & Vysoudil, M. (2015). Urban field classification by "local climate zones" in a medium-sized Central European city: the case of Olomouc (Czech Republic). *Theoretical and Applied Climatology*, *122*(3–4), 531–541. https://doi.org/10.1007/s00704-014-1309-6

Lelovics, E., & Unger, J. (2013). Mapping Local Climate Zones With a Vector-Based Gis Method. *Air & Water Components of the Environment / Aerul Si Apa Compone*, 423–430.

Lelovics, E., Unger, J., Gál, T., & Gál, C. V. (2014). Design of an urban monitoring network based on Local Climate Zone mapping and temperature pattern modelling. *Climate Research*, *60*(1), 51–62. https://doi.org/10.3354/cr01220

Li, Y., Zhang, H., & Kainz, W. (2012). Monitoring patterns of urban heat islands of the fast-growing Shanghai metropolis, China: Using time-series of Landsat TM/ETM+ data. *International Journal of Applied Earth Observation and Geoinformation*, *19*, 127–138. https://doi.org/10.1016/J.JAG.2012.05.001

Lin Zhongli, & Xu Hanqiu. (2016). A study of Urban heat island intensity based on "local climate zones": A case study in Fuzhou, China. In *2016 4th International Workshop on Earth Observation and Remote Sensing Applications (EORSA)* (pp. 250–254). IEEE. https://doi.org/10.1109/EORSA.2016.7552807

Liu, S., Bond-Lamberty, B., Boysen, L. R., Ford, J. D., Fox, A., Gallo, K., … Zhao, S. (2017). Grand Challenges in Understanding the Interplay of Climate and Land Changes. *Earth Interactions*, *21*(2), 1–43. https://doi.org/10.1175/EI-D-16-0012.1

Makokha, G. L., & Shisanya, C. A. (2010). Temperature Cooling and Warming Rates in Three Different Built Environments within Nairobi City, Kenya. *Advances in Meteorology*, *2010*, 1–5. https://doi.org/10.1155/2010/686214

Masson, V., Marchadier, C., Adolphe, L., Aguejdad, R., Avner, P., Bonhomme, M., … Zibouche, K. (2014). Adapting cities to climate change: A systemic modelling approach. *Urban Climate*, *10*, 407–429. https://doi.org/10.1016/J.UCLIM.2014.03.004

Mcpherson, E. G., Van Doorn, N. S., & Peper, P. J. (2016). Urban Tree Database and Allometric Equations, (October), 86. https://doi.org/10.13140/RG.2.2.35769.98405

Middel, A., Häb, K., Brazel, A. J., Martin, C. A., & Guhathakurta, S. (2014). Impact of

urban form and design on mid-afternoon microclimate in Phoenix Local Climate Zones. *Landscape and Urban Planning*, *122*, 16–28. https://doi.org/10.1016/j.landurbplan.2013.11.004

Muhaisen, A. S. (2006). Shading simulation of the courtyard form in different climatic regions. *Building and Environment*, *41*(12), 1731–1741. https://doi.org/10.1016/j.buildenv.2005.07.016

Ng, E., & Cheng, V. (2012). Urban human thermal comfort in hot and humid Hong Kong. *Energy and Buildings*, *55*, 51–65. https://doi.org/10.1016/j.enbuild.2011.09.025

Ng, Y. (2015). A Study of Urban Heat Island using "Local Climate Zones" – The Case of Singapore. *British Journal of Environment and Climate Change*, *5*(2), 116–133. https://doi.org/10.9734/BJECC/2015/13051

Ongoma, V., Muange, P. K., & Shilenje, Z. W. (2016). Potential effects of urbanisation on urban thermal comfort, a case study of Nairobi city, Kenya: A review. *Geographica Pannonica*, *20*(1), 19–31. https://doi.org/10.18421/GP20.01-03

Ongoma, V., Muthama, J. N., & Gitau, W. (2013). Evaluation of urbanisation on urban temperature of Nairobi City, Kenya. *Global Meteorology*, *2*(e1), 1–5. https://doi.org/10.4081/gm.2013.e1

Oyugi, M. O., Odenyo, V. A. O., & Karanja, F. N. (2017). The Implications of Land Use and Land Cover Dynamics on the Environmental Quality of Nairobi City, Kenya, *6*(3), 111–127. https://doi.org/10.5923/j.ajgis.20170603.04

Parlow, E., Vogt, R., & Feigenwinter, C. (2014). The urban heat island of Basel – seen

from different perspectives. *DIE ERDE – Journal of the Geographical Society of Berlin*, *145*(1–2), 96–110. Retrieved from https://www.die-erde.org/index.php/die-erde/article/view/95

Peterson, T. C., & Peterson, T. C. (2003). Assessment of Urban Versus Rural In Situ Surface Temperatures in the Contiguous United States: No Difference Found. *Journal of Climate*, *16*(18), 2941–2959. https://doi.org/10.1175/1520-0442(2003)016<2941:AOUVRI>2.0.CO;2

Polydoros, A., Mavrakou, T., Cartalis, C., Polydoros, A., Mavrakou, T., & Cartalis, C. (2018). Quantifying the Trends in Land Surface Temperature and Surface Urban Heat Island Intensity in Mediterranean Cities in View of Smart Urbanization. *Urban Science*, *2*(1), 16. https://doi.org/10.3390/urbansci2010016

Ragheb, A. A., El-Darwish, I. I., & Ahmed, S. (2016). Microclimate and human comfort considerations in planning a historic urban quarter. *International Journal of Sustainable Built Environment*, *5*(1), 156–167. https://doi.org/10.1016/j.ijsbe.2016.03.003

Ren, C., Cai, M., Wang, M., Xu, Y., & Ng, E. (2016). Local Climate Zone (LCZ) Classification Using the World Urban Database and Access Portal Tools (WUDAPT) Method: A Case Study in Wuhan and Hangzhou. *The Fourth International Conference on Countermeasure to Urban Heat Islands (4th IC2UHI)*, (May), 1–12.

Ren, C., Fung, J. C.-H., Tse, J. W. P., Wang, R., Wong, M. M. F., & Xu, Y. (2017). Implementing WUDAPT product into urban development impact analysis by using WRF simulation result - A case study of the Pearl River Delta Region (1980-2010). *Proceedings of the 13th Symposium on Urban Environment*,

(January), 22–26. Retrieved from http://files/3490/REN et al. - 9.2 Implementing WUDAPT product into urban develop.pdf

Santamouris, M., Haddad, S., Fiorito, F., Osmond, P., Ding, L., Prasad, D., … Wang, R. (2017). Urban Heat Island and Overheating Characteristics in Sydney, Australia. An Analysis of Multiyear Measurements. *Sustainability*, *9*(12), 712. https://doi.org/10.3390/su9050712

Santamouris, M., Paraponiaris, K., & Mihalakakou, G. (2007). Estimating the ecological footprint of the heat island effect over Athens, Greece. *Climatic Change*, *80*(3–4), 265–276. https://doi.org/10.1007/s10584-006-9128-0

Schlünzen, K. H., Hoffmann, P., Rosenhagen, G., & Riecke, W. (2009). Long-term changes and regional differences in temperature and precipitation in the metropolitan area of Hamburg. *International Journal of Climatology*, *30*(8), 1121–1136. https://doi.org/10.1002/joc.1968

Schwarz, N., Schlink, U., Franck, U., & Großmann, K. (2012). Relationship of land surface and air temperatures and its implications for quantifying urban heat island indicators—An application for the city of Leipzig (Germany). *Ecological Indicators*, *18*, 693–704. https://doi.org/10.1016/J.ECOLIND.2012.01.001

See, L., Ching, J., Masson, V., Mills, G., Neophytou, M., Connor, M. O., … Bechtel, B. (2015). Generating WUDAPT ' s Specific Scale-dependent Urban Modelling of Level 1 and Level 2 Data • The need for WUDAPT.

See, L., Perger, C., Duerauer, M., Fritz, S., Bechtel, B., Ching, J., … Masson, V. (2015). Developing a community-based worldwide urban morphology and materials database (WUDAPT) using remote sensing and crowdsourcing for improved

urban climate modelling. In *2015 Joint Urban Remote Sensing Event (JURSE)* (pp. 1–4). IEEE. https://doi.org/10.1109/JURSE.2015.7120501

Shashua-Bar, L., Pearlmutter, D., & Erell, E. (2011). The influence of trees and grass on outdoor thermal comfort in a hot arid environment. *International Journal Of Climatology Int. J. Climatol*, *31*, 1498–1506. https://doi.org/10.1002/joc.2177

Shooshtarian, S., & Ridley, I. (2017). The effect of physical and psychological environments on the users thermal perceptions of educational urban precincts. *Building and Environment*, *115*, 182–198. Retrieved from https://linkinghub.elsevier.com/retrieve/pii/S0360132316305170

Singh, P., Kikon, N., & Verma, P. (2017). Impact of land-use change and urbanisation on urban heat island in Lucknow city, Central India. A remote sensing-based estimate. *Sustainable Cities and Society*, *32*, 100–114. https://doi.org/10.1016/J.SCS.2017.02.018

Smoliak, B. V., Snyder, P. K., Twine, T. E., Mykleby, P. M., Hertel, W. F., Smoliak, B. V., … Hertel, W. F. (2015). Dense Network Observations of the Twin Cities Canopy-Layer Urban Heat Island*. *Journal of Applied Meteorology and Climatology*, *54*(9), 1899–1917. https://doi.org/10.1175/JAMC-D-14-0239.1

Stevan, S., Dragan, M., Lazar, L., Vladimir, M., Daniela, A., & Dragoslav, P. (2013). Classifying urban meteorological stations sites by ‘local climate zones’: Preliminary results for the City of Novi Sad (Serbia). *Geographica Pannonica*, *17*(3), 60–68.

Stewart, I. D., & Oke, T. R. (2012). Local climate zones for urban temperature studies. *Bulletin of the American Meteorological Society*, *93*(12), 1879–1900.

https://doi.org/10.1175/BAMS-D-11-00019.1

Stewart, I. D., Oke, T. R., & Krayenhoff, E. S. (2014). Evaluation of the 'local climate zone' scheme using temperature observations and model simulations. *International Journal of Climatology*, *34*(4), 1062–1080. https://doi.org/10.1002/joc.3746

Stewart, I., & Oke, T. (2006). Thermal Differentiation of Local Climate Zones Using Temperature Observations From Urban and Rural Field Sites (Figure 1).

Stone, B. (2007). Urban and rural temperature trends in proximity to large US cities: 1951–2000. *International Journal of Climatology*, *27*(13), 1801–1807. https://doi.org/10.1002/joc.1555

Stone, B., Hess, J. J., & Frumkin, H. (2010). Urban Form and Extreme Heat Events: Are Sprawling Cities More Vulnerable to Climate Change Than Compact Cities? *Environmental Health Perspectives*, *118*(10), 1425–1428. https://doi.org/10.1289/ehp.0901879

Stone, B., & Rodgers, M. O. (2001). Urban Form and Thermal Efficiency: *How the Design of Cities Influences the Urban Heat Island Effect*. *Journal of the American Planning Association*, *67*(2), 186–198. https://doi.org/10.1080/01944360108976228

Taubenböck, H., Esch, T., Wurm, M., Roth, A., & Dech, S. (2010). Object-based feature extraction using high spatial resolution satellite data of urban areas. *Journal of Spatial Science*, *55*(1), 117–132. https://doi.org/10.1080/14498596.2010.487854

Tzavali, A., Paravantis, J., Mihalakakou, G., Fotiadi, A., Stigka, E., Tzavali, A., …

Stigka, E. (2015). Urban Heat Island Intensity: A Literature Review. *Fresenius Environmental Bulletin*, *24*(December 2016), 4535–4554.

Unger, J. (2004). Intra-urban relationship between surface geometry and urban heat island: review and new approach. *Climate Research*, *27*(3), 253–264. https://doi.org/10.3354/cr027253

Unger, J., Lelovics, E., Gál, T., Bulletin, H. G., Unger, J., Lelovics, E., & Gál, T. (2014). Local climate zone mapping using GIS methods in Szeged. *Hungarian Geographical Bulletin*, *63*(1), 29–41. https://doi.org/10.15201/hungeobull.63.1.3

Vargo, J., Stone, B., Habeeb, D., Liu, P., & Russell, A. (2016). The social and spatial distribution of temperature-related health impacts from urban heat island reduction policies. https://doi.org/10.1016/j.envsci.2016.08.012

Vieira De Abreu-Harbich, L., Labaki, L. C., & Matzarakis, A. (2015). Effect of tree planting design and tree species on human thermal comfort in the tropics. *Landscape and Urban Planning*, *138*, 99–109. https://doi.org/10.1016/j.landurbplan.2015.02.008

Vieira De Abreu-Harbich, L., Labaki, L. C., Matzarakis, A., de Abreu-Harbich, L. V., Labaki, L. C., & Matzarakis, A. (2015). Effect of tree planting design and tree species on human thermal comfort in the tropics. *Landscape and Urban Planning*, *138*, 99–109. https://doi.org/10.1016/j.landurbplan.2015.02.008

Voogt, J. ., & Oke, T.. (2003). Thermal remote sensing of urban climates. *Remote Sensing of Environment*, *86*(3), 370–384. https://doi.org/10.1016/S0034-4257(03)00079-8

Wang, J. X. L., Gaffen, D. J., Wang, J. X. L., & Gaffen, D. J. (2001). Late-Twentieth-Century Climatology and Trends of Surface Humidity and Temperature in China. *Journal of Climate*, *14*(13), 2833–2845. https://doi.org/10.1175/1520-0442(2001)014<2833:LTCCAT>2.0.CO;2

Wang, R., Ren, C., Xu, Y., Lau, K. K.-L., & Shi, Y. (2018). Mapping the local climate zones of urban areas by GIS-based and WUDAPT methods: A case study of Hong Kong. *Urban Climate*, *24*, 567–576. https://doi.org/10.1016/j.uclim.2017.10.001

Warren, C. M. J. (2012). Heat Islands; Understanding and Mitigating Heat in Urban Areas20122Lisa Gartland. *Heat Islands; Understanding and Mitigating Heat in Urban Areas*. London: Earthscan 2011. 192 pp., ISBN: 978-1-84971-298-9 $64.95. *Property Management*, *30*(1), 105–106. https://doi.org/10.1108/pm.2012.30.1.105.2

Weaner, L., & Christopher, T. (2016). *Garden Revolution: How Our Landscapes Can Be a Source of Environmental Change*. Retrieved from https://scholar.google.com/scholar?hl=en&as_sdt=0%2C5&q=%28Weaner+%26+Christopher%2C+2016%29.&btnG=

Zhan, J., Huang, J., Zhao, T., Geng, X., & Xiong, Y. (2013). Modelling the impacts of urbanisation on regional climate change: A case study in the beijing-tianjin-tangshan metropolitan area. *Advances in Meteorology*, *2013*. https://doi.org/10.1155/2013/849479

Zhang, J., & Yao, F. (2009). The characteristics of urban heat island variation in Beijing urban area and its impact factors. In *2009 Joint Urban Remote Sensing Event* (pp. 1–6). IEEE. https://doi.org/10.1109/URS.2009.5137502

Zhang, J., Yao, F., Fu, C., & Yan, X. (2004). Study on response of ecosystem to the East Asian monsoon in eastern China using LAI data derived from remote sensing information*. *Progress in Natural Science*, *14*(3), 279–282. https://doi.org/10.1080/10020070412331343471

Zhang, N., Zhu, L., & Zhu, Y. (2011). Urban heat island and boundary layer structures under hot weather synoptic conditions: A case study of Suzhou City, China. *Advances in Atmospheric Sciences*, *28*(4), 855–865. https://doi.org/10.1007/s00376-010-0040-1

Zhao, X., Li, G., & Gao, T. (2017). Research on Optimization and Biological Characteristics of Harbin Trees Based on Thermal Comfort in Summer. *Procedia Engineering*, *180*, 550–561. https://doi.org/10.1016/J.PROENG.2017.04.214

Zhou, D., Zhao, S., Liu, S., Zhang, L., & Zhu, C. (2014). Surface urban heat island in China's 32 major cities: Spatial patterns and drivers. *Remote Sensing of Environment*, *152*, 51–61. https://doi.org/10.1016/J.RSE.2014.05.017

Zhou, W., Qian, Y., Li, X., Li, W., & Han, L. (2014). Relationships between land cover and the surface urban heat island: seasonal variability and effects of spatial and thematic resolution of land cover data on predicting land surface temperatures. *Landscape Ecology*, *29*(1), 153–167. https://doi.org/10.1007/s10980-013-9950-5

Žuvela-Aloise, M. (2017). Enhancement of urban heat load through social inequalities on an example of a fictional city King's Landing. *International Journal of Biometeorology*, *61*(3), 527–539. https://doi.org/10.1007/s00484-016-1230-z

Žuvela-Aloise, M., Koch, R., Buchholz, S., & Früh, B. (2016). Modelling the potential of green and blue infrastructure to reduce urban heat load in the city of Vienna.

Climatic Change, *135*(3–4), 425–438. https://doi.org/10.1007/s10584-016-1596-2